Defining In Vivo Functions of the Atypical Ubiquitin Conjugating Enzyme, Ube2W

by

Bo Wang

A dissertation submitted in partial fulfillment
of the requirements for the degree of
Doctor of Philosophy
(Neuroscience)
in the University of Michigan
2015

Doctoral Committee:

Professor Henry L. Paulson, Chair
Associate Professor Anthony Antonellis
Assistant Professor Sami J. Barmada
Professor Kojo S. J. Elenitoba-Johnson
Professor Miriam H. Meisler

Acknowledgements

I would like to thank my dissertation mentor, Dr. Henry Paulson, for his full support and expert guidance during my study and research. His diligence, wisdom and patience have always been a great motivation to me. Without the help of him, this dissertation would not have been possible. I would like to express my appreciation to my committee members: Dr. Anthony Antonellis, Dr. Sami Barmada, Dr. Kojo Elenitoba-Johnson and Dr. Miriam Meisler for their support and helpful advice regarding my thesis work. I want to thank all the current and previous members of Henry Paulson laboratory for being so helpful and supportive towards my work; their presence certainly makes everyday enjoyable in lab. Especially the members that directly contribute to my thesis work: Sean Merillat, Dr. Matthew Scaglione, Dr. Li Zeng and Dr. Biswarathan Ramini. I also thank my collaborators for teaching and helping me with several aspects of my thesis project: Dr. Sami Barmada, Dr. Andrzej Dlugosz, Dr. Doris Mangelberger, Dr. David Irani, Dr. Amanda Huber, Dr. Richard Miller, Melissa Han, William Kohl, Dr. Santiago Schnell, Michael Vincent, Dr. Kojo Elenitoba-Johnson, Dr. Venkatesha Basrur, Dr. Matthew Scaglione, Dr. Leslie Thompson and Joseph Ochaba. I am very appreciative towards the helpful discussion with Dr. Roger Albin, Dr. Andrew Lieberman, Dr. Xiaochun Yu, Dr. Chun-Chi Liang

and Dr. Chunjing Bian regarding my thesis work. I also want to thank medical school of Shanghai Jiaotong University for supporting me as a joint MD-PhD student with University of Michigan. The funding sources are acknowledged throughout the dissertation.

Table of Contents

List of Figures

Abstract

Ubiquitination is a common post-translational modification that is critically important to many different cellular pathways. Dysfunction of ubiquitin pathways can disrupt various cellular processes that eventually cause diseases such as Huntington's disease (HD). Unlike typical ubiquitination, which happens at lysine residues of substrates, Ube2W attaches ubiquitin in an atypical manner: to the N-termini of substrates. Disordered N-termini are believed to represent the preferred substrates for Ube2W. In chapter 1, I review recent studies of typical lysine ubiquitination and atypical ubiquitination, including Ube2W-mediated N-terminal ubiquitination. I also review ubiquitin pathways implicated in HD, since the disordered N-terminus of the disease protein, Huntingtin (Htt), is a compelling candidate substrate for Ube2W and the focus of later studies. I then describe the results of two research projects that investigate Ube2W in vitro and vivo functions. In chapter 2, using mice in which the *Ube2W* is knocked out, I present evidence that Ube2W is important for early postnatal survival and plays significant roles in in multiple organ systems; I also provide in vivo evidence that supports the view that Ube2W preferentially targets disordered substrates. In chapter 3, using cultured cells and genetic crosses in mouse models, I show that Ube2W regulates the solubility of mutant Htt. Ube2W deficiency significantly increases

levels of soluble Htt monomers and reduces Htt-mediated neurotoxicity. Chapter 4 concludes the dissertation with thoughts of future studies. Taken together, this dissertation provides in vivo evidence supporting Ube2W's ability to N-terminally ubiquitinate misfolded proteins, which is key to multiple cellular pathways and organ functions. This dissertation establishes novel insights to the in vivo functions of Ube2W and N-terminal ubiquitination.

Chapter One: Ubiquitin pathways and their role in neurodegenerative diseases

1.1 ABSTRACT

The conjugation of ubiquitin to proteins, a process known as ubiquitination, is critical to many cellular processes. Different types of ubiquitination result in a wide range of fates for substrate proteins including proteasomal degradation, altered cellular location, and regulation of enzymatic activity. Typically, ubiquitin is conjugated to one or more lysine residues in a substrate protein. Non-canonical ubiquitination to other amino acids or to the amino-termini of substrates can also occur, but is poorly understood. The specific cellular functions of non-canonical ubiquitination, and amino-termini ubiquitination in particular, are not yet determined. In this introductory chapter, I review recent discoveries regarding non-canonical ubiquitination, including its potential functions. Furthermore, because ubiquitin pathways play an important role in most neurodegenerative diseases associated with protein aggregation and accumulation and will be the focus of chapter three of this thesis, I will review the effect of traditional and non-canonical ubiquitination on a well-known disease target, the Huntington's disease protein, Huntingtin (Htt).

1.2 INTRODUCTION

Ubiquitination is a common post-translational modification that can occur to most proteins, leading to different fates for the modified protein depending on the specific type of ubiquitination. An evolutionarily conserved protein that is 76-amino acids in length, ubiquitin (Ub) is conjugated to substrate proteins in an energy-dependent, sequential reaction: 1) conjugation is initiated by activation of Ub via the Ub-activating enzyme, E1, which forms a high-energy thio-ester bond between C-terminal glycine of Ub and the active site thiol of E1; 2) the Ub-E1 complex then transfers the activated Ub to a Ub conjugating enzyme, E2, which also forms a thio-ester bond between Ub and E2 as in the Ub-E1 complex; 3) Ubiquitin ligase (E3) then comes into play, transferring Ub from the E2 to a substrate via different mechanisms depending on the subtype of E3. A series of ubiquitination events can happen to different sites on a substrate or to another Ub already attached to the substrate, generating monoubiquitination and polyubiquitination, respectively. The ubiquitination process is kept in check by deubiquitinating enzymes (DUBs) that act to cleave pre-formed Ub chains and recycle free Ubs and possibly edit the types of polyubiquitin chains added to substrates (Fig 1).

Typically, Ub is covalently attached to free ε-amino groups on lysine side chains. Additional Ub molecules then can be further attached to any of the seven lysine residues of Ub, giving rise to polyubiquitin chains that contain a wide range of topologically distinct Ub-Ub linkages. Emerging evidence, however, indicates that Ub also can be covalently attached to the α-amino group of a protein's

amino-terminus, the hydroxyl group of serine, threonine or tyrosine residues and the thiol group of cysteine residues(1). These latter kinds of ubiquitination events, termed non-canonical ubiquitination, are understudied compared to the typical, canonical lysine ubiquitination.

Taking into consideration these different Ub-chain lengths, linkages and substrate attachment sites, dramatically different kinds of ubiquitination can occur. The variety of ubiquitination pattern is mainly achieved by different combination of E2/E3 pairs. The regulation of Ub attachment is achieved collaboratively between E2s and E3s. At least 38 E2s are encoded in the human proteome and play an essential role in the diversity of Ub chain assembly. E2s determine chain initiation or elongation, the types of linages in polyubiquitin chain, and, in some cases, substrate site preference. My thesis investigates the in vivo function of an intriguing E2, Ube2W. Ube2W is the only E2 shown to specifically carry out N-terminal ubiquitination.

The various forms of Ub signals regulate a wide spectrum of cellular functions: protein proteasomal degradation; autophagy; DNA damage response; multi-protein complex assembly; subcellular localization; enzymatic activity and the inflammatory response. Given Ub's importance to many physiological processes, specific alterations in Ub signaling can result in drastic effects contributing to various human diseases. For example, dysregulation of ubiquitin pathways is important in neurodegenerative diseases, which are often characterized by protein accumulation and aggregation. Defects in ubiquitin systems, including Ubiquitin-Proteasome System (UPS), are present in

neurodegenerative diseases such as the polyglutamine (polyQ) diseases which are caused by a CAG repeat expansion in the protein coding sequence of the disease gene, resulting in an expanded stretch of glutamine residues in the disease protein. In polyQ diseases such as Huntington's disease (HD), the polyQ expansion causes protein misfolding. Because of the defective ubiquitin system in polyQ disease, misfolded disease proteins tend to oligomerize, accumulate and become detrimental to neuronal health. The exact reason for ubiquitin pathway alteration in neurodegeneration is still unclear, but more insights to the ubiquitin system can be beneficial and hopefully can uncover potential therapies to these diseases.

1.3 CANONICAL LYSINE-MEDIATED UBIQUITIN PATHWAYS

1.3.1 Monoubiquitination

As stated in introduction, ubiquitination can occur on a single residue or several residues of a substrate protein, resulting in monoubiquitination or multi-monoubiquitination (Fig 1). To specify whether the Ub will be further ubiquitinated (i.e. form a polyubiquitin chain), different E2 and E3 partners have evolved to achieve these outcomes. For example, proliferating cell nuclear antigen (PCNA), a key enzyme in DNA repair response, can be targeted for monoubiquitination on Lys164 by the E2 Rad6 and the E3 Rad18. Such monoubiquitination signals the recruitment of multiple polymerases to initiate DNA repair. In contrast, the E2 Ubc13/MMS2 and the E3 Rad5 can further extend the Ub chain on

monoubiquitinated PCNA and such polyubiquitination is important to DNA repair(2–4).

Recent evidence suggests that the E2 is more important in such discrimination and that E2s can preferentially mediate chain initiation, chain elongation or both. Different E2s can partner with the same E3 and substrate, resulting in initial monoubiquitination or subsequent polyubiquitination. The BRCA1-BARD1 E3 ligase recruits any of the four E2s, UbcH6, Ube2E2, UbcM2 and Ube2W, to monoubiquitinate BRCA1, whereas it recruits the E2s Ubc13/MMS2 and Ube2K to polyubiquitinate BRCA1(5–9). Although the exact mechanism for this discrimination is not understood, the structures around the E2 catalytic region and substrate lysines are both considered to be important regulators(10, 11).

The biological functions of monoubiquitination extend far beyond protein degradation. One important function of monoubiquitination is the regulation of endocytosis. A well-known example is epidermal growth factor receptor (EGFR): once activated, EGFR is rapidly multi-monoubiquitinated (monoubiquitination events occurred on multiple substrate lysines) by Cbl E3 ligase family(12, 13) which leads EGFR to interact with ubiquitin binding domains (UBDs) that lie within adaptor proteins such as clathrin coat proteins and EGFR substrate 15 (EPS15)(14). This interaction triggers the assembly of monoubiquitinated EGFR molecules into clathrin-coated vesicles. In the meantime, adaptor proteins such as EPS15 undergo EGFR-coupled monoubiquitination by NEDD4 (E3), further facilitating EGFR endocytosis and subsequent lysosomal degradation(15, 16).

Monoubiquitination can also regulate enzymatic activity of substrate proteins. As a key switch of cellular differentiation and growth, Ras signaling is tightly regulated by monoubiquitination. Monoubiquitination of Lys147 in K-Ras inhibits GAP-mediated GTP hydrolysis, thus increasing its biological effects(17–19). Comparatively, monoubiquitination of Lys117 in H-Ras increases GTP-GDP exchange, thus activating H-Ras via a different mechanism than K-Ras(20). Monoubiquitination is also crucial in DNA damage response. After DNA double strand breaks (DSB), the histone H2A variant H2AX is one of the first proteins recruited to the DSB sites to initiate DNA damage repair. RNF2 and BMI1-mediated H2AX monoubiquitination is required for its phosphorylation and subsequent DNA repair, and a lysine mutation that abolishes H2AX monoubiquitination impairs its recruitment to DNA damage loci(21). Fanconi Anemia pathway is another major DNA repair pathway that is highly regulated by FANCD2 monoubiquitination. Ube2W, the focus of my thesis, together with Ube2T, are able to monoubiquitinate FANCD2 in vitro, but only *Ube2T* knockout renders cells more prone for mitomycin-C induced DNA crosslinking(22–24).

The protein that is the focus of this thesis, Ube2W, is an E2 that preferentially monoubiquitinates substrates on their N-terminal amino group(25). Although the exact in vivo function of such modification is unknown, the lessons from literature suggest a wide range of biological functions for monoubiquitination that are not limited to proteasomal degradation.

1.3.2 Polyubiquitination

After the first Ub is attached to the substrate, subsequent cycles of ubiquitination can target the amino groups on Ubs already attached to the substrate, thus generating polyubiquitin chains. There are eight amino groups in each Ub molecule: an α-NH_2 at the N-terminus and the ε-NH_2 of lysines at position 6, 11, 27, 29, 33, 48 and 63. Much like the mechanism in distinguishing monoubiquitination or polyubiquitination, Ub chain linkage preference can be specified by E2s: examples include K11-specific Ube2S, K48-specific Ube2K, K63-specific Ube2N-Ube2V1, and UbcH5 that can produce K11, K48 and K63 linkages. E2s are not involved in formation of Ub-Ub linkages via the N-terminal methionine (Met1); rather, Met1-linked Ub chains are generated by the linear ubiquitination assembly complex (LUBAC) that includes HOIL-1L, HOIP and sharpin.

The various types of Ub linkages serve as distinct cellular signals (Fig 2). The best-studied type of polyubiquitination is K48-linked Ub chain. A stretch of more than four K48-linked Ubs on a substrate typically serves as a signal for proteasomal targeting and degradation(26). Several E2s are known to generate such chain linkages: Ube2K, Ube2G2 and cdc34. Mutations in key regulatory domains of these E2s result in loss of specificity towards K48-linked Ub chain (9, 27). Once K48-linked polyUb is attached to a substrate, the conjugate must be targeted to the cell's degradation machinery by chaperone or Ub adapter proteins, which recognize and bind to the polyubiquitin stretch. Valosin-containing protein (VCP) is a chaperone and Ub adapter protein, which physically interacts with and

shuttles poly-ubiquitinated substrates to the proteasome to facilitate their degradation(28). Ubiquilin-2 (UBQLN2) is another shuttle protein that contains both UBA domain and UBL domain, through which they can interact with polyubiquitinated substrates and the proteasome. UBQLN2 and related ubiquilins can bring polyubiquitinated substrates to the proteasome. Dominant acting mutations in VCP or UBQLN2 can result in the accumulation of poly-ubiquitinated proteins and carrier patients suffer from neurodegenerative diseases such as Amyotrophic Lateral Sclerosis (ALS) and Frontotemporal Dementia (FTD)(29, 30).

The 26S proteasome can be divided into the catalytic 20S core protease (CP) and 19S regulatory particle (RP). Cooperatively, the 19S RP base and lid recognize K48 linked Ub chains, cleave off Ub moieties, and unfold and import substrate to the CP for degradation. Cooperatively, the chymotrypsin-like, trypsin-like, and caspase-like activities of the 20S CP cleave substrate proteins into small peptides(31). Similarly, K11-linked Ub chain modification on target substrate can also result in proteasomal degradation and plays an important function in mitosis progression(10, 32). In contrast, K63-linked ubiquitination has more diverse non-proteolytic functions: DNA repair(33), stress response(34, 35), signal transduction(36, 37) and intracellular protein trafficking(36).

M1-linked Ub chains are implicated in NF-κB activation: LUBAC promotes linear poly-Ub of RIP2 and serves as an activation signal for IKK kinase complex. Such activation enables IκB polyubiquitination and subsequent proteasomal degradation(38). Alterations in LUBAC and M1-linked Ub signals are implicated in many diseases including variety of solid tumors (lung cancer, breast cancer,

prostate cancer and melanoma) and immune disorders(39). Patients with inactivation or deficiency of heme-oxidized IRP2 Ub ligase-1 (HOIL-1, LUBAC component) suffer from chronic autoinflammation and susceptibility to bacterial infections(40).

Taken together, polyubiquitination has a wide variety of cellular functions that are largely determined by types of ubiquitin chain linkages.

1.4 NON-CANONICAL UBIQUITINATION

1.4.1 Ubiquitinations on internal non-lysine residues

In addition to amino groups, Ub can also be attached to hydroxyl groups of serine, threonine or tyrosine residues and the thiol group of cysteine residues(1). In the past decade, numerous targets have been identified to undergo this non-canonical ubiquitination. Peroxisomal import factor Pxp5 was the first identified substrate of cysteine ubiquitination(41, 42). Lysineless Pxp5 can still be ubiquitinated and Pxp5's N-terminal amine is naturally blocked by co-translational acetylation. Both lines of evidence suggest that Pxp5 ubiquitination occurs at internal non-lysine residues. Cysteine ubiquitination was postulated because reducing agents, which break thioester bonds, can disrupt Pxp5 ubiquitination(43). Indeed, when Cys11 is mutated to arginine, Pxp5 ubiquitination is abolished. Pex20p, a Pxp5 related protein, was later found to be ubiquitinated on cysteine as well(44). Cysteine ubiquitination of Pxp5 and Pex20p is critical to their cellular localization: it serves as a signal to recycle the proteins from the peroxisome to cytosol(41, 43–45). Additionally, Ngn2 is a

proneural transcriptional factor that can be ubiquitinated at many potential ubiquitination sites, including cysteine, lysine, N-terminus, serine and threonine. However, unlike Pxp5 and Pex20p where cysteine ubiquitination plays a nondegradative signaling role, cysteine ubiquitination on Ngn2 is sufficient for its proteasomal degradation(46, 47).

Ubiquitination on hydroxyl groups of serine, threonine or tyrosine of the Major Histocompatibility Complex I (MHC I) heavy chain is critical to its stability; mutations of these residues not only reduce its polyubiquitination, they also stabilize the protein(48). Ngn3 is another example of a protein modified by this type of ubiquitination. Unlike Ngn2, which is ubiquitinated on a cysteine residue, Ngn3 ubiquitination occurs at serines and threonines, serving as a degradation signal(49).

Taken together, ubiquitination on internal non-lysine residues occurs to a limited number of proteins and can target these substrates to various destinies including protein degradation and altered cellular localization. Although only a few proteins have been reported to be modified on these non-canonical sites, with the recent advance in mass spectrometry, these internal non-lysine ubiquitinations are increasingly identified by the resultant signature peptide(50). Identifying more substrates of this type of ubiquitination will lead to a better understanding of the function of this modification.

1.4.2 N-terminal ubiquitination

When it remains unmodified, a protein's N-terminus provides an additional free amino group beyond internal lysines. Ub can be attached to the α-amino group via the same mechanism as occurs with conjugation to lysine residues.

For a small subset of proteins, when all lysine residues are chemically mutated or deleted, ubiquitination still takes place and may serve as a degradation signal. When the free α-amino group is blocked, by a bulky tag or chemically ablation, these substrate proteins could no longer be ubiquitinated and thus were stabilized(51–55). Among these proteins, MyoD was the first identified example of N-terminal ubiquitination: lysine-less MyoD can still be ubiquitinated and degraded. Proteasomal inhibition can completely block the degradation of lysine-less MyoD and lead to an accumulation of ubiquitin-conjugated MyoD. Moreover, when the free α-amino group is blocked with carbamylation or 6 myc tags, Ub can no longer be attached to MyoD and MyoD becomes stabilized both in vivo and in vitro(52). These findings ruled out canonical lysine-mediated ubiquitination of MyoD since ubiquitination still occurs when all lysines are removed, leaving only one intact amino group on the N-terminus of MyoD. N-terminal tagging physically blocked Ub access to the free α-amino group. Taken together, MyoD is the first example of a now growing list of proteins that can be N-terminally ubiquitinated.

Using similar experimental approaches, researchers identified several other examples of N-terminal ubiquitination: ataxin-3(56), cyclin G1(57), Epstein-Barr virus latent membrane protein 1 (LMP1)(53), LMP2A(51), Extracellular

signal-regulated kinase 3 (ERK3)(57), the inhibitor of DNA binding 1 (ID1) protein(58), ID2(59), p19(60), p21(55) and peroxisome proliferator activated receptor γ co-activator 1a (PGC1a)(61). In the case of ataxin-3, ERK3 and p21, there is even more convincing direct evidence from mass spectrometry (MS): a fusion peptide directly linking the N-terminal methionine of substrate and the C-terminal glycine of Ub was identified in vivo(55, 56).

Furthermore, there are 14 Naturally Occurring Lysine-Less Proteins (NOLLPs) encoded in the human proteome and 111 NOLLPs in the viral proteome(62). Lacking the lysine residue that is target for canonical ubiquitination, Ub can only be attached to non-lysine residues including the N-terminus. Indeed, $p16^{INK4a}$ and HPV-58 E7 both proved to be substrates for N-terminal ubiquitination and can be targeted for proteasomal degradation(62).

Currently, all but two known N-terminal substrates (ataxin-3 and LMP2A) can be targeted for proteasomal degradation by N-terminal ubiquitination via K48-linked Ub chain. Among the substrates, cyclin G1, $p16^{INK4a}$, p19 and p21 are key regulators governing the cell cycle: cyclin G1 is a key regulator of cyclin-dependent protein kinases (CDKs) and is implicated in G2/M arrest in response to DNA damage(63, 64). $p16^{INK4a}$, p19 and p21 are three well-studied tumor suppressors that inhibit CDK4 and CDK6, so that they arrest cell cycle at G1 or G2(65); loss of function of either gene can lead to dysregulation of cell cycle and results in various cancers including melanomas and germ cell tumors(66). Since all of them can be targeted for degradation by N-terminal ubiquitination, a

potential important function of N-terminal ubiquitination is the regulation of cell proliferation.

Lessons from classic lysine ubiquitination inform us that ubiquitination is more than just a degradation signal. Accordingly, the potential function of N-terminal ubiquitination in non-degradation pathways needs further investigation.

1.4.3 Ube2W and N-terminal ubiquitination

Ube2W is the only E2 known to mediate N-terminal ubiquitination(56, 67). It is a class I E2 that consists of the catalytic UBC domain without any N-terminal or C-terminal extensions. Ube2W can function with various ubiquitin ligases including the C terminus of Hsc-70-interacting protein (CHIP) and the BRCA1/BARD1 complex to mono-ubiquitinate select substrates at their amino-termini or internal lysines(25, 56, 68–70). Ube2W's structure reveals that it is an unique E2 in two major respects. First, unlike other E2s, Ube2W has an unique binding pocket preceding the highly conserved C91 which is present in all members of this E2 family. Within this pocket, Ube2W has a histidine (H83) in place of the conserved asparagine residue. This asparagine critically stabilizes the oxyanion intermediate after E2-Ub lysine attack and stabilizes the loop preceding the active site(71). When H83 is mutated to asparagine, Ube2W can no longer ubiquitinate its documented substrates (e.g. CHIP and tau)(56). Second, except H83, Ube2W shares a highly conserved UBC core structure with other E2s, however, its C-terminal residues N136-W145 form a highly disordered region positioned beneath the active site C91 (Fig 3). This disordered C-terminus

is critical to substrate interaction, as mutation in one of the residues, W144E, abolishes Ube2W's Ub-transfer activity towards tested substrates (ataxin-3, CHIP, RBP8 and tau) (68). These characteristic structural features of Ube2W may provide clue to its unique activity as an N-terminal ubiquitinating E2.

One Ube2W substrate is ataxin-3, which is mutated in the polyglutamine disorder, Spinocerebellar Ataxia Type 3 (SCA3). Ataxin-3 was already known to be ubiquitinated by other E2s and CHIP at two lysine residues, K117 and K200. However, when Ube2W is present, Ub is instead attached to the N-terminus of ataxin-3 instead of these internal lysines. When carbamylation or a bulky GST tag is used to block ataxin-3's α-amino group, Ub can no longer be attached to ataxin-3 by Ube2W. Mass spectrometry also identified the fusion of ubiquitin C-terminus to ataxin-3's N-terminus, providing direct evidence for N-terminal ubiquitination(56). The same experimental methods proved that SUMO-2 and CHIP also can be N-terminally ubiquitinated by Ube2W(67).

Ube2W is a strict monoubiquitinating E2. Unlike LUBAC, which catalyzes M1-linked linear Ub chains, Ube2W does not extend the Ub chain. This observation is supported by the fact that Ube2W fails to show a noncovalent interaction with Ub whereas covalent interactions between E2s and ubiquitin are a common feature of ubiquitin chain-elongating E2s (6, 72–74). Interestingly, when a 13-amino-acid long human influenza hemagglutinin (HA) is added to the N-terminus of ubiquitin, Ube2W shifts its activity from monoubiquitination to M1-linked linear polyubiquitination, indicating that the HA tag itself can be a robust substrate for Ube2W. The HA tag is highly mobile and disordered compared to

ubiquitin, suggesting that Ube2W prefers disordered substrates. To test this, glycine, the most flexible amino acid, was added to the N-terminus of ubiquitin; whereas 1 glycine did not alter Ube2W ubiquitination pattern, the addition of 3 glycines allowed Ube2W to generate polyubiquitin chains, and chains of 5 and 7 glycines further increased the production of polyubiquitin chains by Ube2W. This activity is lost when prolines, amino acids with bulky side chain, are instead added to the N-terminus.

Despite these recent advances in understanding the activity of Ube2W as a N-terminal ubiquitinating E2, the physiological function of Ube2W-mediated N-terminal ubiquitination was unknown before the start of my thesis. Although most substrates tested thus far can be targeted for degradation after N-terminal ubiquitination, whether this holds true in Ube2W-mediated N-terminal ubiquitination is unclear. Our unpublished data suggest that lysine-less ataxin-3 is degraded nearly as efficiently as WT ataxin-3, suggesting either that Ube2W-mediated ataxin-3 N-terminal ubiquitination does not play an important role in ataxin-3 degradation or that ataxin-3 N-terminal ubiquitination is limited in vivo.

The microenvironment inside the cell is much more complex than in a test tube, especially when studying the N-termini of proteins. Besides ubiquitination, acetylation is another post-translational modification that targets amino groups of protein including at their N-termini. N-terminal acetylation has been well documented since the 1950s when researchers faced difficulty sequencing proteins using the Edman degradation method; they realized that acetylation can “block” protein N-termini from being recognized. In fact, a majority of proteins can

be N-terminally acetylated in some organisms: about 60% in yeast, 30% in *D. melanogaster* and 85% in human cells(75, 76). N-terminal acetylation prevents Ube2W from ubiquitinating these substrates.

Recent evidence from TRIM5α and TRIM21 has provided insight to Ube2W's effect on N-terminally acetylated molecules. Members of the tripartite (TRIM) family, TRIM5 and TRIM21 serve as antibody receptors that neutralize intracellular viruses(77). TRIM5α contains a RING domain, conferring upon it an additional E3 ligase activity. When it interacts with retroviral caspids, TRIM5α generates unanchored K63-linked Ub chains, which stimulate NF-κB translocation and induces antiviral gene expression(78, 79). TRIM21 itself can be polyubiquitinated with K63-linked chains and signals immune pathways. The N-termini of both TRIM5α and TRIM21 are acetylated, rendering them inaccessible to Ube2W. However, Ube2W can still mono-ubiquitinate TRIM5α and TRIM21 on internal lysines (K45 and K50 of TRIM5α) identified by mass spectrometry. After Ube2W initiates the Ub chain, Ube2N/Ube2V2 is recruited and extends K63-linked chains. When deacetylating reagents chemically unblock TRIM5α N-termini, Ube2W shifts its preference towards N-termini(69, 70). These results suggest that while Ube2W has a strong preference toward N-termini of proteins, when the α-amino group is inaccessible, Ube2W is capable of mediating ubiquitination to some lysine residues.

1.5 UBIQUITIN PATHWAYS IN HUNTINGTON'S DISEASE

Ubiquitin pathways are implicated in many neurodegenerative diseases including Huntington's disease (HD). For my thesis studies, I became particularly interested in HD because Huntingtin (Htt), the disease protein in HD, is intrinsically misfolded at its N-terminus. This property suggests that Htt is an attractive candidate substrate for Ube2W-mediated N-terminal ubiquitination. The function of Htt N-terminal ubiquitination is unknown. Here, I review the current knowledge of ubiquitin pathways involved in neurodegenerative diseases including HD.

1.5.1 Polyglutamine diseases and other neurodegenerative diseases

Accumulation of ubiquitinated proteins is commonly observed in neurodegenerative diseases. Inclusion body (IB) formation is a characteristic pathological hallmark shared by many neurodegenerative diseases such as Alzheimer's Disease (AD), Parkinson's Disease (PD), Amyotrophic Lateral Sclerosis (ALS), and the polyglutamine (polyQ) diseases. It is believed that dysfunction of the ubiquitin-proteasome system (UPS) or defects in other ubiquitin-dependent pathways contributes to the accumulation of ubiquitinated proteins, which are then recruited to inclusion bodies. Currently, however, there is disagreement regarding the cause of neuron death and the potential pathogenic role of inclusions in neurodegeneration. Whether the inclusion itself is directly toxic, simply a marker of abnormal protein accumulation, or even a protective strategy adopted by neurons to "wall off" extra protein load, remains

under debate. Regardless, dysregulation of ubiquitin-mediated protein quality control pathways is implicated in many of these neurodegenerative diseases. Mutations in genes encoding numerous ubiquitin pathway proteins cause various neurodegenerative diseases. For example, loss of function mutation in CHIP, a E3 ligase that works with Ube2W, causes ataxia(80, 81). Loss of Ube3A, an E3 ligase that specifically generates K48-linked Ub chains, causes Angelman syndrome, which presents as ataxia, myoclonus and other behavioral phenotypes(82, 83).

The polyQ diseases include at least nine neurodegenerative disorders: six forms of spinocerebellar ataxias (SCA) type 1, 2, 3, 6, 7, and 17; (SCA3 is also known as Machado-Joseph disease, or MJD/SCA3); Huntington's disease (HD); dentatorubral pallidoluysian atrophy (DRPLA); and spinal and bulbar muscular atrophy (SBMA). PolyQ diseases are characterized by the pathological expansion of a CAG trinucleotide repeat in the protein-coding region of the otherwise unrelated disease genes, which is translated to an expanded polyQ stretch in the disease proteins. The biochemical properties of expanded polyQ promote abnormal folding, oligomerization and aggregation of the disease protein. Protein quality control systems, including chaperones and ubiquitin-proteasome system (UPS), are important cellular machineries coping with this aberrant protein load(113). In normal conditions, chaperones help proteins fold correctly and the UPS targets unwanted or misfolded proteins for degradation and keeps them at a healthy level inside the cell. Several lines of evidence have implicated perturbations in protein quality control systems in various polyQ diseases.

Molecular chaperones are involved in several key cellular pathways, including folding of nascent proteins, refolding of misfolded or denatured proteins and translocation of proteins(84). Heat shock proteins (HSPs) comprise the majority of chaperones and are central to protein folding and refolding. Induction of HSPs by Heat shock factor protein-1 (Hsf1), a transcription factor, significantly reduces polyQ inclusion formation and cytotoxicity in cultured cells and animal models of HD and SBMA(85–87), while deficiency of Hsf1 accelerates and exacerbates disease phenotypes (86, 87). Cell-based time-lapse microscopy has shown that increasing Hsf1 concentration leads to decreased mutant huntingtin (Htt) IB formation(88). There is some disagreement about how Hsf1 regulates Htt inclusion perhaps because conclusions were based on results in different model systems(85–88). Studies using more physiologically precise disease models, such as knock-in mouse models, may provide more definitive evidence. Hsp40 and Hsp70 are two major HSPs that have been shown to regulate misfolded polyQ proteins. They have been shown consistently to decrease IB formation and suppress toxicity in various polyQ models, including SCA1, SCA3, SBMA and HD(84, 89–96). Therapeutic approaches using chaperones have been extensively investigated. Small molecules such as 17-AAG and geldanamycin, which can activate Hsf1, have been shown to ameliorate polyQ aggregation, disease severity and neurodegeneration in both cellular and animal models(97–99).

In the case of the UPS, although multiple pieces of evidence suggest UPS involvement in polyQ inclusion formation and disease progression, there is

uncertainty regarding the primary cause of protein accumulation. Some studies suggest that a significant problem in polyQ diseases is proteasome dysfunction(100–103). PolyQ expansion induces polyQ-containing peptides that are capable of clogging and inhibiting normal proteasome activity(100, 101, 103). Other studies suggest otherwise, arguing instead that mutant Htt can be degraded efficiently in cultured cells(104, 105). However, only proteasome function is measured in these scenarios without taking into account of the whole UPS, which includes E1, E2, E3 and DUBs. To test the function of UPS, degron reporters such as Ub^{G76V} and CL1 are fused to fluorescent protein so that UPS activity can be measure quantitatively by fluorescence(106–109). CL1 degron is a highly destabilizing tag targeting fusion protein for degradation through UPS. In cellular models of HD, introducing CL1 degron showed an accumulation of fluorescent signal, indicating decrease of UPS activity(109, 110). Ub^{G76V} is an ubiquitin mutant that binds protein N-terminally and serves as a degradation signal through UPS. The G76 mutation disables Ub removal by DUB and enables subsequent polyubiquitination(111). In R6 mice where human mutant Htt is constitutively overexpressed, no global UPS impairment was observed(112, 113); however, when $HttQ^{94}$ expression is acutely induced, a transient UPS impairment is observed in mouse striatum(113). Thus, transient and constitutive expression of mutant Htt result in completely different UPS responses. It is possible when mutant Htt is constitutively expressed, other compensatory mechanisms, such as chaperone system, are recruited to handle misfolding protein load; another possibility is that such long-term UPS impairment is too minimal to reach the

threshold of the limited detection methods. Taken together, UPS impairment is implicated in HD and other polyQ diseases.

It is important to keep in mind that proteasomal degradation is only one of many potential outcomes of ubiquitination, as discussed earlier. Ubiquitinated proteins inside inclusion bodies contain K11-, K48- and K63-linked Ub chains. K11- and K48-linked Ub chains are proteasomal degradation signals, while K63 linked Ub chain has a wide range of non-proteolytic functions. Recent evidence suggests the potential involvement of K63-linked Ub chains in regulating inclusion formation. In cultured cells overexpressing disease proteins that cause AD, FTD/ALS or PD, K63-linked ubiquitination promotes the formation of inclusion bodies(114–117).

To conclude, protein quality control systems are critically important in maintaining protein homeostasis; dysfunction in any of the key protein quality control systems can contribute to polyQ protein accumulation and cytotoxicity. Ubiquitin pathways including K11, K48 and K63 linked Ub chain modifications regulate polyQ protein stability and aggregation.

1.5.2 Huntington's disease and the disease protein, Huntingtin

The final sections of this chapter review the recent discoveries on ubiquitin pathways involved in a specific polyQ disease, Huntington's disease (HD). In HD, the CAG repeat expansion encodes a polyQ stretch in disease protein huntingtin (Htt). In individuals without an expansion, the polyQ length is between 10 and 35 residues in length and may help regulate protein interactions and gene

transcription(118, 119). When the polyQ length exceeds a threshold of ~40 glutamines, it causes disease(120). The severity of HD is polyQ length-dependent as increasing repeat length correlates with earlier onset of disease, more severe clinical and pathological presentations(121, 122). The most common HD alleles bear 40-50 CAG repeats. HD patients with these lengths tend to manifest classic HD symptoms including involuntary movements such as chorea and dystonia, neuropsychiatric symptoms and cognitive deficits. Repeats greater than 50 CAG repeats in length tend to cause earlier onset, juvenile HD that often includes additional symptoms beyond the classic symptoms noted above, including seizures and generalized slowness of movement(123). HD is a slowly progressive disease usually leading to death within 20 years of symptom onset. Histopathologically, HD displays a progressive spreading pattern of brain involvement: initially, the brain region affected most prominently is the striatum, with preferential loss of medium spiny neurons that express dopamine D2 receptors and the neurotransmitter enkephalin(124–127). The cerebral cortex also is involved as disease progresses but, unlike most other polyQ diseases, the cerebellum is relatively spared in HD(128–130).

Like other polyQ diseases, polyQ-expanded Htt protein is highly misfolded. It exists as three distinct states in cells: soluble monomers, soluble oligomers and insoluble aggregates(25, 26) (Fig 4). Htt aggregates present as inclusion bodies in neuronal nuclei, perinuclear regions and neurites(131–133). Immunohistochemical studies revealed that these inclusion bodies contain N-terminal fragments of Htt, ubiquitin, proteasomal components and numerous

other proteins (132). Lines of studies suggest that the N-terminus of Htt plays a key role in Htt processing: alteration or modification to Htt's N-terminus can result in dramatic changes in Htt level, localization and inclusion formation. Firstly, the N-terminus of Htt is polyQ containing since the CAG expansion occurs within exon1 of *Hdh* gene, thus generating a polyQ stretch at the very N-terminus (starting from the 18th amino acid). Secondly, the first 17 amino acids (N17) of Htt, located immediately before the polyQ stretch, are critical to cytosolic localization of the protein. Through N17, Htt can bind to cytoplasmic membrane in order to be exported from nucleus(134–137). In vitro, N17 promotes the formation of oligomers and aggregation of mutant Htt(138, 139), but deleting N17 has also been shown to significantly increase Htt nuclear localization and worsen disease phenotype in a BAC-HD mouse model(140). Thirdly, multiple protein post-translational modifications can occur at the N-terminus of Htt including acetylation, phosphorylation, SUMOylation and ubiquitination(141) (Fig 5). All four modifications are critical to Htt levels and cytotoxicity(142–145).

To conclude, the HD disease protein Htt is intrinsically disordered at its N-terminus, partly due to N17 and partly due to the polyQ stretch, and this disorder may be critical to regulating Htt levels, localization and inclusion formation.

1.5.3 Huntingtin Ubiquitination

The discovery of ubiquitin and proteasomal subunits in HD inclusion bodies supports the importance of ubiquitination and the UPS in HD pathogenesis. However, the roles of ubiquitination and the proteasome in HD are

not fully understood. To date, two main theories have been proposed: 1. Ubiquitinated mutant Htt can no longer be degraded by the proteasome, and thus accumulates as inclusion bodies(109, 110, 112, 146–148); 2. Ubiquitination of mutant Htt is a non-degradation signal, with proteasome subunits being secondarily recruited to inclusions as cell's coping mechanism towards such mutant Htt accumulation(112, 149). These theories may not be mutually exclusive to and both may contribute to HD pathogenesis.

The most straightforward possibility is that ubiquitinated mutant Htt is itself a proteasomal substrate. As discussed in the previous section, two proposed scenarios might contribute to the inclusion formation: a) the increased burden of misfolded protein overwhelms the UPS system; and b) long polyQ stretches, derived from Htt by proteolytic cleavage, clog the proteasome and inhibit its normal function. In both cases, a defective proteasome would accelerate the accumulation of mutant Htt. This idea is supported by multiple cell and animal models in which HD is modeled by expression of an N-terminal fragment of Htt (109, 110, 112, 146–148). However, mixed findings were achieved in a more physiologically precise mouse model: proteasome function remains unaltered in R6 mouse(112, 149). In a doxycycline-inducible Hdh^{Ex1} transgenic mouse, the Ub^{G76V}-GFP reporter accumulates when Hdh^{Ex1} expression is induced(113). So, up to now, there is still disagreement on the exact function of UPS in HD pathogenesis.

Besides Ub monomers and proteasome subunits, inclusions of postmortem HD brain also stained positively with anti-K63-linked ubiquitin

antibodies(109, 143, 150). As described above, unlike K48-linked Ub chains, K63-linked Ub chains serve as a non-proteolytic signal. When nuclear mutant Htt is biochemically pulled-down, K63-linkage is found to be the main ubiquitination species(143). The existence of K63-linked mutant Htt favors the hypothesis that ubiquitination of Htt represents a non-proteolytic signal. When lysine 63 of ubiquitin is mutated to arginine (K63R), K63-linked Ub chain can no longer be formed. In HD cell models where the N-terminal fragment of Htt was overexpressed, coexpression of K63R ubiquitin significantly decreased polyubiquitination of mutant Htt. In the same model, when all other lysines except K63 of ubiquitin were mutated to arginines, there was an increase in mutant Htt polyubiquitination. Taken together, these results suggest that, at least in cell models, K63-linked Ub chains are the main type of mutant Htt ubiquitination(143). In vivo validation of this idea would be very valuable.

However, the exact function of K63-linked Htt ubiquitination is still unclear. It has been postulated that K63-linked ubiquitinated Htt is caused by failed Htt degradation through K48-linked Ub chain(143, 150), since K63-linked ubiquitination has been linked to autophagic clearance of inclusions and accompanies UPS impairment(117, 151, 152). In another study, however, the presence of K63-linked Ub chains enhanced polyQ inclusions and targeted polyQ protein for subsequent autophagic clearance, thus contributing to the life cycle of IBs(116, 117).

In addition to ubiquitination, SUMOylation may play an important role in HD pathogenesis. In HD patient brains, there is accumulation of SUMOylated

insoluble proteins including Htt(145). Like ubiquitination, SUMOylation is a post-translational modification that targets protein lysine amino groups. Unlike the case with ubiquitination, N-terminal SUMOylation and other non-canonical SUMOylations have not been identified. SUMOylation participates in a wide range of cellular activities including the regulation of protein cellular localization, transcription control and protein interactions(153, 154). There are four different SUMO isoforms in mammals: SUMO-1 and SUMO-2 are ~50% identical at a protein level, while SUMO-2 and SUMO-3 are nearly identical and SUMO-4 is a precursor form expressed in kidney, spleen and thymus(153, 155, 156). Similar to ubiquitination, substrate SUMOylation involves a cascade of enzymes: E1 activating enzyme (AOS1/Uba2), E2 conjugating enzyme (Ubc9) and E3 ligases (PIAS, Pc2 and RanBP2). Since only one set of E1 (SAE1/SAE2) and E2 (UBC9) has been identified for SUMOylation, it is believed that E3s specify SUMOylation substrates. PIAS (protein inhibitor of activated STAT) family is one of the best-characterized SUMO E3 ligase families. PIAS protein has RING finger domains, which assists in the attachment of SUMO to target substrates.

Emerging evidence suggests that mutant Htt SUMOylation plays a key regulatory role in HD pathogenesis. Under stress conditions, Htt can be phosphorylated at S13 and S16 by inflammatory kinase (IKK) and lead to an increase polySUMOylation of truncated Htt (Htt^{ex1})(142). K6 and K9 of Htt^{ex1} are most susceptible to SUMOylation of both SUMO-1 and SUMO-2; mutation of these lysines can abolish Htt^{ex1} polySUMOylation(145). However, SUMO-1 and SUMO-2 showed a different regulatory role in mutant Htt aggregation and

inclusion. SUMO-1 modification of Htt^{ex1} reduces aggregation and solubilizes the protein(144). However, SUMO-2 is shown to cause Htt^{ex1} to insolubilize and accumulate. Overexpressing PIAS1, the E3 ligase for Htt SUMOylation, can also increase mutant Htt aggregation, reproducing the same cellular phenotype with SUMO-2 overexpression(145). In $Htt^{ex1}Q_{93}$ expressing drosophila model, knockdown of PIAS1 significantly decreases SUMOylation of Htt and rescues the eye degeneration(144, 145).

In summary, both ubiquitination and SUMOylation of the N-terminal domain of Htt appear to participate in some manner in HD pathogenesis. However, non-canonical ubiquitination of Htt at its N-terminus has not been studied. Given the disordered nature of Htt's N-terminal fragment, it is predicted to be a strong candidate target for non-canonical ubiquitination by Ube2W. The biological role of such modification is the key question of my second part of thesis.

FIGURE 1. Process of ubiquitin conjugation

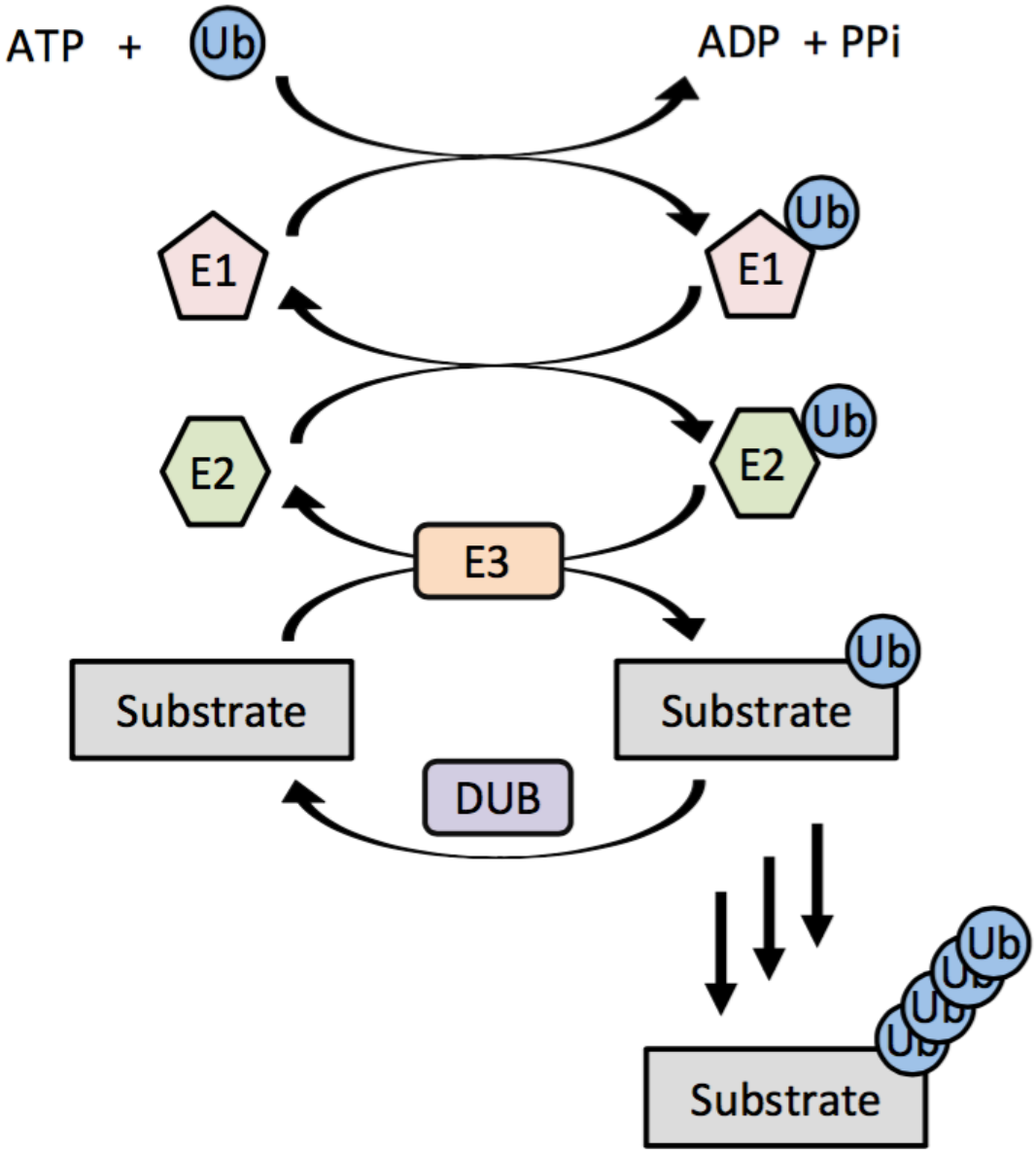

FIGURE 2. Different types of ubiquitin chains

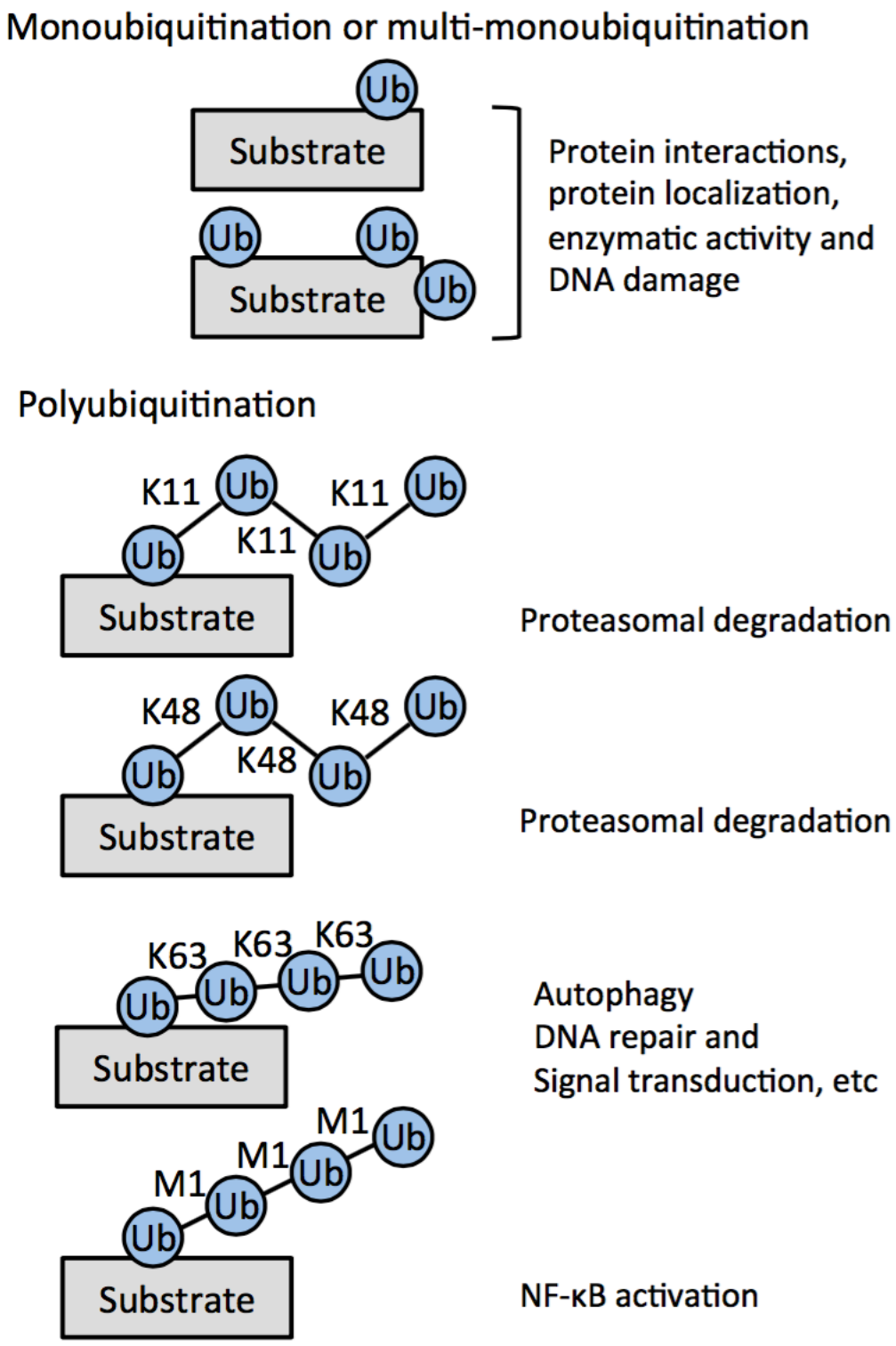

FIGURE 3. Ube2W's unique structure allows N-terminal ubiquitination

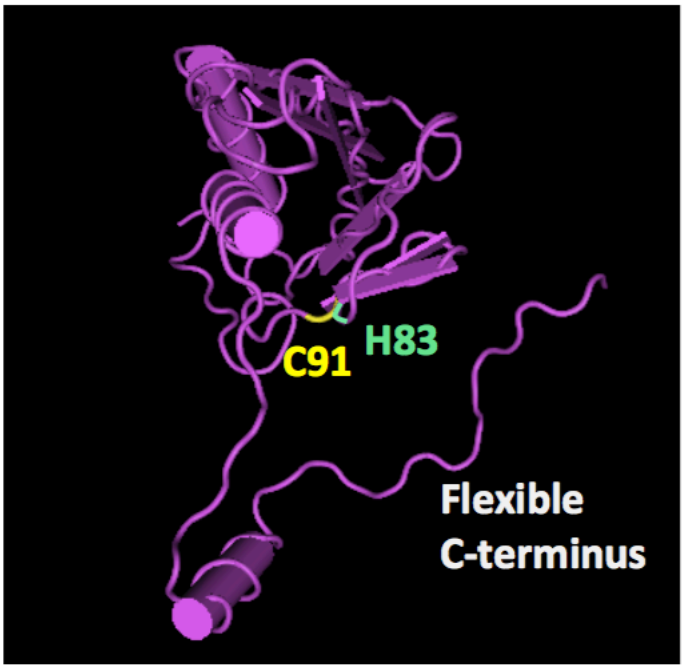

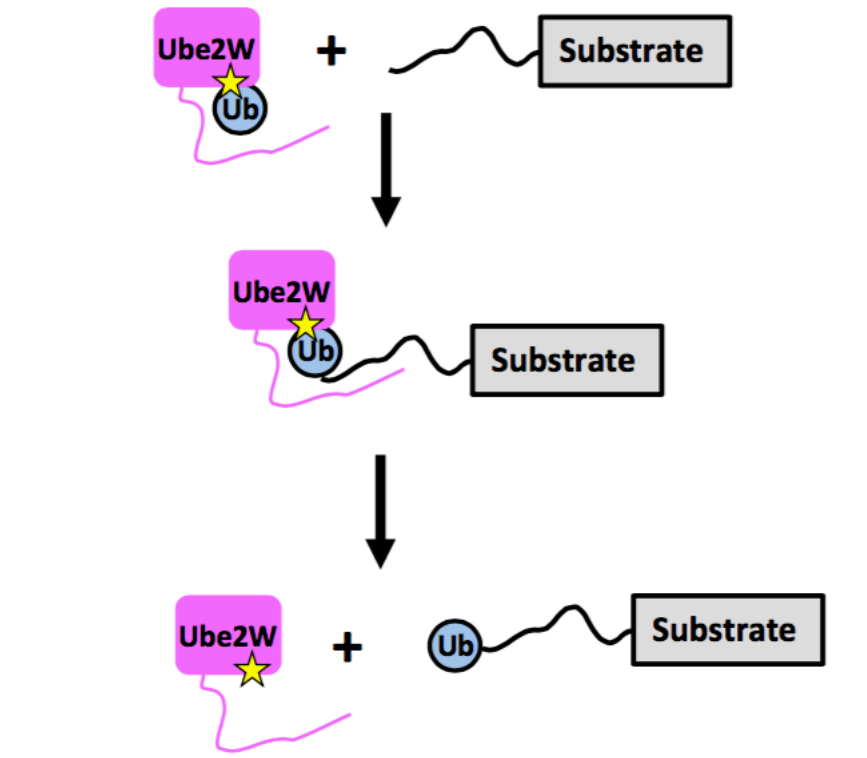

FIGURE 4. Htt aggregation and related molecular pathogenesis of HD

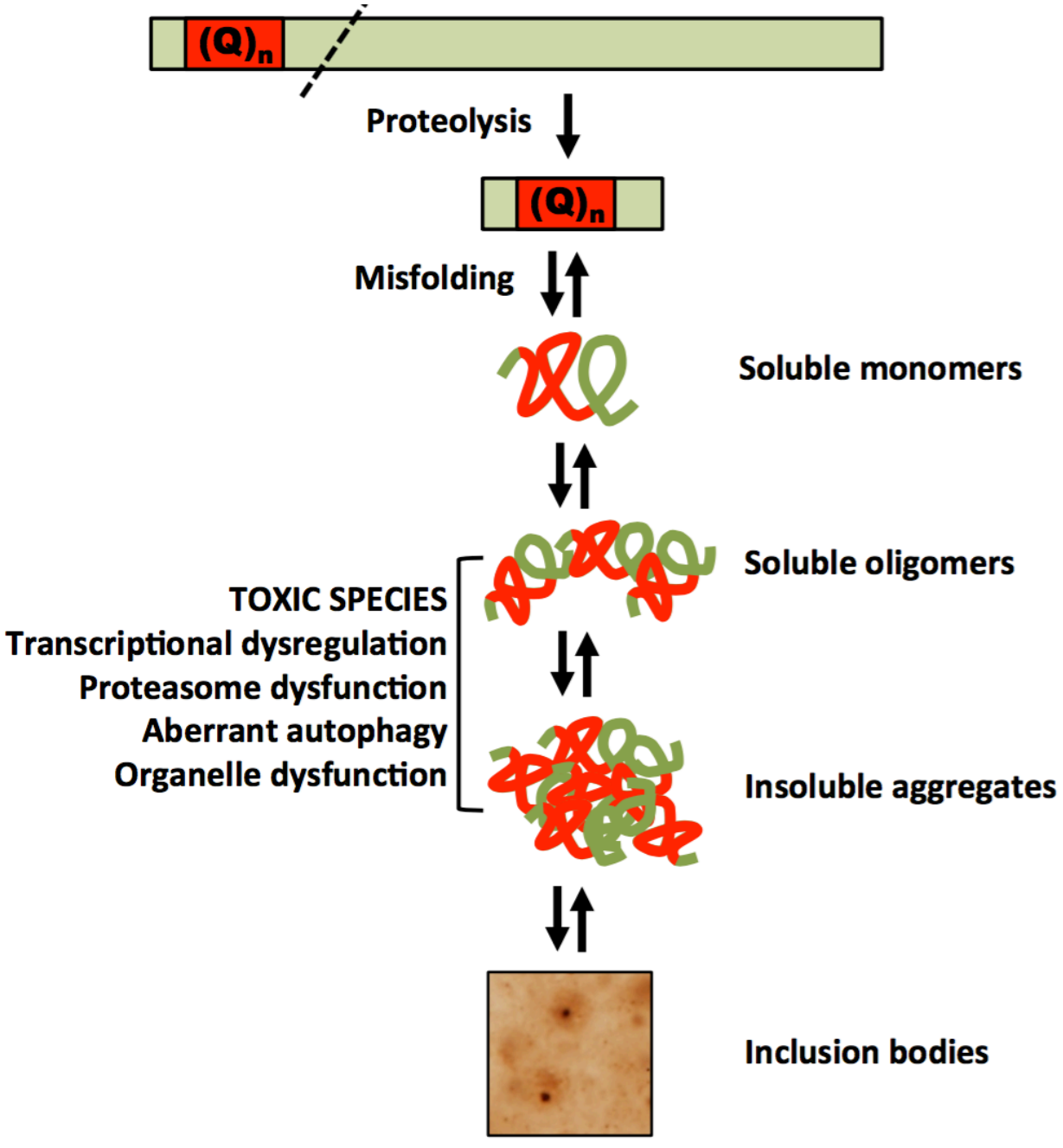

FIGURE 5. Post-translational modification of Htt N-terminus

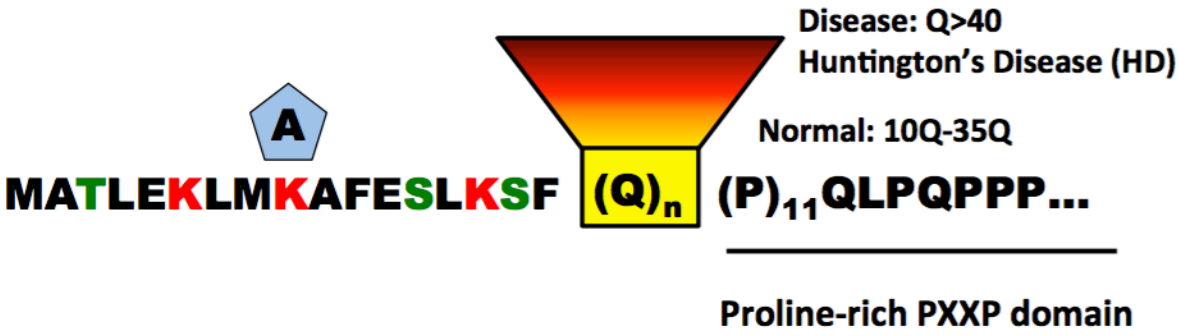

Acetylation site: K9
Phosphorylation sites: T3, S13 and S16
SUMOylation and ubiquitination sites: K6, K9 and K15

1.6 FIGURE LEGENDS

FIGURE 1. Process of ubiquitin conjugation

Ubiquitin (Ub) conjugation is initiated by activation of Ub via the Ub-activating enzyme, E1, which forms a high-energy thio-ester bond between C-terminal glycine of Ub and the active site thiol of E1; 2) the Ub-E1 complex then transfers the activated Ub to a Ub conjugating enzyme, E2; 3) Ubiquitin ligase (E3) then comes into play, transferring Ub from the E2 to a substrate via different mechanisms depending on the subtype of E3. Deubiquitinating enzymes (DUBs) act to cleave pre-formed Ub chains and recycle free Ubs and possibly edit the types of polyubiquitin chains added to substrates. Additional ubiquitin molecules can be added onto the first to create polyubiquitin chains on substrate proteins.

FIGURE 2. Different types of ubiquitin chains

In canonical ubiquitin pathways, ubiquitin is usually attached to the ε-amino group of lysine (K) residues in substrates. The transfer of a single ubiquitin to one (monoubiquitination) or multiple (multi-monoubiquitination) sites can inhibit interactions, change protein localizations, modulate protein activities or participate in DNA damage response. Ubiquitin itself contains seven lysine residues, which can function as acceptor sites for another ubiquitin moiety during ubiquitin chains formation. In addition, the amino terminus of a substrate-linked ubiquitin can serve as an acceptor for the formation of linear ubiquitin chains. Depending on the connection between linked ubiquitin molecules, ubiquitin chains can differ in structure and function. K48- and K11-linked ubiquitin chains

target proteins for degradation by the 26S proteasome. K63–linked chains usually mediate autophagy, DNA damage repair or signal transduction. M1-linked ubiquitin chains involve in NF-κB activation.

FIGURE 3. Ube2W's unique structure allows N-terminal ubiquitination
Ube2W (purple) has an unique binding pocket preceding the highly conserved C91 (yellow) which is present in all members of this E2 family. Within this pocket, Ube2W has a histidine (H83, cyan) in place of the conserved asparagine residue. Ube2W C-terminal residues N136-W145 form a highly disordered region positioned beneath the active site C91 and participate in substrate binding. These characteristic structural features allow Ube2W to function as an N-terminal ubiquitinating E2.

FIGURE 4. Htt aggregation and related molecular pathogenesis of HD
Full-length Htt usually undergo proteolytic cleavage that generates polyQ containing N-terminal fragment, which is highly misfolded. It exists as three distinct species in cells: soluble monomers, soluble oligomers and insoluble aggregates. Oligomeric and aggregating Htt are believed to be the toxic species in cells by inhibiting normal transcription, proteasome function, autophagy and normal organelle function.

FIGURE 5. Post-translational modification of Htt N-terminus

Several amino acids of N-terminal Htt are subjected to post-translational modifications. Each modification is colored on the schematics: acetylation as blue pentagon, phosphorylation as green, ubiquitination, and SUMOylation as red.

Chapter Two: Ube2W deficiency causes multi-system defects in mice

2.1 ABSTRACT

Ube2W ubiquitinates amino-termini of proteins rather than internal lysine residues, showing a preference for substrates with intrinsically disordered amino-termini. The in vivo functions of this intriguing E2, however, remain unknown. We generated *Ube2W* germline KO mice that proved to be susceptible to early postnatal lethality without obvious developmental abnormalities. While the basis of early death is uncertain, several organ systems manifest changes in *Ube2W* KO mice. Newborn *Ube2W* KO mice often show altered epidermal maturation with reduced expression of differentiation markers. Mirroring higher Ube2W expression levels in testis and thymus, *Ube2W* KO mice showed a disproportionate decrease in weight of these two organs (~50%), suggesting a functional role for Ube2W in the immune and male reproductive systems. Indeed, *Ube2W* KO mice displayed sustained neutrophilia accompanied by increased G-CSF signaling, and testicular vacuolation associated with decreased fertility. Proteomic analysis of a vulnerable organ, pre-symptomatic testis, showed a preferential accumulation of disordered proteins in the absence of Ube2W, consistent with the view that Ube2W preferentially targets disordered

polypeptides. These mice further allowed us to establish that Ube2W is ubiquitously expressed as a single isoform localized to the cytoplasm and that the absence of Ube2W does not alter cell viability in response to various stressors. Our results establish that Ube2W is an important, albeit not essential, protein for early postnatal survival and normal functioning of the multiple organ systems.

2.2 INTRODUCTION

Protein ubiquitination is critical to many cellular processes. The sequential action of ubiquitin-activating enzyme (E1), ubiquitin-conjugating enzyme (E2) and ubiquitin ligase (E3) results in isopeptide bond formation between the carboxyl-terminus of ubiquitin and an amino group on the substrate protein. Typically, this isopeptide linkage occurs through the ε-amino group of one or more lysine residues in the substrate (157), though linkage through non-lysine residues has also been described, including esterification on cysteine, serine and threonine residues as well as isopeptide bond formation with the α-amino group at the amino-terminus of substrates (46, 51–53, 59–62, 158).

Different ubiquitination events can specify distinct fates for substrate proteins. Well established examples include a role for mono-ubiquitination in altering the localization or activities of targeted proteins (159), the role of K48-linked poly-ubiquitin chains in targeting substrates for proteasomal degradation (32, 160), and the role of K63-linked Ub chains in recruiting binding partners that facilitate various cellular pathways including the stress response, DNA repair,

and intracellular trafficking (161). In contrast, the function of amino-terminal substrate ubiquitination is poorly understood. Thus far, this process has only been implicated in proteasomal degradation of a subset of proteins including a few naturally occurring, lysine-less proteins (NOLLPs): $p16^{INK4a}$, Puma and Human Papillomavirus Oncoprotein-58 E7 (60, 62, 158, 162).

Ube2W is the only E2 known to mediate amino-terminal ubiquitination (56, 67). It can function with various ubiquitin ligases including the C terminus of Hsc-70-interacting protein (CHIP) and the BRCA1/BARD1 complex (5, 25, 163) to mono-ubiquitinate select substrates at their amino-termini, with an apparent preference for substrates having intrinsically disordered amino-termini (68). In addition, mono-ubiquitination of FANCD2, which can be mediated by Ube2W(23), is critical for activation of the Fanconi Anemia (FA) tumor suppressor pathway in the DNA damage response (22, 159), but the role of Ube2W in DNA damage pathways is not well studied. Ube2W also forms noncovalent homodimers which are not essential to its ubiquitin transfer activity (164).

Despite growing knowledge of the biochemical properties of Ube2W, its in vivo functions remain elusive. Here we generated and characterized *Ube2W* KO mice to facilitate study of the physiological functions of this enzyme.

2.3 EXPERIMENTAL PROCEDURES

Animals-Three *Ube2W* gene-trap ES cell clones ($Ube2w^{tm1a(EUCOMM)Wtsi}$) were obtained from EuComm and used to generate *Ube2W* chimeras. Germline transmission of *Ube2W* gene trap was successfully obtained. *Ube2W* KO mice

were generated by intercrossing *Ube2W* heterozygous KO mice. All mice in this study were maintained on a pure C57BL/6 genetic background, housed in cages with a maximum number of five animals and maintained in a standard 12-hour light/dark cycle with food and water *ad libitum*. Genotyping was performed using DNA isolated from tail biopsy at the time of weaning. *Ube2W* KO genotype was determined by PCR amplification of a fragment of *Ube2W* gene. Mice were euthanized at specific ages, anesthetized with ketamine/xylazine, and perfused transcardially with phosphate-buffered saline.

PCR primers-For *Ube2W* KO genotyping:
5'AAAGGAAGAGCCCAGTATGGACCCT3' and
5'AGAGTCCCTGCAGCTATTAC3'.
Ube2W For: 5'ATGGTTTCATCATGGCGTCAATGCAG3';
1-Rev: 5'GATATGACCATTGCTATACACATGAGG3';
2-Rev: 5'TCAGGTGACCATAGAACTCACATG3';
3-Rev: 5'TCAACAAGTGTCATCATGATACCACCA3'.

Western blotting-Protein lysates from different organs were generated by lysis in radioimmunoprecipitation assay (RIPA) buffer containing protease inhibitors (Complete-mini; Roche Diagnostics, Indianapolis, IN), followed by sonication and centrifugation. The supernatants were collected, total protein concentration was determined using the BCA method (Pierce, Rockford, IL) and then stored at −80 °C. Forty microgram of total proteins per sample were resolved in 15% sodium dodecyl sulfate–polyacrylamide gel electrophoresis gels, and corresponding polyvinylidene difluoride membranes were incubated

overnight at 4 °C with primary antibodies: rabbit anti-Ube2W (1:1,000; 15920-1-AP; Protein Tech Group), mouse anti-GAPDH (1:10,000; MAB374; Millipore), rabbit anti-Histone H3 (1:10,000; #9715; Cell Signaling Technology), rabbit anti-$G_{\alpha\ i\text{-}2}$ (1:1,000; sc-4222; Santa Cruz Biotechnology), mouse anti-Hsp90 (1:1,000; Enzo Life Sciences) and goat anti-protamine-2 (1:250; sc-23104; Santa Cruz Biotechnology). Bound primary antibodies were visualized by incubation with a peroxidase-conjugated anti-mouse or anti-rabbit secondary antibody (1:10,000; Jackson Immuno Research Laboratories, West Grove, PA) followed by treatment with the ECL-plus reagent (Western Lighting; PerkinElmer, Waltham, MA) and exposure to autoradiography films.

Histological analysis-All tissues were fixed overnight at room temperature in 10% neutral buffered formalin, transferred to 70% EtOH, processed, and paraffin embedded. For immunohistochemical staining, tissue was sectioned at 5 µm, deparaffinized, and rehydrated prior to antigen retrieval in boiling citrate-based buffer (0.01 mol/L citric acid, pH 6.8). Endogenous peroxidases were quenched with 3% H_2O_2, followed by blocking in 5% goat serum and incubation with primary antibodies (Keratin 1 1:1000 , AF109, Covance, cat#PRB-165P; Keratin 5 1:2000, AF138, Covance cat# PRB-160P; Keratin 10 1:1000, Covance, cat# PRB-159P; loricrin 1:1000, Covance, cat# PRB-1459). Bound antibodies were detected with the Vector M.O.M. peroxidase (Vector Laboratories, Burlington, CA), using SigmaFast diaminobenzidene as a peroxidase substrate (Jackson ImmunoResearch, West Grove, PA)

Flow-cytometry-Cells were isolated from thymus, spleen, liver, and lymph nodes (axillary, brachial, and inguinal pooled) by passing through a 70 um nylon mesh filter into a 50ml conical tube. Blood was collected in EDTA-coated tubes, spun, and plasma was collected for multiplex analysis. Cells were resuspended in PBS and layered over lympholyte M to isolate viable lymphocytes. All cell preparations were ACK lysed and washed before analysis. For surface staining, cells were suspended in PBS with 2% FCS containing Fc Block (50 ng/ml) prior to incubation with fluorochrome-conjugated Abs (anti–mouse Ly-6C, AL21, BD; anti–mouse Ly-6G, 1A8, BD; anti–mouse CD11b, M1/70, eBioscience; anti–mouse CD11c, N418, eBioscience; anti–mouse CD4, RM-45, eBioscience; anti–mouse CD45, 30-F11, eBioscience; anti–mouse CD19, MB19-1, eBioscience; anti–mouse CD8, 3-6.7, eBioscience and anti–mouse MHCII (I-A/I-E), M5/114.15.2, eBioscience. The stained cells were analyzed with a FACSCanto II flow cytometer using FACSDiva software (v6.1.3, Becton Dickinson). Data were analyzed using FlowJo software (v9.3.2, TreeStar).

Bead-based multiplex analysis-Plasma levels of G-CSF and GM-CSF were measured with customized multiplex magnetic bead based arrays (EMD Millipore) according to the manufacturer's protocol. Data were collected using the Bio-Plex 200 system (Bio-Rad Laboratories). Standards were run in parallel to allow quantification of individual factors. The data shown indicates levels that fell within the linear portion of the corresponding standard curve.

Differential proteome analysis using tandem mass tag (TMT) labeling and mass spectrometry-Protein lysates from 4-week-old mice testis were generated

by lysis in RIPA buffer containing protease inhibitors (Complete-mini; Roche Diagnostics, Indianapolis, IN), followed by sonication and centrifugation. The supernatants were collected and total protein concentration was determined using the BCA method (Pierce, Rockford, IL). Enzymatic digestion with trypsin and TMT labeling was performed essentially according to the manufacturer's protocol (Thermo Scientific). 100 mg of peptide from each sample was labeled with TMT labeling reagents. The peptides from 3 wild type samples were labeled with TMT reagent channels 126, 127 and 128. Peptides from 3 KO samples were labeled with TMT reagent channels 129,130 and 131. Further processing of these samples using 2D-LC was done as described below.

Peptides were reconstituted in strong cation exchange (SCX) buffer A (5 mM KH_2PO_4, pH 3, 5% acetonitrile) and separated on a Polysulfoethyl A column (1 x 150 mm, 5 mm particle size, Thermo Scientific) using Dionex Ultimate 3000 RSLC nano system at a flow rate of 50 ml/min. Elution buffer B consisted of buffer A with 1 M NaCl. A linear gradient of 35% buffer B over a period of 45 min followed by a 5 min wash with 100% Buffer B and re-equilibration with buffer A for 20 min was used. Approximately 50 ug of peptides were separated per injection. An on-line 214 nm UV detector guided the collection and pooling of fractions.

The SCX fractions with 214 nm absorbance were desalted using in-line m-Precolumn (5 mm x 300 mm inner diameter, C18 PepMap100, 5 mm, Thermo Scientific) and loaded directly onto a nano-RP column (Acclaim PepMap RSLC, 15 cm x 75 mm inner diameter, 2 mm C18 media). Peptides were separated

using acetonitrile/0.1% formic acid gradient system (2-30% acetonitrile over 50 min followed by 95% acetonitrile wash for 5 min) at a flow rate of 300 nl/min on a Dionex Ultimate 3000 RSLC nano system. Eluted peptides were directly introduced into Orbitrap Fusion Tribrid ETD mass spectrometer (Thermo Fisher Scientific) equipped with nano-flex source. The mass spectrometer was set to collect a survey spectrum in the Orbitrap with a resolution of 60,000 followed by data-dependent HCD spectra on most abundant ions for the next 3 seconds. For HCD, normalized collision energy was set to 35, maximum inject time was 120 ms, maximum ion counts were set to 1e5 and product ions were analyzed in Orbitrap cell (resolution 15,000).

Protein identification and quantification was performed using Proteome Discoverer 1.4 (Thermo Fisher Scientific). The data was searched against a mouse protein database, a subset of UniProtKB (51629 entries), by considering trypsin enzyme specificity, and a maximum of 2 missed cleavages. Precursor and product ion tolerance were set to 20 ppm and 0.02 Da respectively. Carbamidomethylation of cysteines and TMT labeling of lysines and peptide N-termini are considered as fixed modifications. Allowed variable modifications included oxidation of methionine and deamidation of asparagine and glutamine residues. Percolator algorithm was used for discriminating between correct and incorrect spectrum identification. The false discovery rate (FDR) was calculated at the peptide level and peptides with <1% FDR were retained. The quantification was performed using the reporter ion intensities which were extracted using Proteome Discoverer.

Protein disorder analysis-Disorder was examined using the IUPred long (Dosztanyi et al., 2005; Dosztanyi et al., 2005) and DisEMBL (Linding et al., 2003) disorder prediction algorithms. Primary sequences for all proteins included in our disorder analysis were obtained from UniProt (The UniProt Consortium, 2015). Specifically, 3,905 protein sequences were obtained from the *Mus musculus* reference proteome file (Proteome ID: UP000000589, accessed on 4/28/2015), while 598 isoform sequences were retrieved from the UniProt isoform file (accessed on 5/23/2015). Of the total population of 4,503 proteins, those with completely defined primary sequences were included in our disorder assessment, while 76 proteins with ambiguous and/or undetermined amino acid residues were excluded. Within the remaining 4,427 proteins, protein length varied from 35 amino acids (Transcription elongation factor A N-terminal and central domain-containing protein; UniProt accession: A2AFP8) to 33,467 amino acids (Titin; UniProt accession: E9Q8K5). Following the collection of disorder scores, a binary classification of "disordered" or "ordered" was assigned to each residue using algorithm-specific threshold values of disorder. To characterize disorder we chose to examine the percentage of disordered amino acid residues as well as continuous length disorder (CLD) both in N-terminal regions and in full-length sequences. Regions with CLD were defined as any sequence of two or more consecutive amino acids with individual disorder scores above the algorithm-specific threshold value. The two-sided Kolmogorov-Smirnov test was used to compare the percent disorder distribution in the target and reference populations; p-values less than 0.05 were deemed significant.

Primary and secondary cell culture-Tail skin biopsies (3 to 5 mm) were obtained and cultured as follows: Skin samples were washed with PBS and ethanol, then diced, and digested overnight in collagenase type II (400 U/ml; 1,600 U total per tail; Gibco-Invitrogen, Carlsbad, CA) dissolved in Dulbecco's modified Eagle's medium (DMEM) supplemented with 10% heat-inactivated fetal bovine serum (HyClone, Logan, Utah), antibiotics, and fungizone (complete medium). Incubation was at 37°C with 10% CO_2. After overnight collagenase treatment, cells were separated from remaining tissue by filtering through a 45-micron mesh, centrifuged, and resuspended in complete medium. Approximately 2.5×10^5 cells in 5 ml of medium were seeded into tissue culture flasks of 25-cm^2 surface area, and this was called passage 0. A complete media change was made after 3-4 days. 7 days after cell isolation the cultures were trypsinized (using 0.05% trypsin) and placed into 75-cm^2 flasks ($0.6x10^6$ cells) or 175-cm^2 flasks (1.2×10^6 cells). Each culture was passaged at a 7-day interval, with complete media changes being made on day 4 between passages. Cells used in the assays described were confluently plated at ~10^5 cells/well in the third passage.

Stress assays-Stress assays were performed as previously described (165) with slight modifications. Briefly, cells were plated confluently (10,000 cells/well) into 96-well plates, allowed to adhere overnight. For the glucose deprivation assay cells were washed with PBS and then media containing differing amounts of glucose was added with the cells incubated for 6 hours. Survival was measured at the 6-hour point. Cells in the other assays were

washed with PBS and given media consisting of DMEM with only BSA added for 24 hours. Cells were dosed with stressor for 6 h, after which cells were washed with PBS and returned to the DMEM media containing only BSA as a supplement. Survival was measured the following day by WST-1 (Roche) reduction. Stressors used in study: Thapsigargin and Tunicamycin are both from Calbiochem (EMD Chemicals, San Diego, CA); Cadmium Chloride is from Fluka (Sigma/Aldrich); MMS is from Aldrich (Sigma/Aldrich, St Louis, MO); Hydrogen peroxide, glucose and ammonium chloride are from Sigma (St Louis, MO)

2.4 RESULTS

Production of *Ube2W* KO mice

To produce *Ube2W* KO mice, we acquired three EuComm ES cell lines bearing the targeting vector (Fig 6A-i) [EPD0156-4- C08, -C07, and -G06], two of which (C07 and C08) contained euploid chromosome counts. Blastocysts from C07 and C08 were injected into pseudopregnant females to produce chimeric mice. Upon breeding of chimeric mice, black progeny were selected for genotyping to confirm germ line transmission (data not shown). To generate "Floxed" *Ube2W* mice with the potential to engineer conditional knockout mice, we crossed mice with Flp recombinase-expressing mice to delete the lacZ and Neo cassette (Fig 6A-ii). Further crosses to Cre recombinase-expressing mice resulted in deletion of exon 3 of *Ube2W*, a critical 103bp exon whose absence leads to a frame shift causing premature termination of the protein and loss of

functional Ube2W expression (Fig 6A-iii). *Ube2W* heterozygous KO mice were then bred to produce progeny of all three genotypes (Fig 6B).

Ube2W is a widely expressed, predominantly cytoplasmic protein

Little is known about the expression of Ube2W and its subcellular localization. The availability of *Ube2W* KO mice allowed us to analyze Ube2W expression in vivo. Lysates from different tissues were immunoblotted with a polyclonal anti-Ube2W antibody. A single, major immunoreactive protein of approximately 16 kDa was detected in every WT tissue examined but was absent in KO mice (Fig 6C). Among tissues examined, the testes, pancreas and thymus displayed the highest Ube2W expression, while the heart and liver showed the lowest Ube2W expression.

The cross-reactivity of existing anti-Ube2W antibodies to other proteins limits their utility in immunofluorescence studies to assess subcellular localization of Ube2W. Instead, we used cell fractionation to define its intracellular residence. Cell extracts obtained from mouse embryonic fibroblasts (MEFs) were fractionated into membrane, cytosol and nuclear fractions by differential centrifugation (see EXPERIMENTAL PROCEDURES). Ube2W partitioned in the cytosolic fraction, showing little expression in membrane and nuclear fractions (Fig 6D). Similar results were obtained for extracts derived from mouse brain lysates (data not shown). In addition, human myc-tagged Ube2W equivalent to the mouse protein was transiently expressed in transfected HEK293 cells to

visualize subcellular localization. Human Ube2W also showed a diffuse cytoplasmic pattern with little staining in the nucleus (Fig 6E).

Isoform 1 is the major expressed Ube2W isoform in mouse

As shown in Figure 2, three potential protein isoforms of *Ube2W* are predicted in mouse: Isoforms 1 and 3 each contain six coding exons while isoform 2 has seven coding exons, two of which are unique to isoform 2. All three isoforms share exons 1-3 (Fig 7A, yellow) and exon 5. Isoforms 2 and 3 contain a shortened exon 4 that lacks the first 79bp of exon 4, resulting in a frame shift that alters the carboxyl-terminal half of the predicted protein (Fig 7A, green). Isoform 2 also skips exon 6 and uniquely contains exons 7 and 8 that would encode a different protein segment (Fig 7A, red). In isoform 3, the stop codon in exon 6 occurs further downstream because of the frame-shift in exon 4.

To elucidate which isoforms are expressed in vivo, first strand cDNA was generated from WT and *Ube2W* KO MEFs, the latter to ensure the specificity of PCR amplification. Specific primer pairs were used to amplify and identify the three predicted *Ube2W* isoforms. The forward primer, identical for all three isoforms, binds exon 1. Reverse primer 1 (Rev-1) binds the extended exon 4 present only in isoform 1, resulting in PCR amplification of an isoform 1 product differing in size in WT versus KO cells. PCR products of the expected size for isoform 1 were observed (Fig 7B) and confirmed by sequencing. Reverse primer 2 (Rev-2) binds to exon 8 and thus can only amplify isoform 2, generating different size products for WT and KO cells. No PCR products corresponding to

isoform 2 were observed (Fig 7B). Due to the similarity between isoforms 1 and 3, there is no specific primer pair for isoform 3. Isoforms 1 and 3 can be distinguished, however, by the longer PCR product for isoform 1 reflecting its extended exon 4. Predicted isoform 3 was not detected in WT or KO cells (Fig 7B).

These results indicate that, at least in MEFs, isoform 1 is the predominant if not only expressed form of Ube2W. Because Ube2W protein runs as the same size protein in all tissues examined, we suspect that isoform 1 is the major expressed isoform in most if not all tissues.

Methionine 30 is the transcriptional start site for Ube2W

The *Ube2W* murine transcript contains two possible start codons, each with predicted Kozak sequences. Either or both could be used as the initiating site for translation. The predicted encoded proteins, termed here Met1 and Met30, have expected molecular weights of 20.7 kDa and 17.3 kDa, respectively. To determine which start site initiates translation of the single Ube2W protein species detected in mouse, we cloned the two predicted forms of Ube2W isoform 1 into pcDNA3.1 from WT MEFs, and expressed them in transfected HEK293 cells. Lysates from cells overexpressing Met1 or Met30 were analyzed on anti-Ube2W immunoblots, run adjacent to lysates from WT, heterozygous and homozygous *Ube2W* KO MEFs for size comparison. (Transiently expressed Ube2W is highly overexpressed in these cells, and the low level of endogenous human Ube2W in HEK293 cells is not detectable in this short exposure.) Ube2W

in MEFs electrophoresed identically to overexpressed Met30 at an apparent molecular weight of ~16 kDa, the same size as Ube2W in various mouse tissues shown earlier (Fig 6C). No Ube2W species existed corresponding to Met1 (Fig 7C). While these data indicate that both start sites can be used to generate Ube2W protein, the downstream start site appears to be the preferred initiation site in normal murine tissues and MEFs.

Ube2W KO mice are susceptible to postnatal lethality and growth retardation

Ube2W heterozygous mice (HET) were crossed to obtain *Ube2W* KO mice. Although *Ube2W* KO mice appear to undergo normal prenatal development, they are susceptible to death near or soon after birth. Whereas only 1 of 13 (7.7%) WT and 3 of 38 (7.9%) HET pups died at postnatal day 0 (P0), 6 of 18 (33.3%) KO pups died at P0. *Ube2W* KO mice showed continued lethality until postnatal day 2 (P2): 0 of 39 (0%) WT pups, 1 of 38 (2.6%) HET pups and 4 of 18 (22.2%) KO pups died on postnatal days 1 or 2. After P2, *Ube2W* KO mice displayed no further increased lethality: 1 of 13 (7.7%) WT pups, 1 of 38 (2.6%) HET pups and 1/18 (5.5%) KO pups died between P2 and 16 weeks of age. To assess when susceptibility to early lethality first appears in KO mice, embryonic day 18.5 (E18.5) embryos were extracted and examined: 0 of 9 (0%) WT embryos, 1 of 16 (6.2%) HET embryos and 1 of 10 (10%) KO embryos were nonviable, indicated by the absence of a heart beat (Fig 8A and B). In total, 55.6%

of *Ube2W* KO mice died before P2, revealing an important role for *Ube2W* in early postnatal survival.

Histopathologic examination of major organs did not detect any significant morphologic differences in KO embryos/pups at E16.5, E18.5 and P0 at the microscopic level (Fig 8C). Furthermore, whole-mount *Ube2W* KO mice showed no evidence of increased apoptosis, measured by terminal deoxynucleotidyl transferase dUTP nick end labeling (TUNEL) staining at E16.5, E18.5 and P0 (data not shown).

Two reported Ube2W substrates are the neurodegenerative disease proteins Ataxin-3 and Tau (25, 56), suggesting a potentially important role for Ube2W in brain. To eliminate Ube2W expression selectively in the Central Nervous System (CNS), we crossed *Ube2W* Flox/Flox mice with Nestin promoter-driven, Cre recombinase-expressing mice. Analysis of these mice showed that *Ube2W* expression was eliminated in the brain and spinal cord but persisted in other organs. *Ube2W* Nestin-KO mice did not show postnatal lethality, and were recovered at the expected Mendelian ratios (19 of 35 genotyped mice were KO, in line with the breeding strategy prediction of 50%). Thus, the postnatal lethality of *Ube2W* KO mice is not due to overt brain dysfunction.

While the organismal morphology of *Ube2W* KO mice appears normal at birth, *Ube2W* KO pups weighed significantly less than WT and HET littermates overtime. This decreased body weight was maintained throughout postnatal development in male and female mice. Adult *Ube2W* KO mice remained

approximately 20% smaller than WT mice (Fig 8E and F). Most organs showed a proportionate decrease in size, commensurate with the overall reduced body size. The testis and thymus (Fig 8D), however, showed a disproportionate weight decrease of approximately 50%, indicating a potential important function for Ube2W in these organs.

Ube2W deficient mice display altered epidermal differentiation

One possible cause of early postnatal lethality is a defect in the protective barrier provided by skin. Indeed, histological analysis of P0 pups revealed striking alterations in the epidermis of *Ube2W* KO mice, except in the scalp. Normal epidermis contains 4 cellular compartments, which include a single layer of undifferentiated basal cells that give rise to several layers each of spinous cells, granular cells, and anucleate cornified cells (Fig 9A). The most severe phenotype was observed in dorsal skin: KO mice showed a loss of granules normally found in the granular cell layer and more distinct cell borders compared to WT epidermis (Fig 9A). Further, immunostaining revealed a reduction and altered distribution of loricrin, a granular cell marker that is incorporated into terminally differentiated, cornified cell envelopes in the cornified cell layer. Compared to its cytoplasmic distribution pattern in the stratum granulosum of WT skin, loricrin in KO skin is localized to the periphery of epidermal cells in the upper epidermis (Fig 9B). Cells expressing Keratin 1 (K1) and Keratin 10 (K10) normally exist in the stratum granulosum and spinosum, but were detected only in the lower suprabasal cell layer in KO mice (Fig 9C). In contrast,

immunostaining for the basal cell marker K5 was similar in KO and WT mice (Fig 9D). This abnormal skin phenotype was observed in 4 out of 6 P0 KO mice analyzed. Collectively, these data establish that the loss of Ube2W can result in severely altered epidermal differentiation.

Ube2W KO mice display neutrophilia and increased G-CSF recruitment

Due to high Ube2W expression in the thymus and a disproportionate decrease in thymus weight in *Ube2W* KO mice, we sought to determine whether Ube2W regulates development of the immune system. Immune cells were extracted from major immune organs including thymus, spleen, liver, lymph nodes (axillary, brachial, and inguinal pooled) and blood, and analyzed by flow cytometry according to quantification of cell types using established cell surface markers. $CD45^+$, $CD11b^+$, $CD11C^-$, $Ly6C^+$, $Ly6G^+$, neutrophils comprised 5.55% ± 1.95% of total cells of the blood in *Ube2W* KO mice, which was significantly compared to that of WT mice (0.68% ±0.09%) (Fig 10A-C). In 6 of 10 KO mice tested, neutrophils were also more abundant in lymph nodes. Other immune cell types including $CD4^+$ T cells, $CD8^+$ T cells, B cells, monocytes and dendritic cells were not significantly altered in blood or other immune organs of *Ube2W* KO mice (data not shown).

The increased numbers of neutrophils in blood of *Ube2W* KO mice led us to hypothesize greater chemokine-driven mobilization from bone marrow. Indeed, *Ube2W* KO mice showed a significant increase in serum G-CSF levels but lower serum GM-CSF levels, suggesting the increase in G-CSF in *Ube2W* KO mice

results in aberrant neutrophil recruitment from the bone marrow (Fig 10D and E). To quantify neutrophil trafficking in WT and *Ube2W* KO mice, peritonitis was induced by intraperitoneal injection of thioglycollate. After 4 hours, neutrophils were recovered by peritoneal lavage and analyzed by flow-cytometry. While there was no statistically significant difference in total neutrophils recruited, there was a trend toward an increased population of immature neutrophils in peritoneal lavage, identified by lower Ly6C expression ($p=0.09$), suggesting a premature exit of these cells from the bone marrow in *Ube2W* KO mice (Figure 10F).

Ube2W KO male show decreased fertility accompanied by testicular vacuolation

Because Ube2W is expressed robustly in the testis and testis weight is disproportionately decreased in *Ube2W* KO mice, we suspected an important function for Ube2W in testis. Consistent with this hypothesis, in breeding pairs of *Ube2W* KO males and WT females, nearly half of *Ube2W* KO males failed to generate litters, suggesting infertility. To assess possible changes in testicular cellular integrity and spermatogenesis, we performed histochemical analyses of testes and epididymides from 16-week-old WT and *Ube2W* KO mice.

Whereas testes from WT mice were histologically normal (Figure 11A), showing cells corresponding to each phase of germ cell maturation from spermatogonia to spermatozoa, testes of KO mice displayed variable degeneration and atrophy of seminiferous tubules, ranging from mild and focal vacuolation of the basal layer of spermatogonia (Figure 11B) to marked decrease

in tubule diameter with diffuse tubular atrophy, vacuolation, and the absence of spermatocytes and spermatids (Figure 11C). Compared to WT epididymides that typically showed abundant mature spermatozoa (Figure 11D), KO epididymides showed variable sperm levels ranging from a normal amount of mature spermatozoa corresponding to a mildly vacuolated testis (Figure 6E) to a complete absence of mature spermatozoa corresponding to a severely vacuolated testis (Figure 11F). The epithelium and interstitial Leydig cells of *Ube2W* KO mice appeared normal. Ovaries from 16-week-old female *Ube2W* KO and WT mice showed no overt difference in size and structure (data not shown).

Ube2W KO mice testes show accumulation of disordered proteins

Because of the potential importance of Ube2W in the male reproductive system, we analyzed and compared protein expression profiles in pre-symptomatic 4-week-old WT versus *Ube2W* KO testis, using TMT-labeled LC-MS/MS to compare expression profiles. At 4 weeks, mice testes are structurally and functionally mature but have not yet developed the distinct vacuolation pathology of *Ube2W* KO mice. We analyzed three technical replicates each from WT and *Ube2W* KO testis. Among 4,544 proteins identified in testis with at least two peptide spectrum matches (PSMs), 135 proteins showed more than a 1.5-fold increase in *Ube2W* KO testis. This group, which represents potential Ube2W substrates, comprised the target group for subsequent bioinformatics analysis. Bioinformatic analysis of protein disorder was based on the percent of disordered amino acids in each protein (percent disorder) identified by IUPred (166).

Compared to the reference group (4,309 identified proteins excluding the target group), the target group of enriched proteins shows a significantly skewed distribution of disorder ($p=0.02$ by Kolmogorov-Smirnov test), with higher disorder percentages being more prevalent in the target group (Fig 12A). A similar, negative-skewed distribution of protein disorder is observed when using DisEMBL prediction of COILS (Fig 12B) (167), further suggesting an accumulation of relatively disordered proteins in *Ube2W* KO testis. These results are consistent with the *in vitro* evidence that Ube2W preferentially ubiquitinates disordered substrates (68). This preference of Ube2W, however, is believed to be most critical for disorder at the N-terminus. Accordingly, we also analyzed the prevalence of continuous length disorder (CLD) in the target group, which can provide more detail regarding the organization of disorder than percent disorder. Using a CLD stretch of disordered amino acids of at least 30 aa as the threshold (168, 169), we examined the existence of IUPred-based CLD in both full length proteins (100% amino acids) and the N-terminus of proteins (first 2.5%, 5% and 10% amino acids). Consistently, the target group showed a greater percentage of proteins with a CLD in the N-terminus (Fig 12C). This feature is also more prevalent in the target group of proteins, when using the DisEMBL prediction of COILS (Fig 12D).

Among proteins in the target group, protamine-2 is an attractive candidate because its levels were increased nearly four-fold in *Ube2W* KO testis via proteomic analysis and because it has highly disordered characteristics,

predicted by both IUPred and DisEMBL. Indeed, by Western blot protamine-2 is significantly elevated in 4 week-old testis from *Ube2W* KO mice (Fig 12E and F).

Ube2W deficiency does not alter cell tolerability to DNA interstrand crosslinking

DNA damage repair pathways are critical to testicular function. Because FANCD2 can be monoubiquitinated by Ube2W in vitro and monoubiquitinated FANCD2 is a critical component of the Fanconi Anemia (FA) pathway regulating DNA repair after interstrand crosslinking, we investigated the susceptibility of *Ube2W* KO MEFs to DNA interstrand crosslinking. When DNA crosslinking was introduced by Mitomycin C (MMC) treatment for 24hrs, Ube2W KO MEFs failed to show a significant increase in MMC-induced toxicity (Figure 13A). Earlier (Fig 6) we showed that Ube2W is a cytoplasmic protein in MEFs, suggesting that Ube2W would not be available to mono-ubiquitinate FANCD2 in the nucleus. Accordingly, we tested whether Ube2W translocates to the nucleus in response to DNA damage. After MMC or UV treatment, Ube2W remained in the cytoplasm without translocation to the nucleus (Figure 13B). Despite Ube2W's capacity to mono-ubiquitinate FANCD2 in vitro, its ability to do so in vivo remains uncertain.

Loss of Ube2W does not impair the cellular response to various cytotoxic stressors

Increased early postnatal stress of various types, including oxidative and endoplasmic reticulum (ER) stress, contributes to diseases of the newborn (170–

172). Because ubiquitin signaling has been implicated in the cellular response to such stresses, we sought to determine whether the loss of *Ube2W* renders cells prone to various cell stressors. Skin-derived fibroblasts harvested from *Ube2W* KO and control heterozygous mouse tails were treated with stressors targeting various cellular pathways: tunicamycin and thapsigargin (ER stress), H_2O_2 (ROS stress), MMS (DNA damage stress), cadmium (heavy metal stress), glucose deprivation (nutrient stress), and NH_4Cl (autophagy stress). A median lethal dose (LD50) was measured for each stressor and the value compared between *Ube2W* KO and control cells. *Ube2W* KO fibroblasts did not show altered susceptibility to any stressor tested. We conclude that, at least in fibroblasts, *Ube2W* is not essential to the cellular response to common cellular stressors (Figure 14).

2.5 DISCUSSION

Protein ubiquitination is critically important to diverse aspects of many different cellular pathways. The enzyme cascade mediating ubiquitination achieves the necessary rich diversity of substrate ubiquitination through pairing a limited pool of E2s (38 in humans) with a wide range of E3s (estimated at more than 1000 in humans) (173). Each E2 engages multiple E3 partners to carry out diverse substrate-specific ubiquitination events, thus the loss of any given E2 can have profound deleterious effects on an organism. In mice, for example, deletion of Ube2I, Ube2L3, Ube2N or BIRC6 results in lethality in utero (174–178); while deletion of Ube2A, Ube2B or Ube2D2a causes infertility (179, 180). Our results in

Ube2W KO mice establish that Ube2W, an atypical E2 implicated in N-terminal ubiquitination, contributes to vital ubiquitin pathways involving multiple organ systems.

Ube2W is the only known mammalian E2 that ubiquitinates substrates on their N-termini rather than on internal lysine residues (56, 67). Ube2W may preferentially target substrates with intrinsically unfolded amino-termini (68), but its expression and function in vivo are poorly understood. Our data reveal widespread Ube2W expression in the mouse, particularly of Ube2W isoform 1, with protein translation beginning at the second predicted Kozak sequence. Compared to the predicted Ube2W protein initiated from the first Kozak sequence, this smaller Ube2W species lacks 29 amino acids that include a predicted nuclear-localization signal. Thus, it is perhaps not surprising that the major expressed isoform of Ube2W is a cytoplasmic protein in mouse embryonic fibroblasts and in transfected cells (Fig 6D). When mouse tissue lysates are separated by SDS-PAGE, Ube2W exists as a single species of approximately 16 kDa, suggesting conservation of isoform expression across different tissues.

In contrast to the early embryonic lethality of several other E2s, the early postnatal lethality of *Ube2W* KO mice is not fully penetrant: 60% of *Ube2W* KO mice died between E18.5 and P2 in the C57Bl/6 background. The susceptibility to early lethality indicates an important, but not essential, early postnatal function for Ube2W. The incomplete penetrance of this phenotype could reflect compensatory up-regulation of other E2s or E3s serving similar functions. We have measured levels of known Ube2W-interacting E3 ligases, including CHIP,

BRCA1 and FANCD2 in MEFs, none of which is altered in *Ube2W* KO cells (data not shown). Conceivably other as yet unknown E2/E3 pairs compensate for Ube2W deficiency, or ubiquitination of the amino-termini of specific substrates may be redundant with additional posttranslational signaling events. Our data further suggest that the loss of *Ube2W* does not cause a dramatic change in stress-induced cell effects, implying that other effects beyond basic cellular stress pathways are involved in this early postnatal lethality.

The altered epidermal differentiation pattern observed in P0 KO mice suggests delayed or impaired maturation of stratum granulosum and spinosum. The sequential differentiation of epidermis is essential for post-natal survival. The loss of keratohyalin granules and altered Loricrin immunostaining in *Ube2W* KO P0 mice suggest a defect in barrier function, which can result in early postnatal lethality due to excessive water loss (reviewed in 37, 38). In *Ube2W* KO mice, the 60% postnatal lethality we observe is a similar percentage to that of the altered skin phenotype, suggesting a potential link between the epidermal differentiation defect and early postnatal lethality. Further studies are needed to establish whether *Ube2W* KO mice are susceptible to dehydration concomitant with these observed skin abnormalities. Further analysis of the pathogenesis of skin defects in *Ube2W* KO mice also may shed light on specific ubiquitin-dependent pathways critical to normal epidermal differentiation.

The neutrophilia observed in *Ube2W* KO mice could result from different scenarios. We favor the view that sustained neutrophilia in adult *Ube2W* KO mice is secondary to increased expression of neutrophil-mobilizing cytokines since G-

CSF levels were higher in the serum of *Ube2W* KO mice. Increased G-CSF together with neutrophilia can be observed in systemic bacterial infections, but the fact that this phenotype was consistently observed at different stages of development in mice kept in pathogen-free conditions argues against this possible explanation. Moreover, recruitment of neutrophils is intact in *Ube2W* KO mice, arguing against an intrinsic neutrophil defect and further supporting the view that neutrophilia is a secondary event reflecting increased serum G-CSF. G-CSF is primarily degraded by neutrophil elastases, but there is no published literature suggesting ubiquitin-associated degradation of G-CSF. G-CSF synthesis occurs in different cell populations, including monocytes, endothelium and keratinocytes, so perhaps Ube2W plays a regulatory role in G-CSF secreting cells to govern circulating blood neutrophils. The decreased GM-CSF level in *Ube2W* KO mice is probably secondary to neutrophilia, as the increased number of circulating neutrophils in *Ube2W* KO mice likely would capture more GM-CSF through their GM-CSF receptors, resulting in the decreased levels seen in *Ube2W* KO mice.

A key question regarding Ube2W is: what are its natural target substrates? The testis, which appears vulnerable to the loss of Ube2W based on the observed vacuolation in seminiferous tubules and high rate of male infertility, provided us an opportunity to begin addressing this question. Specifically, we examined changes in the testis proteome in the absence of Ube2W. In *Ube2W* KO testis, bioinformatic analysis revealed an accumulation of proteins with increased disorder, consistent with the recent view that Ube2W may

preferentially target substrates with disordered N-termini (68). The extreme N-termini (approximately the first five amino acids) may be the key determinant for substrate recognition by Ube2W (21), but most proteins in the mouse proteome (70-80%) are predicted to show disorder in the first five amino acids, based on DisEMBL analysis (with COILS, Hotloops and REM465). Accordingly, we were unable to discern differences linked to the extreme N-termini. By expanding our analysis of N-termini to first 2.5%, 5% and 10% of proteins, however, we noted that proteins enriched in *Ube2W* KO testis are more likely to contain stretches of disordered amino acids. This preferential accumulation of disordered proteins in *Ube2W* KO testis is consistent with the view that Ube2W preferentially ubiquitinates disordered substrates and that such ubiquitination serves as a degradation signal. More work is required, however, to establish that Ube2W-mediated ubiquitination favors disordered proteins and regulates their steady state levels. The testicular proteome offers numerous candidate proteins for such future analysis, including protamine-2, an intrinsically disordered testicular protein that we confirmed was increased in the absence of Ube2W.

Ubiquitin pathways are known to be important to the maintenance of testicular structure and function. Knockout models of many E3 ligases including RNF8 have shown similar testicular vacuolation defects and infertility(183–185). Moreover, DNA damage pathways are implicated in spermatogenesis: RNF8, FANCD2 and BRCA1 all participate in DNA damage pathways and can interact with Ube2W in vitro. Ube2W deficient fibroblasts, however, failed to show a significant difference in the cellular response to a form of DNA damage:

mitomycin C induced DNA crosslinking. This result is consistent with a recent study in which Ube2W was shown to efficiently mono-ubiquitinate FANCD2 yet a Ube2W-deficient chicken cell line did not show increased sensitivity to mitomycin C-induced lethality (22). Although Ube2W is capable of ubiquitinating FANCD2, it may be functionally redundant in the cellular response to DNA damage response. Moreover, when cells were stressed with mitomycin C, Ube2W failed to be recruited into the nucleus, making it physically difficult for Ube2W to participate directly in DNA damage repair. Taken together, these results lead us to believe that testicular vacuolation in *Ube2W* KO mice is not likely to be due to a defective DNA damage response.

In summary, utilizing a novel *Ube2W* KO mouse model we have established that Ube2W is a widely expressed, predominantly cytoplasmic E2 that plays an important, nonessential role in several divergent organ systems. Our data indicate that Ube2W functions as a significant factor in mouse postnatal survival as well as in skin differentiation, G-CSF related immune response and male fertility. We stress that we closely examined only these three divergent organ systems based on clues provided by the *Ube2W* KO mice. Accordingly, we have not ruled out Ube2W's involvement in other organ systems. Moreover, all studies were performed on a pure C57Bl/6 genetic background and led to incompletely penetrant phenotypes. Further analysis of Ube2W deficiency in different inbred murine strains could exacerbate or lessen these phenotypes, and thereby provide additional genetic clues to the in vivo role of Ube2W. Finally, the

availability of *Ube2W* KO mice should facilitate the identification of key physiological substrates for this unusual E2 in affected tissues.

FIGURE 6. Generation of *Ube2W* KO mouse and expression of Ube2W

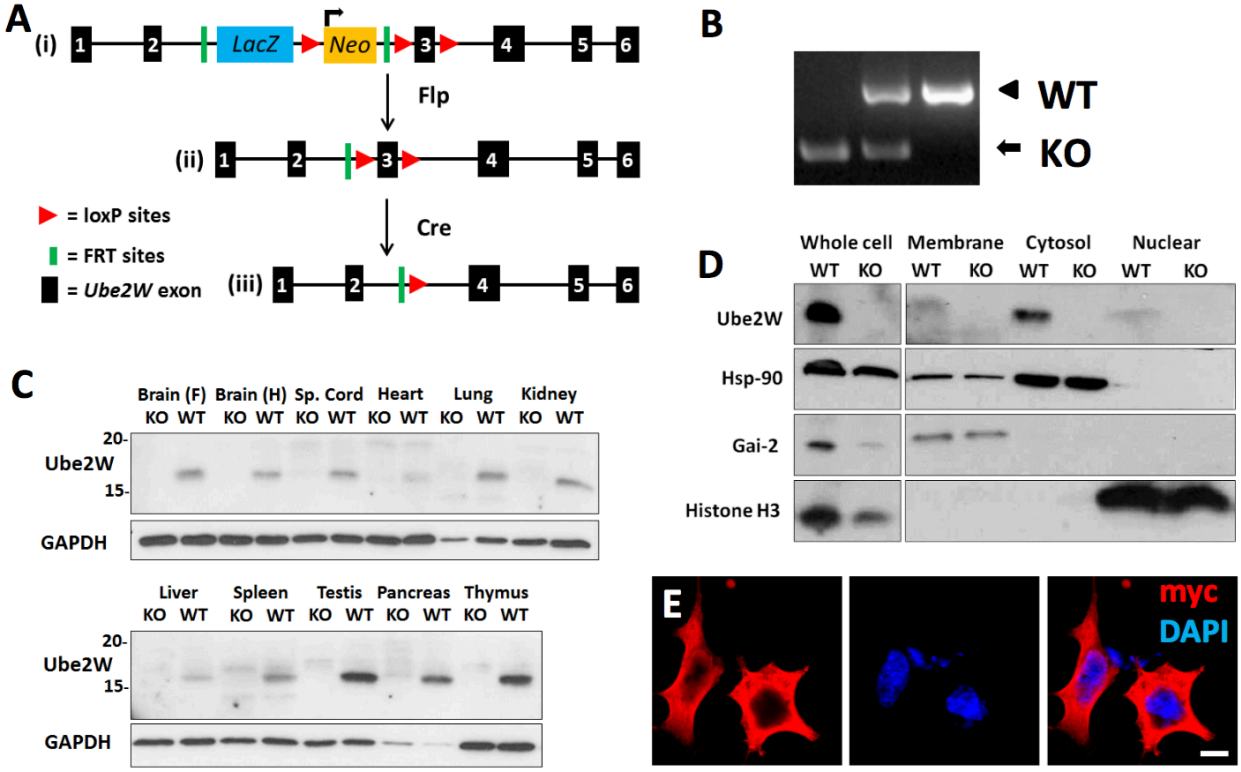

FIGURE 7. Ube2W isoform 1 beginning at Met30 is the predominant Ube2W species in mouse.

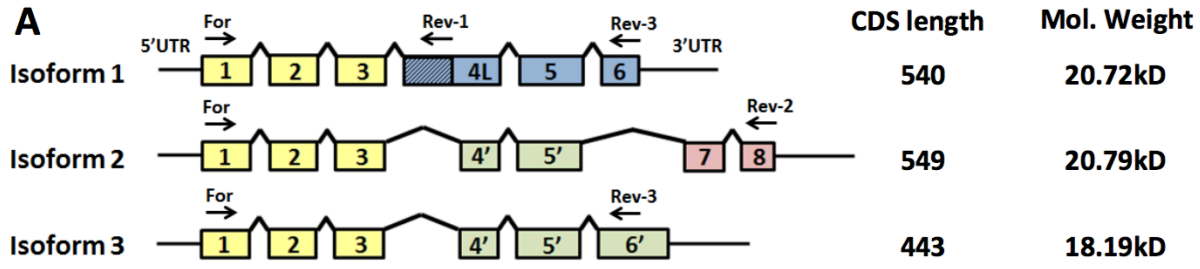

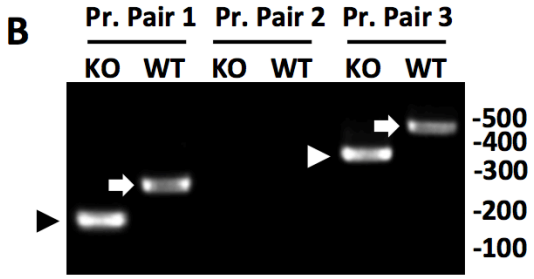

	Pr. Pair 1		Pr. Pair 2		Pr. Pair 3	
Isoform	WT	KO	WT	KO	WT	KO
1	281	178			456	353
2			(475)	(372)		
3					(377)	(274)

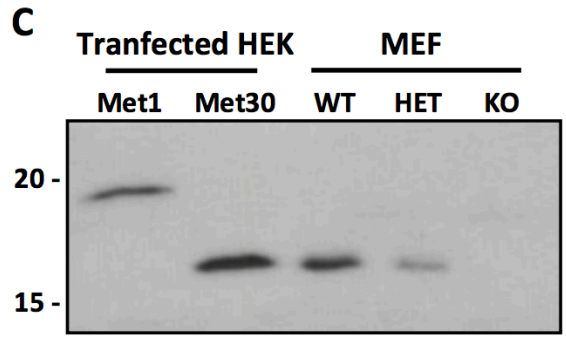

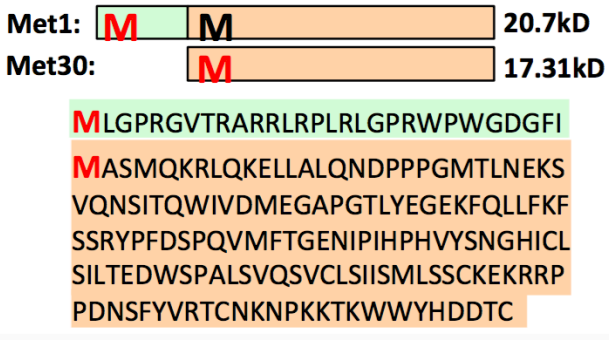

FIGURE 8. *Ube2W* KO mice are susceptible to early postnatal lethality and show retarded growth.

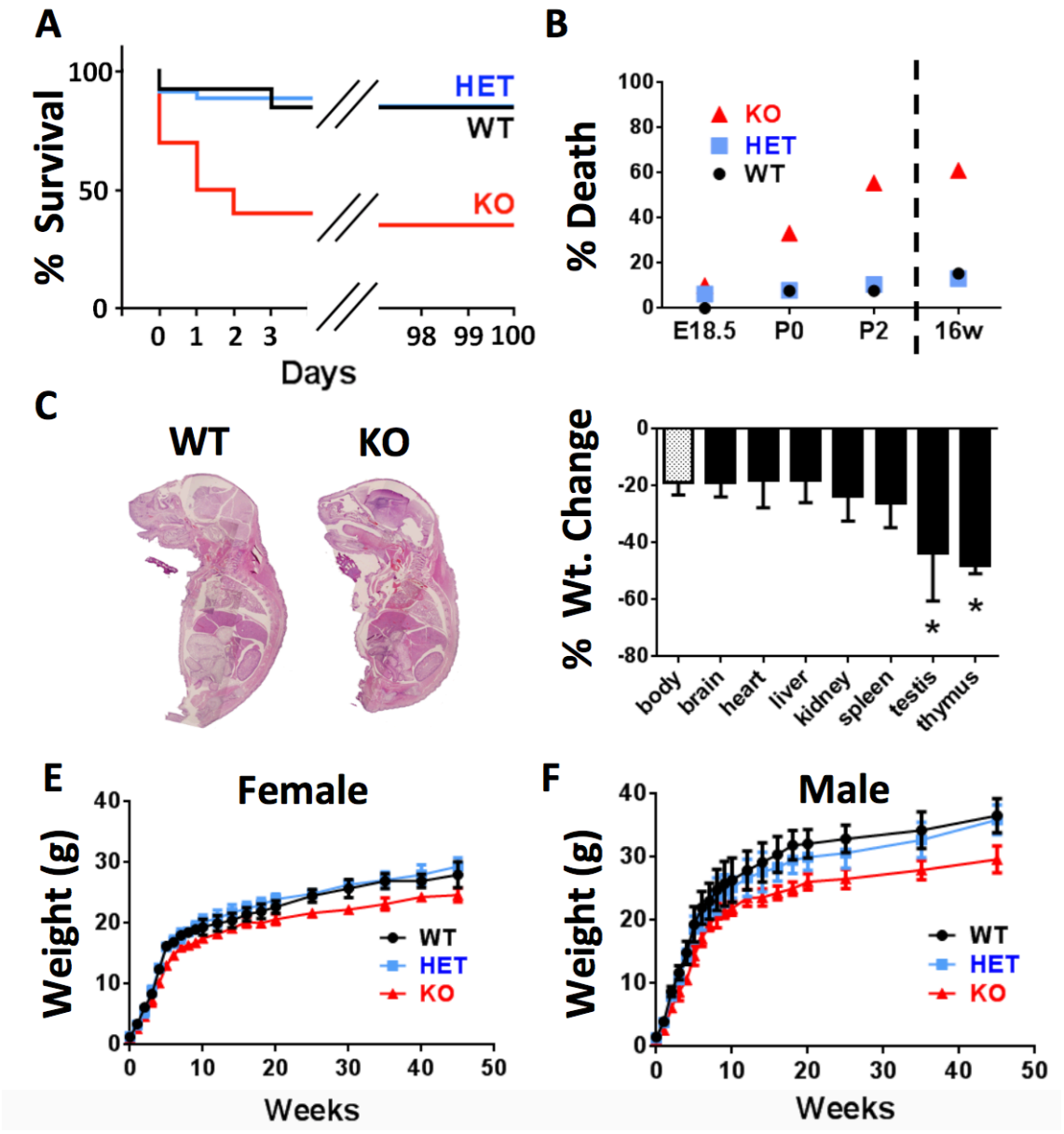

FIGURE 9. Defective skin terminal differentiation in *Ube2W* KO mice.

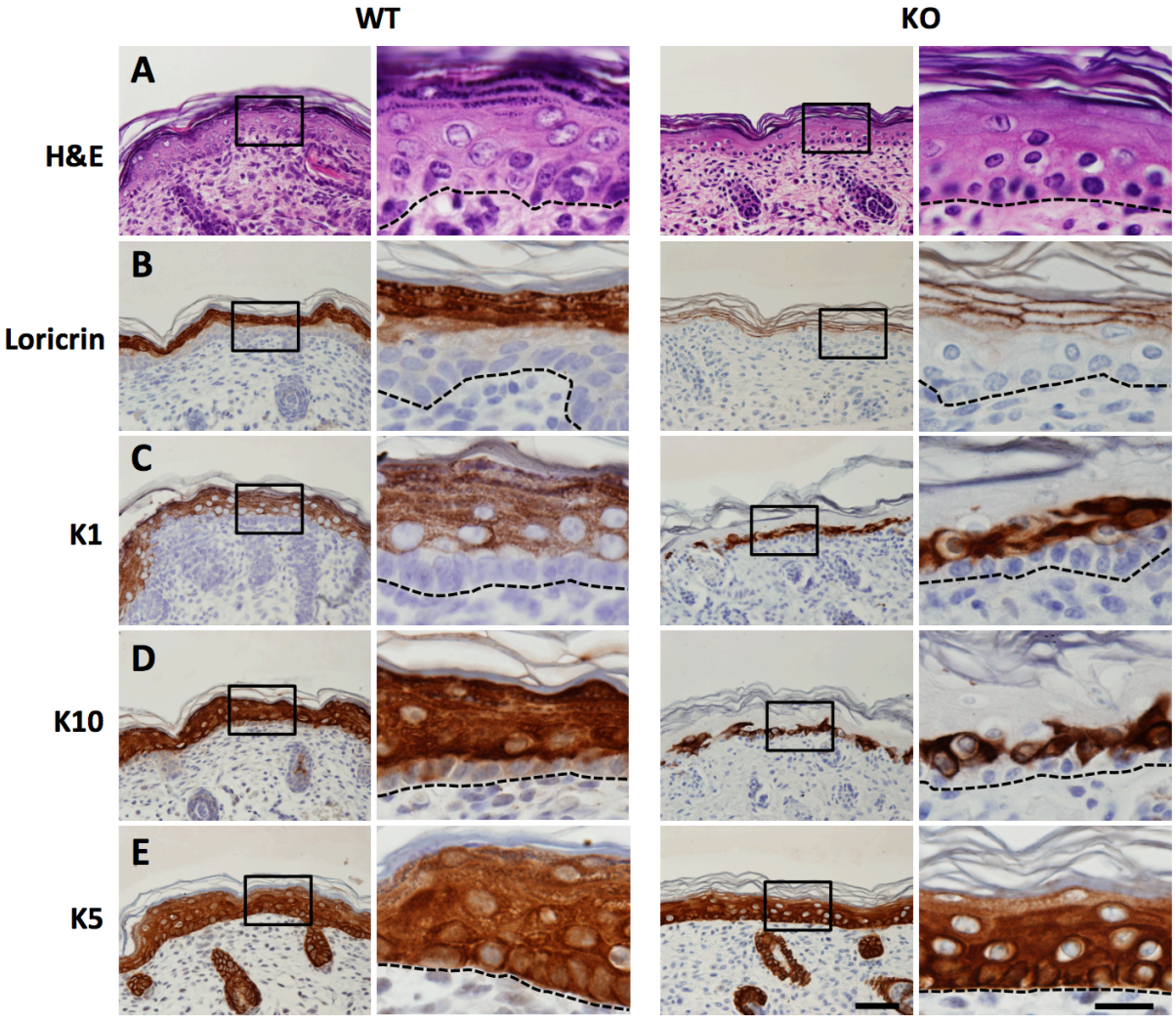

FIGURE 10. *Ube2W* KO mice show neutrophilia and increased G-CSF signaling.

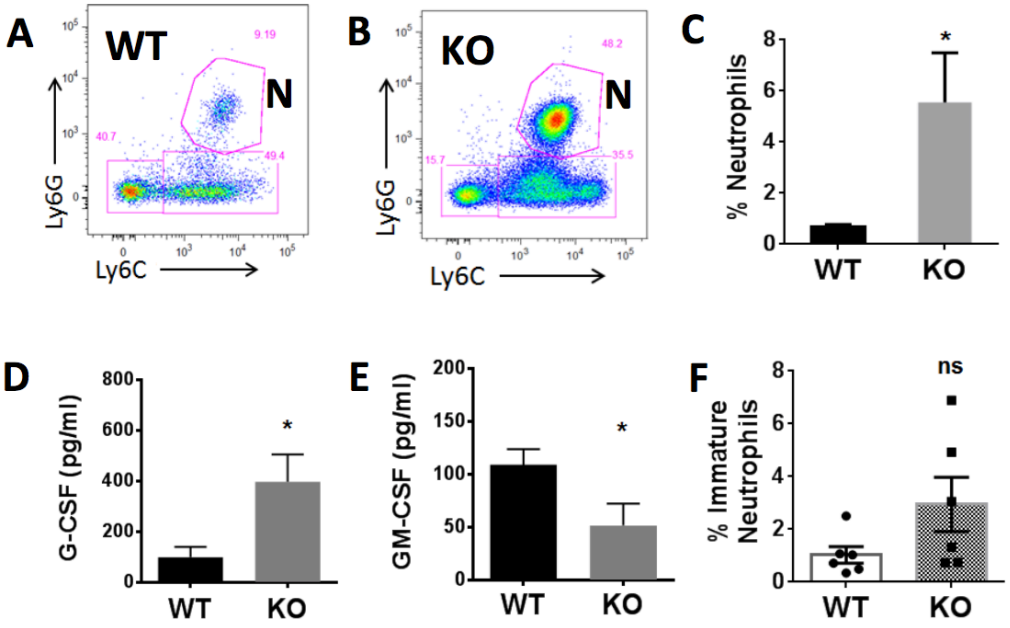

FIGURE 11. Testicular vacuolation in *Ube2W* KO mice.

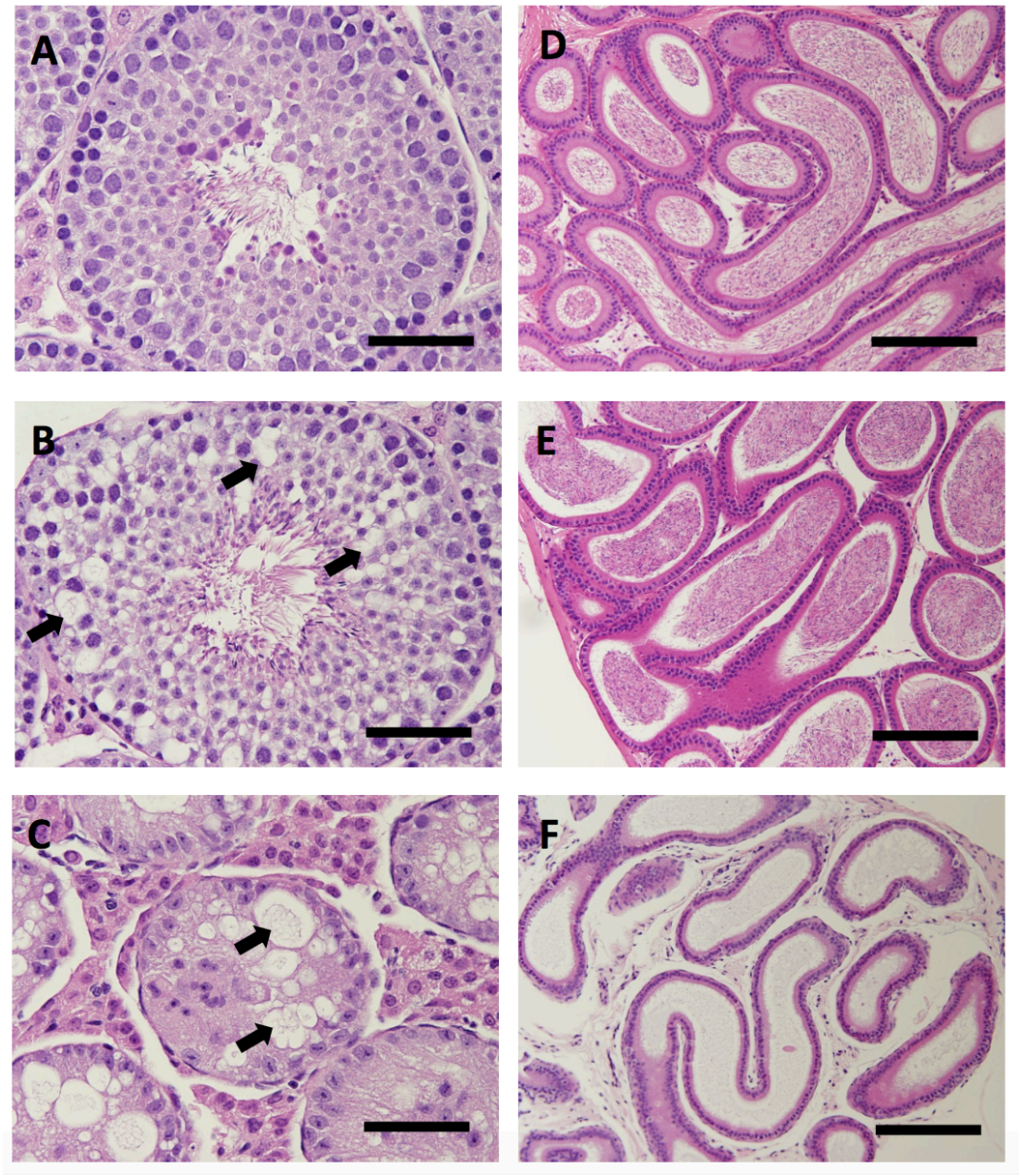

FIGURE 12. Testicular proteomic analysis shows a preferential accumulation of disordered proteins in *Ube2W* KO mice.

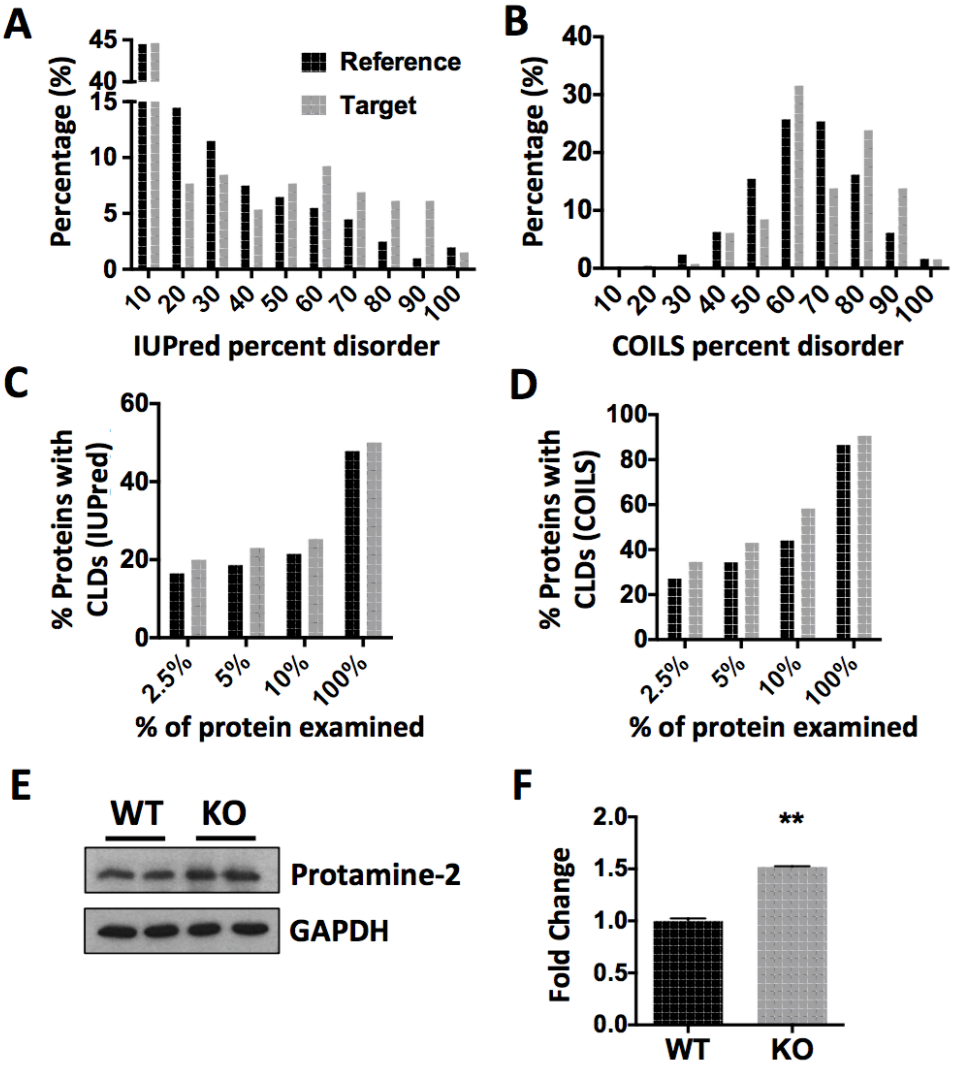

FIGURE 13. *Ube2W* deficiency does not alter cell tolerability to DNA interstrand crosslinking.

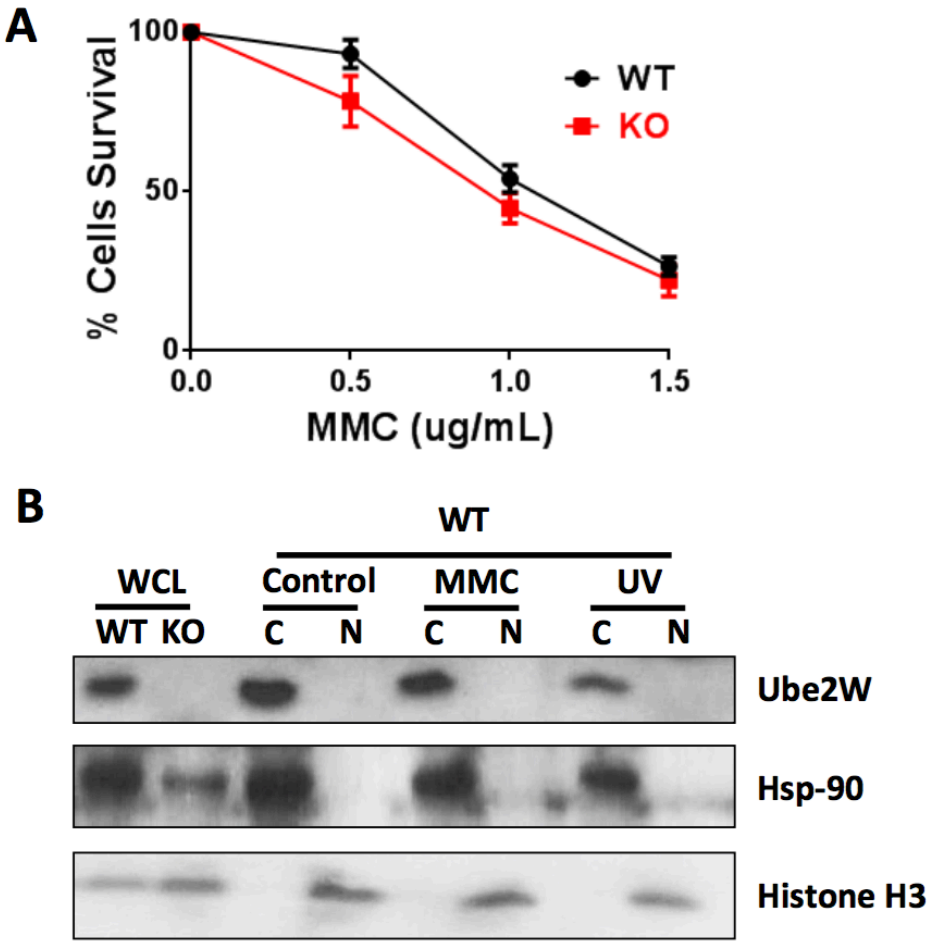

FIGURE 14. *Ube2W* KO skin-derived fibroblasts show no difference in response to various cell stressors.

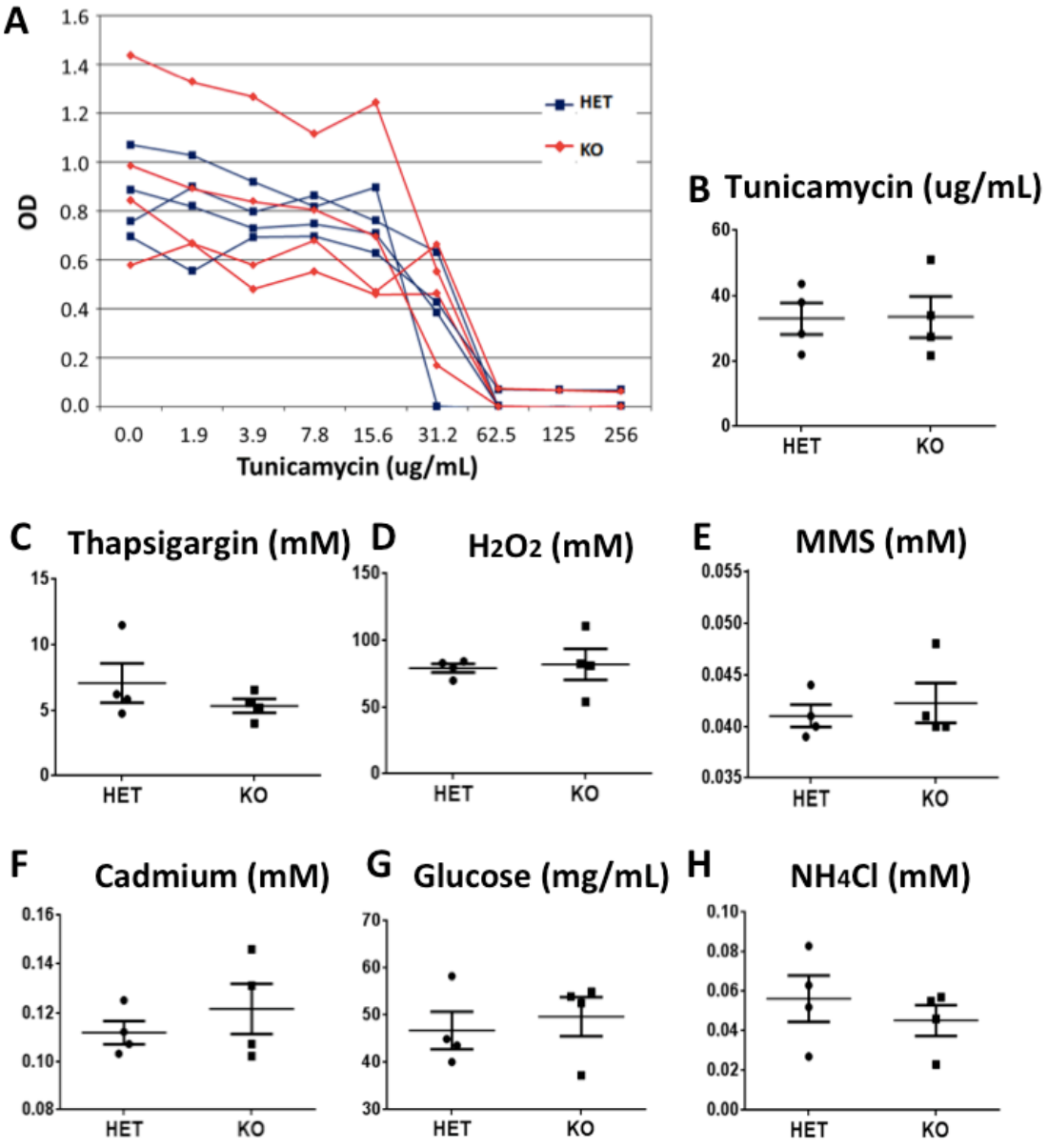

2.6 FIGURE LEGENDS

FIGURE 6. Generation of *Ube2W* KO mouse and expression of Ube2W.

A. Targeting strategy of *Ube2W* KO mouse: targeting vector is shown in (i), Flp-FRT recombination results in deletion of *lacZ* and *Neo* gene shown in (ii), further Cre-loxP recombination results in deletion of *Ube2W* exon 3 shown in (iii), this frameshift mutation causes loss of *Ube2W* expression. B. Gel electrophoresis of PCR amplification products from *Ube2W* KO and WT mice. WT size: 925bp, KO size: 394bp. C. Western blot of tissue lysates from *Ube2W* KO and WT mice, probed with anti-Ube2W and anti-GAPDH antibody as loading control. (30ug protein loaded per lane.) D. Western blot of cell fractionation lysates from KO and WT mouse embryonic fibroblasts (MEFs) probed with anti-Ube2W, Hsp-90 (cytosolic), Gai-2 (membrane-bound) and Histone H3 (nuclear) antibodies. (15ug protein loaded per lane.) E. Immunofluorescence (anti-myc, red; DAPI, blue) on HEK293 cells transiently transfected with myc tagged, human Ube2W equivalent to murine isoform 1 (Scale bar = 10 μm)

FIGURE 7. Ube2W isoform 1 beginning at Met30 is the predominant Ube2W species in mouse.

A. Schematic diagram of predicted murine *Ube2W* isoforms. Colored boxes indicate *Ube2W* coding exons. Common protein sequences across isoforms are represented in the same colors. Coding sequence length and predicted molecular weight are listed. Arrows indicate primers used in (B). Pr. Pair 1: For and Rev-1; Pr. Pair 2: For and Rev-2; Pr. Pair 3: For and Rev-3. B. PCR

amplification of *Ube2W* first strand cDNA from KO and WT MEFs. Expected band sizes are listed in table; numbers in parentheses indicate predicted bands that were not observed. Arrowheads and arrows denote bands corresponding to KO and WT isoform 1, respectively. C. Diagram on right shows two possible Ube2W protein sequences beginning at different potential start Methionines (Met1 and Met 30). Green color indicates peptide sequence unique to Met1. Western blot of HEK 293 cells overexpressing Ube2W Met1 or Ube2W Met30 (0.2ug total protein loaded), run adjacent to MEF lysates from WT, heterozygous and KO mice (20ug total protein loaded), probed with anti-Ube2W antibody.

FIGURE 8. *Ube2W* KO mice are susceptible to early postnatal lethality and show retarded growth.

A. Survival curves for WT (black, n=13), heterozygous (blue, n=38) and homozygous *Ube2W* KO mice (red, n=18). *Ube2W* KO mice display early lethality before postnatal day 2. Data at P0 represents number of both mice that either died in utero or were dead immediately upon birth. Heterozygous mice show normal survival curves. B. Representative bar graph of *Ube2W* KO mice lethality at embryonic day 18.5, postnatal day 0, postnatal day 2 and 16 weeks; shown as percentage. C. Representative images of H&E stained whole embryo, sagittal section (E18.5). *Ube2W* KO embryos show no apparent overt histological difference in internal organs. D. Proportionate organ weight decrease in *Ube2W* KO mice compared to decrease in whole body weight. Error bars indicate SEM (n=8). E. Representative growth curve (means and ranges) of female WT (circles,

n=11), heterozygous (squares, n=14) and homozygous *Ube2W* KO (triangles, n=10) mice. F. Representative growth curve (means and ranges) of male WT (circles, n=9), heterozygous (squares, n=11) and homozygous *Ube2W* KO (triangles, n=9) mice.

FIGURE 9. Defective skin terminal differentiation in *Ube2W* KO mice. Images of dorsal skin from P0 WT (left two columns) and *Ube2W* KO (right two columns) mice. Column 2 and 4 are higher magnification of inserts in column 1 and 3. Dashed lines indicate basal cell layer. A. Hematoxylin and Eosin (H&E) staining of dorsal skin. Wild-type epidermis contains basal (b), spinous (s), granular (g), and cornified (c) cell layers. Note absence of keratohyalin granules in mutant epidermis. B. Restricted expression of granular cell marker Loricrin to the cell periphery in *Ube2W* KO skin, compared with cytoplasmic expression in WT epidermis. C and D. Expression of spinous cell markers Keratin 1 (K1) and Keratin 10 (K10) in 1-2 layers of suprabasal cells in *Ube2W* KO mice skin, compared with expression in WT spinous layers that persists in granular cell layers. E. Immunostaining of basal cell marker Keratin 5 (K5) shows a similar pattern in wild-type and *Ube2W* KO skin. Scale bar=50 μm, insert scale bar=20 μm.

FIGURE 10. *Ube2W* KO mice show neutrophilia and increased G-CSF signaling. A and B. Representative flow-cytometry sorting of neutrophils in WT (A) and *Ube2W* KO (B) mouse blood. N= neutrophils ($CD11b^+Ly6G^+Ly6C^+$). C.

Percentage of neutrophils in all $CD11b^+CD45^+$ blood cells from WT (black) and *Ube2W* KO (grey) mice. n=10. D and E. Serum levels of G-CSF (D) and GM-CSF (E), measured by bead-based multiplex analysis. n=6. F. Percentage of immature neutrophils ($CD11b^+Ly6G^+Ly6C^{low}$) in all $CD11b^+CD45^+$ cells from intraperitoneal lavage 4 hours after thioglycollate injection. n=6. All graphs indicate means; error bars denote SEM. *, $P < 0.05$.

FIGURE 11. Testicular vacuolation in *Ube2W* KO mice.

A-C. Images of H&E stained seminiferous tubules from 16-week-old WT (A) and *Ube2W* KO (B and C) mice. Testes from KO mice show variable vacuolations within seminiferous tubules, ranging from focal vacuolation of spermatogonia and spermatocytes (B, arrows) to diffuse vacuolation and loss of spermatocytes with marked atrophy of seminiferous tubules (C). D-F. Images of H&E stained epididymis (D-F) from the WT (D) and *Ube2W* KO (E and F) mice shown in A-C. Epididymi from *Ube2W* KO mice showed no histological abnormalities but a variable reduction in mature sperm (E-F). Bars= 50 μm (A-C); 100μm (D-F).

FIGURE 12. Testicular proteomic analysis shows a preferential accumulation of disordered proteins in *Ube2W* KO mice.

A. Distribution of full length proteins according to IUPRED calculation of percent disorder (PD). p=0.02 (KS test). In panels A-D, the reference set (black bars) includes all identified testicular proteins minus the target set (gray bars) of proteins whose levels are increased >1.5 fold in *Ube2W* KO mouse testis. B.

Distribution of full length proteins according to DisEMBL-COILS calculation of percent disorder (PD). P=0.004 (KS test). C. Percentage of proteins containing continuous length disorder (CLD) of at least 30 amino acids, according to IUPRED, based on analysis of the amino-terminal first 2.5%, 5% or 10% of the protein or the full protein sequence. D. Percentage of proteins containing CLDs of at least 30 amino acids, according to DisEMBL-COILS, based on analysis of the amino-terminal first 2.5%, 5% or 10% of the protein or the full protein sequence. E. Western blot confirmation of increased levels for a top identified target protein, Protamine-2; GAPDH as loading control. (30ug total protein loaded per lane.) F. Quantification of Western blot in panel E. p=0.002, n=2.

FIGURE 13. *Ube2W* deficiency does not alter cell tolerability to DNA interstrand crosslinking.

A. MEF survival after 24–hour treatment with increasing concentrations of mitomycin C (MMC). B. Western Blot of different cell fractionation lysates from WT and *Ube2W* KO mouse embryonic fibroblasts (MEFs) after treatment with MMC or UV radiation, blotted with anti-Ube2W, Hsp-90 (cytosolic) and Histone H3 (nuclear) antibodies. (15ug total protein loaded per lane.)

FIGURE 14. *Ube2W* KO skin-derived fibroblasts show no difference in response to various cell stressors.

A. Representative cell survival at various tunicamycin concentrations; the figure shows results for fibroblasts from four individual *Ube2W* KO and heterozygous

(HET) mice. B. Compilation of LD_{50} results from experiments as in panel A; each symbol representing a different donor mice. C-H. Compilation of LD_{50} results for treatment with thapsigargin (C), H_2O_2 (D), MMS (E), cadmium (F), glucose deprivation (G), and NH_4Cl (H). All graphs show means +/- SEM. *, $P < 0.05$. n=4

Chapter Three: Ube2W regulates mutant Huntingtin solubility

3.1 ABSTRACT

Huntington's Disease (HD) is caused by polyglutamine (polyQ) expansion in the HD disease protein, huntingtin (Htt). PolyQ expansion leads to Htt misfolding and accumulation as inclusion bodies within neurons. Ube2W is the only ubiquitin conjugating enzyme (E2) that ubiquitinates substrates at the disordered amino-termini. Htt is known to have an intrinsically disordered amino terminus. In this study, I tested whether Ube2W is capable of regulating Htt. To investigate this potential non-canonical ubiquitination of Htt, I performed studies in immortalized cells, primary neurons and a knock-in (KI) mouse model of HD to study the effect of Ube2W deficiency on Htt levels, inclusion formation and neurotoxicity. In cultured cells, functional deficiency of Ube2W markedly decreases inclusion formation and increases the level of soluble monomers, while reducing Htt cytotoxicity. Consistent with this result, the absence of Ube2W in *HdhQ*$_{200}$ KI mice significantly increases levels of HttQ$_{200}$ soluble monomers without altering Htt inclusion and expression of striatal markers. This study sheds light on the potential function of non-canonical N-terminal ubiquitination in an important neurodegenerative disease and supports the view that post-

translational modification at or near the N-terminus of Htt modulates Htt solubility and aggregation formation.

3.2 INTRODUCTION

Accumulation of ubiquitinated proteins is commonly observed in neurodegenerative diseases, shared as a pathological hallmark shared by many neurodegenerative diseases including Huntington's disease (HD). HD is the most common polyglutamine (polyQ) disease. The CAG repeat expansion encodes a polyQ stretch in the disease protein huntingtin (htt). When the polyQ length exceeds a threshold of ~40 glutamines, it becomes pathogenic(120). HD patients typically develop various clinical signs and symptoms including involuntary movements such as chorea and dystonia, neuropsychiatric symptoms and cognitive deficits. Histopathologically, HD displays a progressive spreading pattern: the brain region first affected is the striatum, particularly the loss of medium spiny neurons that express dopamine D2 receptors, DARPP-32 and the neurotransmitter enkephalin(124–127).

In HD, the polyQ stretch resides very near the N-terminus of htt and contributes to the disorderness and misfolding of htt. Expanded Htt becomes insoluble and forms inclusion bodies in neuronal nuclei, perinuclear regions and neurites(131–133). Immunohistochemical studies revealed that these inclusion bodies contain N-terminal regions of htt, ubiquitin, proteasomal components and numerous other proteins(132). The discovery of ubiquitin and proteasomal

subunits in HD inclusion bodies supports the importance of ubiquitin-dependent pathways in HD pathogenesis. However, the exact roles of ubiquitination in HD are not fully understood. Studies have shown that numerous components of ubiquitin-dependent systems can contribute to and alter htt degradation, aggregation and cytotoxicity. K11, K48 and K63-linked polyubiquitin-modified proteins have been identified in HD inclusion bodies, suggesting a regulatory role of either the proteasome or autophagy systems in htt inclusion formation. Furthermore, ubiquitin-like molecules such as SUMO have proved to be important regulators in htt aggregation(144, 145).

Ubiquitin (Ub) conjugation involves a sequential action of enzymes to target ubiquitin to substrates: Ub-activating enzyme (E1), Ub conjugating enzyme (E2) and Ub ligase (E3). Taking into consideration different Ub-chain lengths, linkages and substrate attachment sites, dramatically different kinds of ubiquitination can occur. The variety of ubiquitination pattern is mainly achieved by different combinations of E2/E3 pairs. Recently, Ube2W was identified as the only E2 that can recognize disordered N-termini of proteins and initiate ubiquitination at the α-amino group(56, 67, 68). Ube2W can function with various ubiquitin ligases including the C terminus of Hsc-70-interacting protein (CHIP) and the BRCA1/BARD1 complex to mono-ubiquitinate select substrates at their amino-termini(25, 56, 68–70).

Given the highly disordered nature of the N-terminal domain of Htt, I predict it to be a strong candidate target for Ube2W. Currently the function of Htt N-terminal ubiquitination is unknown. In this chapter, I utilize different model

systems to study the effect of Ube2W deficiency to Htt protein levels, aggregation and neurotoxicity.

3.3 EXPERIMENTAL PROCEDURES

Animals - *Ube2W* germline KO mice were generated as described in chapter 2. *Ube2W* neuronal KO mice were generated by crossing *Ube2W* Flox/Flox mice (described in chapter 2) with Nestin promoter driven Cre transgenic mice from Jackson Laboratory (B6.Cg-Tg(Nes-cre)1kln/J), in which Cre is expressed in central nervous systems. All mice in this study were maintained on a pure C57BL/6 genetic background, housed in cages with a maximum number of five animals and maintained in a standard 12-hour light/dark cycle with food and water *ad libitum*. Genotyping was performed using DNA isolated from tail biopsy at the time of weaning, otherwise indicated. Genotype was determined by PCR amplification of a fragment of gene-of-interest. To model Huntington's disease, I utilized the heterozygous HD-KI Q_{200} (*Hdh*Q_{200}) mouse model expressing murine Htt with ~200 CAG repeats(186, 187). Mice were euthanized at specific ages, anesthetized with ketamine/xylazine, and perfused transcardially with phosphate-buffered saline.

PCR primers - For *Ube2W* KO genotyping:
5'AAAGGAAGAGCCCAGTATGGACCCT3' and
5'AGAGTCCCTGCAGCTATTAC3';

Cre genotyping: 5'GTCCAATTTACTGACCGTACACC3',
5'GTTATTCGGATCATCAGCTACACC3',
5'CTAGGCCACAGAATTGAAAGATCT3' and
5'GTAGGTGGAAATTCTAGCATCATCC;

Flox genotyping: 5'AAAGGAAGAGCCCAGTATGGACCCT3' and
5'TGTGTTTTGTTTTAATCTTTCTGGCC3';

Hdh genotyping: 5'CCCATTCATTGCCTTGCTG3' and
5'GCGGCTGAGGGGGTTGA3';

Hdh qRT-PCR: 5'TTGTGTTAGATGGTGCCGAT3' and
5'GTTGAAGGGCCAGAGAAGAG3'.

Transfection and immunofluorescence imaging - Human embryonic kidney 293 (HEK293) cells were cultured in DMEM, supplemented with 10% FBS, 100U/ml penicillin/streptomycin. Transfections were carried out with lipofectamine 2000 (Invitrogen) as described previously(187). GFP fluorescence was visualized by Olympus IX-71 fluorescence microscope.

Plasmids - pcDNA3.1-$Htt^{ex1}Q_{103}$-GFP and pGW1-mApple has been reported previously(187–189); pCMV6-Ube2W plasmid was from Origene (RC204985), C91A and W144E mutations were introduced using Quikchange Lightning Site-Directed Mutagenesis (#210518, Agilent Technologies); pGW1-Htt^{ex1}-(Q_{17} or Q_{72})-EGFP were kindly provided by Dr. Steven Finkbeiner(190).

Western blotting - Protein lysates from different cells were generated by lysis in radioimmunoprecipitation assay (RIPA) buffer containing protease inhibitors (Complete-mini; Roche Diagnostics, Indianapolis, IN), followed by

sonication and centrifugation. The supernatants were collected. For transfection experiments, transfected cells were lysed with 0.5% Triton X-100 lysis buffer containing 150 mM NaCl, 20 mM Tris/HCl, pH 8.0, 5 mM EDTA and complete Mini Protease Inhibitor tablets. Insoluble material was further lysed with 2X Laemmli buffer. Total protein concentration was determined using the BCA method (Pierce, Rockford, IL) and then stored at −80 °C. Proteins were resolved in sodium dodecyl sulfate–polyacrylamide gel electrophoresis gels, and corresponding polyvinylidene difluoride membranes were incubated overnight at 4 °C with primary antibodies: rabbit anti-Ube2W (1:1,000; 15920-1-AP; Protein Tech Group), mouse anti-GAPDH (1:10,000; MAB374; EMD Millipore), rabbit anti- α tubulin (1:10,000; #2144; Cell Signaling Technology), rabbit anti-GFP (1:1,000; sc-8334; Santa Cruz Biotechnology), mouse anti-polyglutamine (1:2,000; MAB1574; EMD Millipore), mouse anti-Huntingtin (1:250, MAB2166, EMD Millipore), rabbit anti-Hsp40 (1:1,000; #4868, Cell Signaling Technology), rabbit anti-Hsp60 (1:1,000; ab46798, abcam), mouse anti-Hsp70 (1:1,000; SPA-810, Enzo Life Sciences) and mouse anti-Hsp90 (1:1,000; SAP-830, Enzo Life Sciences). Bound primary antibodies were visualized by incubation with a peroxidase-conjugated anti-mouse or anti-rabbit secondary antibody (1:10,000; Jackson Immuno Research Laboratories, West Grove, PA) followed by treatment with the ECL-plus reagent (Western Lighting; PerkinElmer, Waltham, MA) and exposure to autoradiography films.

^{35}S-Methionine labeling and immunoprecipitation - At 24h after transfection, cells were labeled with 100 µCi of ^{35}S-Met (Perkin Elmer) in Cys/

Met-free DMEM. When indicated, cells were washed and incubated with ice-cold PBS and then lysed in RIPA buffer (pH 7.4) containing protease inhibitors (Roche). Lysates were immunoprecipitated overnight with anti-GFP, boiled in SDS sample buffer with 0.1 M DTT, and analyzed by Tris-Acetate SDS-PAGE.

Histological analysis - All tissues were fixed 96hrs at 4 degree in 4% Formaldehyde solution in PBS, transferred to 30% sucrose in PBS, processed, and sectioned. For immunohistochemical staining, tissue underwent antigen retrieval in boiling citrate-based buffer (0.01 mol/L citric acid, pH 6.8). Endogenous peroxidases were quenched with 3% H_2O_2, followed by blocking in 5% goat serum and incubation with primary antibodies (anti-Huntingtin 1:250, sc8767, Santa Cruz Biotechnology). Bound antibodies were detected with the Vector M.O.M. peroxidase (Vector Laboratories, Burlington, CA), using SigmaFast diaminobenzidene as a peroxidase substrate (Jackson ImmunoResearch, West Grove, PA).

Primary neuron culture and transfection - Cortical neurons were dissected from P0 WT or *Ube2W* KO pups and cultured at 0.6×10^6 cells per milliliter for 4 d in vitro before transfection, as described previously(191). Transfection of primary neurons was performed using Lipofectamine 2000 (Invitrogen). A total of 0.2 µg DNA (total) and 0.5 µL Lipofectamine 2000 was used per well in 96-well plates. Cells were incubated with Lipofectamine/DNA complexes for 20 min at 37 °C before rinsing and changing to normal culture media. Rest of the transfection was performed according to manufacture recommendation.

Automated fluorescence microscopy – Cultured primary mouse neurons were imaged by automated fluorescent microscopy (188–190, 192). The system is consisted of an inverted microscope (Nikon Eclipse Ti) equipped with the Perfect Focus System (Nikon), a high-numerical aperture 20× objective lens, a digital camera, a Lambda XL lamp (Sutter) and an ASI MS2000 stage to automatically control the platform. Neurons were imaged inside a thermo chamber, in which temperature and CO_2 concentration was maintained at 37^{o}C and 5% respectively.

Image analysis – 25 raw images were taken from each well of primary neurons. Raw images were stitched together to represent a larger area. According to the sequence and alignment, stitched images were stacked together to represent time-elapse change of fluorescence. Neuronal survival was calculated by a software algorithm developed in ImageJ (192). The time of death for each neuron was recorded as the last time a neuron was confirmed to be alive (left censoring). Intensities of transfected proteins were determined automatically in Fig 3 by segmentation of neuronal cell bodies in ImageJ and measurement of mean pixel intensity within each region of interest. Statistical analyses and the cumulative hazard plots were generated using custom-written scripts and the survival package within R (192).

RNA extraction and qRT-PCR - RNA was extracted from frontal brain of mice using TRIzol® (Life Technologies) and further purified using the RNeasy kit with on-column DNase I digestion (Qiagen). For qPCR, 1 µg of RNA was reverse-transcribed using iScript™. 0.5 µl was used with the SYBR®

GreenMasterMix and each reaction was performed in triplicate. qRT-PCR was performed on the Bio-Rad iCycler with MyIQ single color real-time PCR detection system module with the following parameters: 95°C at 3 min, (95°C 10 s, 55°C 30 s) Å~ 40, 95°C 1 min, 55°C 1 min. The fold change in transcript levels was calculated using the ΔΔCt method(193). Gapdh was used as controls. The primers used for qRT-PCR are listed above. For figure 6A and 6B, qRT-PCR was performed with TaqMan® Gene Expression Master Mix (#4369016, Life technologies). qRT-PCR was performed on the applied biosystems 7500 real-time PCR system and the remainder of the transfection protocol was per the manufacturer's suggestions. Primers used for TaqMan qRT-PCR are from Life technologies (Drd2: Mm00438545_m1, Ppp1r1b: Mm00454892_m1 and Actb: Mm00607939_s1).

3.4 RESULTS

Ube2W regulates Htt inclusion formation in cultured cells

$Htt^{ex1}Q_{103}$-GFP overexpression in HEK293 cells results in nuclear inclusion formation (Fig 15A). Visualized by fluorescence microscope, the formation of GFP-positive Htt inclusions was studied when Ube2W or its mutants were co-expressed with $Htt^{ex1}Q_{103}$-GFP. C91 is Ube2W's enzymatic active site cysteine. Mutating C91 to alanine results in failed Ub transfer to substrate while still allowing Ube2W to bind substrate. Amino acid W144 lies near the C-terminus of Ube2W, and is critically important for substrate binding. Mutating W144 to glutamic acid results in failed substrate binding while retaining Ube2W's capacity

as an enzyme since its active site cysteine remains(68). Both mutants are predicted to disrupt Ube2W-mediated $Htt^{ex1}Q_{103}$ ubiquitination. When WT Ube2W is co-expressed with $Htt^{ex1}Q_{103}$, inclusion number and size are significantly increased. In contrast, when either Ube2W mutant is co-expressed with $Htt^{ex1}Q_{103}$, inclusion number and size are significantly decreased (Fig 15). Neither Ube2W nor its mutants alters cell viability (data not shown).

Biochemically, mutant Htt exists in three distinct states in cells: soluble monomers, soluble oligomers and insoluble aggregates(194, 195). Accordingly, lysates from transfected cells were separated into soluble and insoluble fractions based on solubility in a nonionic detergent (0.5% Triton-X100). Coexpression of the Ube2W mutant, W144E, dramatically increases soluble monomeric Htt. WT Ube2W results in a trend toward decreasing Htt soluble monomers, while the Ube2W mutant, C91A, shows a trend toward increasing Htt soluble monomers, although these did not reach statistical significance (Fig 16A and C). In the insoluble fraction, Htt exists as two species that are discernible by gel electrophoresis: high molecular weight (HMW) Htt in the stacking gel and monomeric Htt in the resolving gel. Both Ube2W mutants, W144E and C91A, significantly reduced levels of HMW and monomeric Htt in the insoluble fraction. In contrast, Ube2W overexpression showed no statistically significant change in levels of HMW or monomeric Htt in the insoluble fraction (Fig 16A, D and E).

Ube2W does not alter Htt translation in cultured cells

To study whether Ube2W affects htt synthesis or degradation, I measured Htt translation using ^{35}S-Methionine pulse-labeling. HEK293 cells overexpressing $Htt^{ex1}Q_{103}$ with WT Ube2W or the C91A mutant were pulse-labeled for 20 mins with ^{35}S-Methionone to label all newly synthesized proteins. Labeling efficiencies were similar among different cell populations. After the 20 mins labeling and cell lysis, anti-GFP immunoprecipitation (IP) captured the soluble $Htt^{ex1}Q_{103}$-GFP present in cell lysates and the radioactive signal representing newly synthesized Htt was visualized by autoradiography. The rate of $Htt^{ex1}Q_{103}$ translation was similar regardless of which form of Ube2W was coexpressed (Fig 16B and F). Due to Htt's tendency to aggregate over time, a pulse labeling followed by long chase times is technically difficult due to the inability to assess the aggregated Htt species by gel autoradiography.

Ube2W deficiency results in decreased Htt inclusion formation and reduced neurotoxicity

To investigate the consequences of Ube2W deficiency in vivo, I generated primary neuronal cultures from WT or conditional *Ube2W* KO mice in which the Nestin promoter results in Ube2W deletion in the nervous system. To assess the potential relationship between Ube2W and $Htt^{ex1}Q_{72}$-mediated neurotoxicity, I measured single-cell fluorescence and cell survival by automated fluorescence microscopy (AFM)(188–190, 192, 195). Using longitudinal AFM, I determined the risk of death for neurons expressing EGFP alone (as a control), normal repeat $Htt^{ex1}Q_{17}$-EGFP, or expanded repeat $Htt^{ex1}Q_{72}$-EGFP. AFM measures the

lifespan of individual neurons and gauges the impact of prespecified factors on the risk of death. The qualitative measures used to estimate cell death in these assays, loss of mApple fluorescence or disruption of cell integrity, are equally sensitive as conventional measures such as additional staining for apoptotic markers (195)(Fig 17A). I calculated risk of death for each population of neurons through Cox proportional hazards analysis, resulting in a hazard ratio (HR) analogous to measurements of relative risk in human clinical trials. Upon simple EGFP overexpression, neurons lacking Ube2W showed significantly increased neuronal cell death compared to neurons expressing Ube2W. In contrast, upon expression of mutant $Htt^{ex1}Q_{72}$-EGFP, neurons lacking Ube2W showed a statistically significant reduction in risk of death. Importantly, *Ube2W* KO neurons did not show a significant difference in risk of death from expression of $Htt^{ex1}Q_{17}$-EGFP overexpression (Fig 17B).

To assess the effect of Ube2W on EGFP or Htt^{ex1} expression levels, I measured the fluorescence signal separately in each of hundreds of EGFP- or $Htt^{ex1}Q_n$-EGFP-expressing neurons 24 hours after transfection, a time when $Htt^{ex1}Q_{72}$-EGFP inclusion body formation is minimal. In neurons expressing EGFP alone, EGFP fluorescence did not differ between WT and *Ube2W* KO neurons. In contrast, the absence of Ube2W resulted in significantly decreased fluorescence signal for both $Htt^{ex1}Q_{17}$-EGFP and $Htt^{ex1}Q_{72}$-EGFP (Fig 17C-E). To further study Ube2W's effect on Htt inclusion formation, I quantified $Htt^{ex1}Q_{72}$-EGFP inclusion formation in transfected neurons. The number of neurons with $Htt^{ex1}Q_{72}$-EGFP inclusions was decreased by 20% in the absence of Ube2W (Fig

17F). These inclusion-negative neurons showed diffuse EGFP signal that persisted to the endpoint of the experiment (216hr).

Ube2W deficiency increases soluble monomeric $HttQ_{200}$

To further study Ube2W's effect on mutant Htt in vivo, heterozygous *$HdhQ_{200}$* KI mice were crossed with *Ube2W* germline KO mice. At 32 weeks of age, frontal brain lysates including the striatum, the most involved region in HD, were prepared in RIPA buffer and separated by gel electrophoresis. Strikingly, soluble mutant $HttQ_{200}$ monomers were significantly increased by approximately 5-fold in the absence of Ube2W (Fig 18A and C). A similar increase in soluble $HttQ_{200}$ was also observed in 46 week-old in *Ube2W* KO mice (data not shown). Moreover, in *$HdhQ_{200}$* KI mice, the absence of Ube2W caused an increase in WT Htt monomers by approximately 3 fold (Fig 18A and B). In comparison, *Ube2W* KO mice not crossed to *$HdhQ_{200}$* KI mice failed to show any change in WT Htt levels. Thus, the increase in WT Htt in *$Ube2W^{-/-}$, $HdhQ_{200}$* mice appears to be secondary to coexpression of mutant $HttQ_{200}$. In these experiments, in which RIPA buffer was the lysis buffer and analyzed by SDS-PAGE, no Htt signal was observed in the stacking gel, which would represent detergent-resistant HMW Htt species.

To exclude the possibility that the observed changes reflected transcriptional differences, I investigated whether Ube2W affects *Hdh* transcription (both WT and mutant) by qRT-PCR. Ube2W deficiency did not alter

Hdh transcript level, arguing that Ube2W instead affects Htt expression at a translational or post-translational stage (Fig 20C).

$HttQ_{200}$ inclusion bodies in striatum are not altered by Ube2W deficiency

Inclusion bodies in neurons are a pathological hallmark of HD. Due to polyQ expansion, $HttQ_{200}$ forms widespread neuronal inclusion bodies in striatum, cortex, hippocampus and cerebellum of $HdhQ_{200}$ KI mice, beginning at ~32 weeks of age. To determine whether the marked increase in $HttQ_{200}$ monomers correlated with a change in size or number of inclusion bodies, I performed immunostaining with an N-terminal Htt antibody on brain sections from 32 and 46 week old mice (Fig 19A and B). At 46 weeks old, striatum of both groups showed robust presence of inclusion bodies with no significant difference in inclusion number or size in the presence or absence of Ube2W (Fig 19C and D). This result suggests that Ube2W preferentially affects levels of soluble $HttQ_{200}$ without altering levels of insoluble, aggregated disease protein.

Ube2W deficiency does not alter transcript levels of striatal markers in $HdhQ_{200}$ mice

Medium spiny neurons in striatum are the most affected neuronal population in HD and are known to be affected in $HdhQ_{200}$ mice. Expression levels of two striatal neuronal markers, Dopamine D2 receptors (*Drd2*) and DARPP-32 (*Ppp1r1b*), decline dramatically over the course of disease in human HD patients and animal models(186, 196–199). Their transcript levels have been

shown to be sensitive measurements of HD pathology in mice(127). Indeed, at 46 weeks of age transcript levels for both markers decreased significantly in *HttQ$_{200}$* het KI mice, suggesting striatal neuronal dysfunction(127, 200). Ube2W deficiency failed to lead to a significant alteration in transcript levels of these striatal markers (Fig 20A and B). Thus, the presence or absence of Ube2W does not appear to affect the degree of HttQ$_{200}$-mediated striatal neuron dysfunction.

Levels of key molecular chaperones are unchanged in *Ube2W* KO mice

Protein chaperones and protein-folding machinery are important regulators in mutant Htt processing and HD pathology (as discussed in Chapter 1). Accordingly, I sought to determine whether the Ube2W-mediated increase in HttQ$_{200}$ monomers reflects a change in key components of the protein-folding machinery. The heat shock protein (hsp) family is a group of proteins implicated in correct protein folding. I measured expression levels of four members of hsp family: hsp40, hsp60, hsp70 and hsp90. Only hsp70 showed a decrease in *Ube2W$^{-/-}$, HdhQ$_{200}$* mice; other hsp family members were not significantly altered (Fig 21). A decrease in hsp70 has been reported in various HD mouse models, however, whether it correlates with HD progression is not fully understood(186, 201). These results argue that Ube2W deficiency does not cause the observed increase in HttQ$_{200}$ monomers simply by changing levels of key quality control molecular chaperones.

3.5 DISCUSSION

Htt normally is highly disordered at the N-terminus. In HD, where polyQ expansion occurs 18 amino acids into the protein coding sequence, the degree of disorderness of Htt is further increased and the disordered disease protein tends to misfold, aggregate and accumulate as inclusion bodies (IBs). Ubiquitin pathways have been shown to regulate Htt levels, IB formation and disease progression(144, 145, 114, 112, 113, 143, 202, 203). Given its highly disordered N-terminus, Htt is predicted to be a candidate substrate of Ube2W N-terminal ubiquitination. However, such non-canonical ubiquitination of Htt has not been studied before. In this chapter, I utilized different model systems to show that Ube2W deficiency leads to increase in soluble Htt levels, while reducing aggregation and neurotoxicity in cellular models. This study provides evidence supporting the importance of ubiquitin pathways in HD and in particular sheds light on the possible function of N-terminal ubiquitination of Htt.

A decrease in Htt solubility is likely critically important to HD pathogenesis. As mentioned earlier, Htt can exist in three distinct states in cells: soluble monomers, soluble oligomers and insoluble aggregates(194, 195, 204). Preceding aggregation, Htt oligomers are considered to be a more toxic species than monomers and aggregates(194, 205–208). Using FRET confocal microscopy, researchers showed that neuronal cells containing oligomers die faster than those with either monomers or inclusions(194). In drosophila, polyphenol epigallocatechin-gallate reduces oligomeric species by promoting inclusion formation with a corresponding protective effect towards Htt

neurotoxicity(206). In contrast to toxic oligomers, Htt insoluble aggregates have protective effects by recruiting and neutralizing toxic oligomers(191, 194, 195, 209, 210) (Fig 5).

Htt monomers are generally believed to be non-toxic species, however, there is limited in vivo evidence to support this argument(194). In this chapter, I observed a significant increase in Htt monomers when Ube2W is deficient or absent, accompanied by increased neuronal survival in cultured cells (Fig 15, 16 and 17). This evidence suggests an inverse correlation between monomeric Htt levels and cytotoxicity. The increase in Htt monomers observed here could result from reduced oligomerization of monomers or solubilization of Htt oligomers, with the cytoprotective effect achieved by indirectly decreasing toxic oligomers. In order to prove this hypothesis, further experiments are proposed to visualize Htt oligomers. In cellular models where HD is modeled by Htt^{ex1} overexpression, a combination between split fluorescence tagging (such as bimolecular fluorescence complementation, BiFC) and time-lapse confocal microscopy allows visualization and quantification of Htt oligomers specifically(211). Furthermore, oligomers can be visualized using biochemical approaches: filter retardation assays and SDS-agarose gel can determine Htt oligomers by their characteristic high molecular weight. More detailed approaches are discussed in future directions in chapter 4. To conclude, Ube2W deficiency leads to increased Htt monomers and reduced cytotoxicity. This study provides evidence supporting the view that Htt monomers are relatively non-toxic species.

What is the mechanism by which Ube2W alters solubility of mutant Htt? I have considered three hypotheses: 1. N-terminal ubiquitination of Htt is a stabilizing signal that contributes to Htt aggregation; 2. N-terminal ubiquitination of Htt alters other post-translational modification(s) of Htt N-terminus, thus indirectly promoting Htt aggregation; and 3. Ube2W ubiquitinates other proteins that regulate Htt, such as SUMO-2, a documented Ube2W substrate that increases Htt aggregation(145). At the time of thesis defense, I am still in the process of investigating these individual hypotheses.

The exact biological role of Ube2W-mediated ubiquitination is not fully understood. Based on limited studies, a role in proteasomal degradation has been proposed. As discussed in chapter 1, researchers have identified at least 13 proteins that can be N-terminally ubiquitinated(56, 58, 52, 158, 53, 51, 62, 55, 60, 61). All but two known N-terminal substrates (ataxin-3 and LMP2A) are targeted for proteasomal degradation by N-terminal ubiquitination via lys48-linked polyubiquitination. Additionally, in chapter 2, I showed an accumulation of disordered proteins in *Ube2W* KO testis, indicating that Ube2W-mediated N-terminal ubiquitination likely functions as a degradation signal. A derivative form of N-terminal ubiquitination further supports this hypothesis. Specifically, an N-terminal mutant ubiquitin fusion has been widely used as a “degron” that targets the protein for degradation by the UPS. For example, Ub^{G76V}-GFP can be used as a proxy of UPS activity due to its rapid proteasomal degradation(108, 110, 109, 212). The G76V mutation inhibits Ub removal from substrates by DUBs and allows subsequent polyubiquitination(108). This evidence indicates that N-

terminal ubiquitination of GFP serves as a signal for proteasome degradation. These lines of evidence suggest that Ube2W-mediated N-terminal ubiquitination can target proteins for degradation. However, because Ube2W is a strict monoubiquitinating enzyme, it does not determine subsequent Ub chain linkage(5, 25, 56, 68, 69). As reviewed in chapter 1, cellular functions of ubiquitination are not limited to degradation pathways. Working with Ube2N/Ube2V2, Ube2W is able to generate K63-linked ubiquitin chains on TRIM5α and TRIM21. Such non-proteolytic K63-linked polyubiquitination is critical to regulating the reverse transcription activity of TRIM5α and TRIM21(69, 70). Accordingly, the potential functions of N-terminal ubiquitination in non-degradative pathways cannot be ruled out. Further studies are required to identify the Ub chain linkages of Htt N-terminal ubiquitination and its biological function with respect to Htt solubility.

Besides direct N-terminal ubiquitination, alternative mechanisms, such as SUMOylation, can also cause alteration in Htt monomers. SUMO-2 itself can be N-terminally monoubiquitinated by Ube2W in vitro(67), though the biological function of this signal is still unknown. It is possible that Ube2W ubiquitinates SUMO-2 already conjugated to Htt. SUMO-2 modification of Htt^{ex1} decreases Htt solubility: it favors Htt accumulation and decreases monomers(145). Similar to the findings here with Ube2W mutants, SUMO-2 knockdown in cells significantly decreases insoluble Htt species. Based on this finding, it is likely that Ube2W-mediated N-terminal ubiquitination on SUMO-2 is a prerequisite for Htt SUMOylation. Thus inhibiting Ube2W would cause the same effect as abolishing

SUMO-2. Further studies will be important to address this alternative hypothesis (see also chapter 4).

While more work remains, my studies on Ube2W and HD have begun to provide insight into how the ubiquitin system can regulate misfolded proteins contributing to diseases.

FIGURE 15. Ube2W alters $Htt^{ex1}Q_{103}$-GFP inclusion formation in HEK293 cells

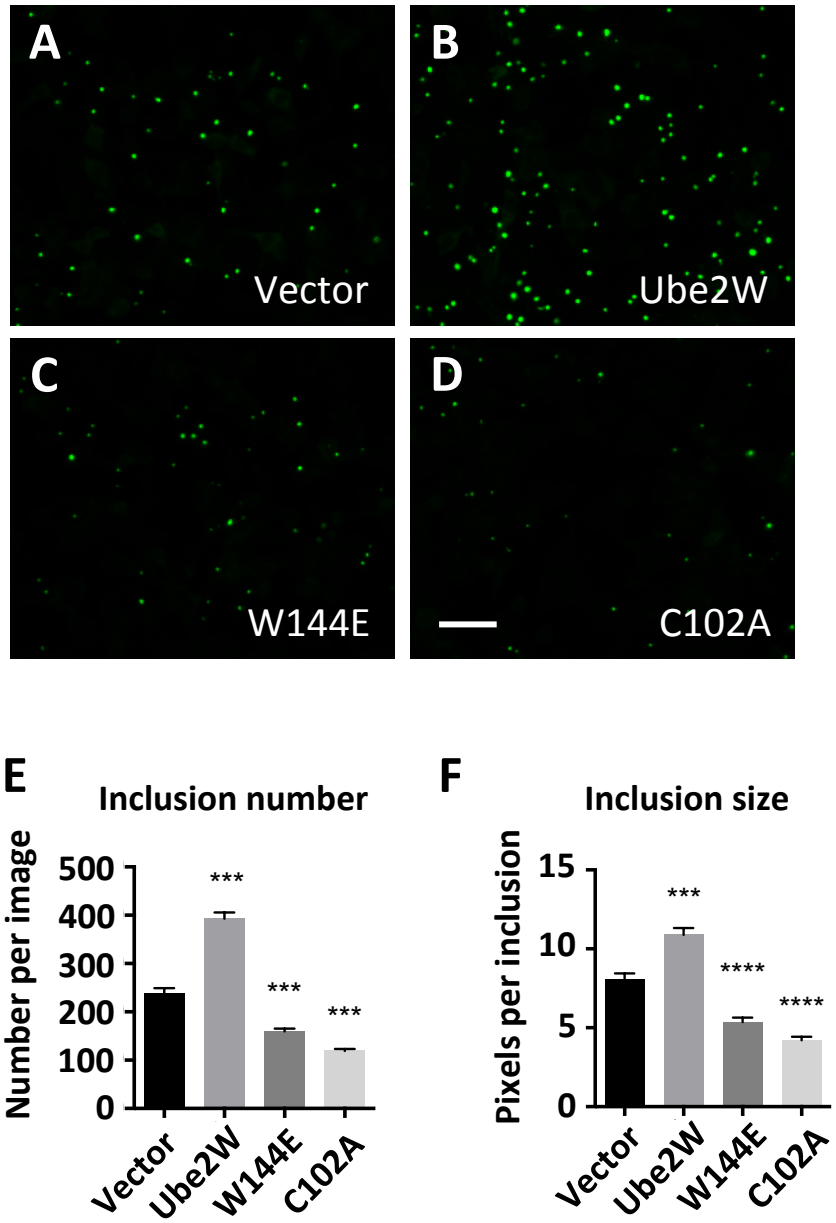

FIGURE 16. Ube2W alters solubility of $Htt^{ex1}Q_{103}$

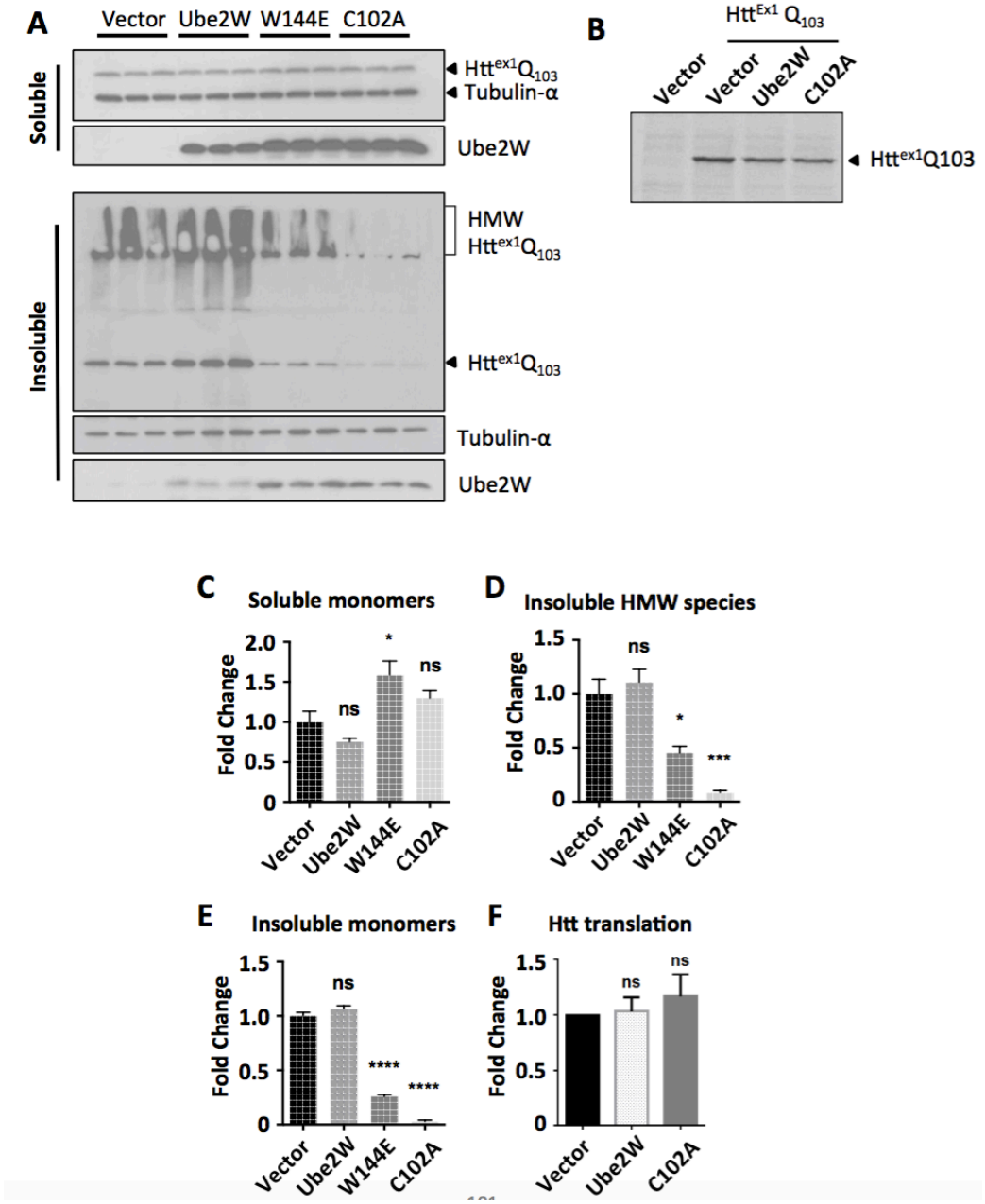

FIGURE 17. Ube2W deficiency results in decreased $Htt^{ex1}Q_{72}$ inclusion formation and increased neuronal survival

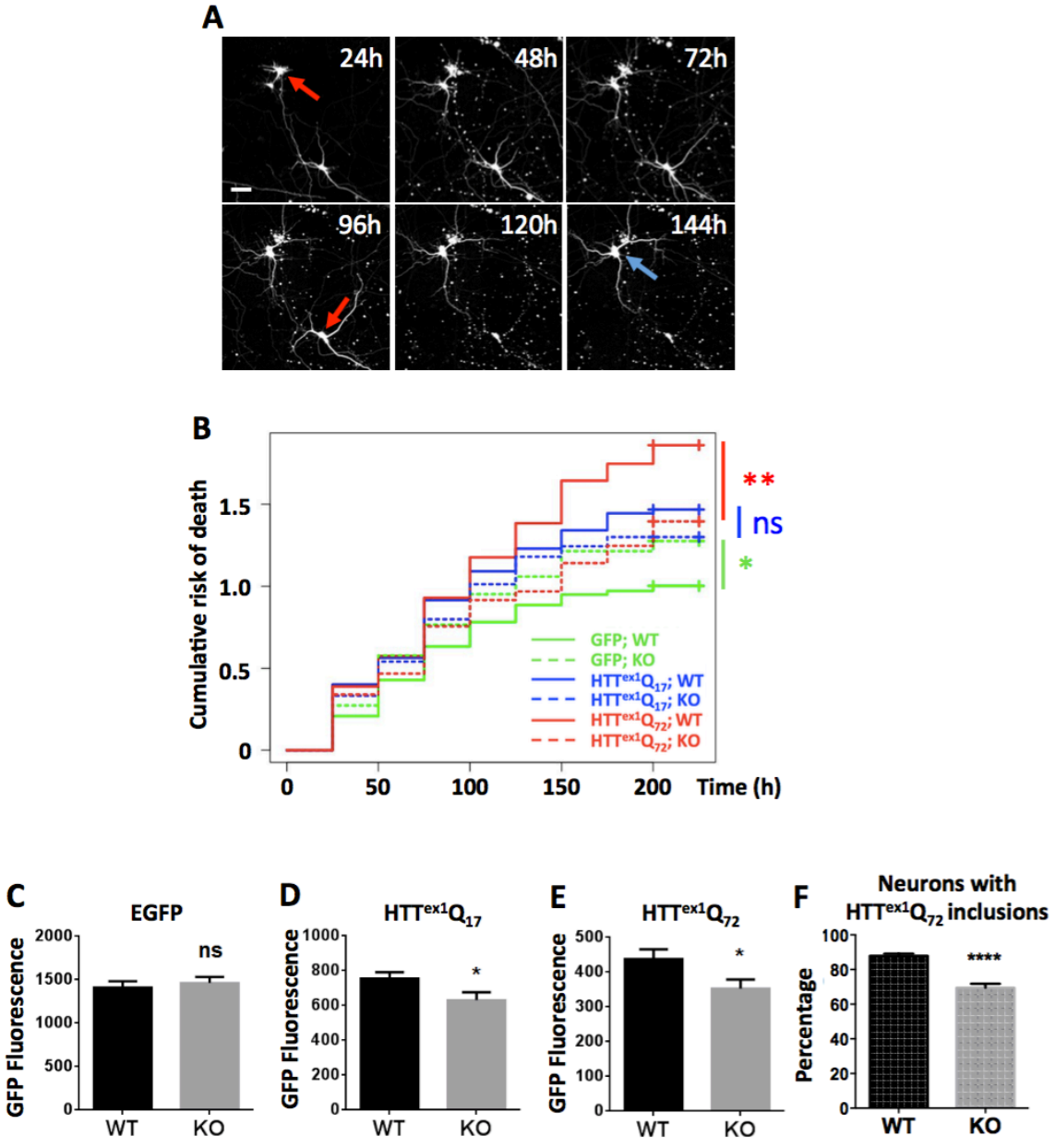

FIGURE 18. Ube2W deficiency increases soluble Htt levels in *HdhQ200* KI mice

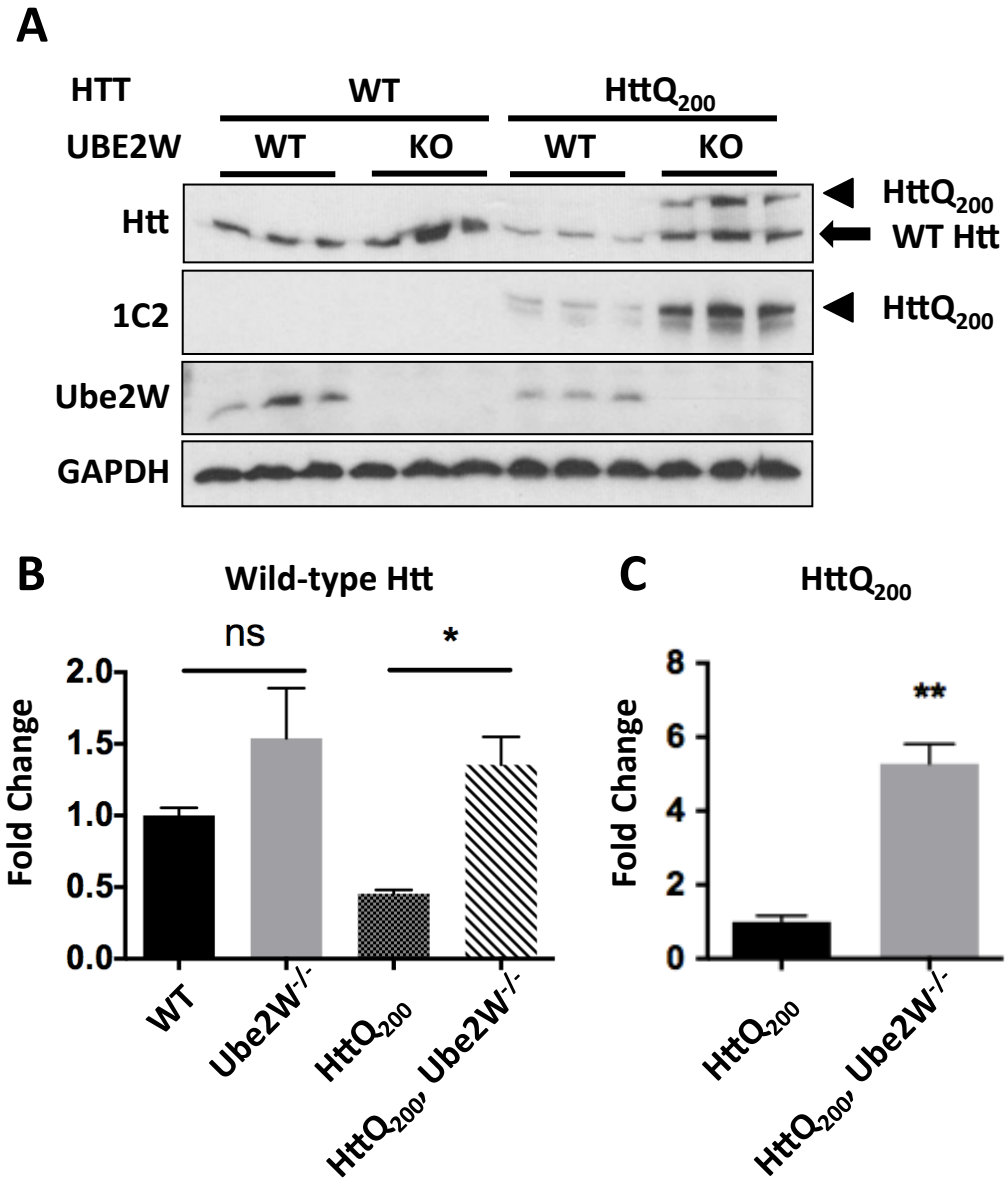

FIGURE 19. Absence of Ube2W does not alter $HttQ_{200}$ inclusion levels in striatum of *$HdhQ_{200}$* KI mice.

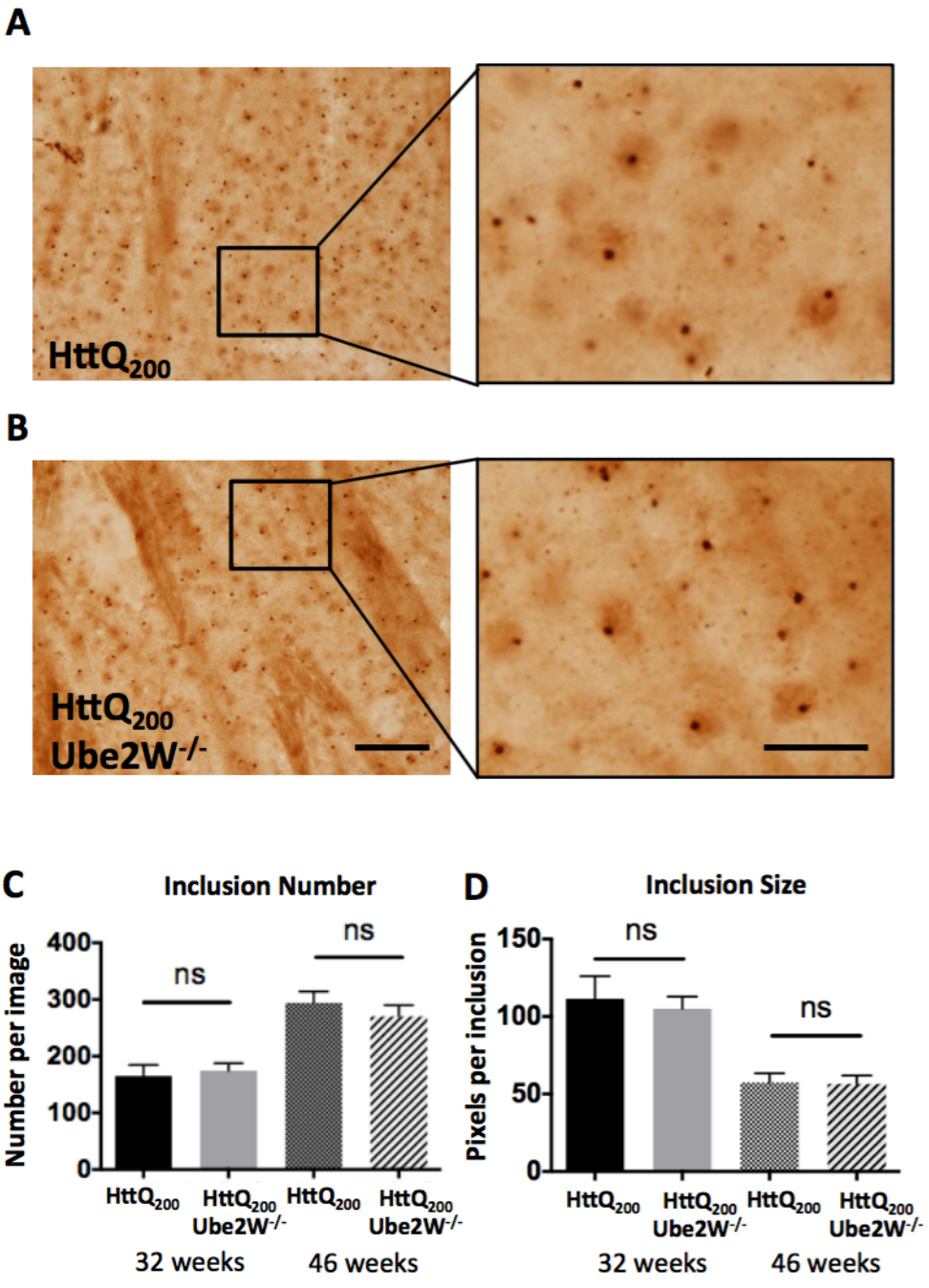

FIGURE 20. Ube2W deficiency does not alter transcript levels of striatal neuronal markers in *HdhQ$_{200}$* het KI mice.

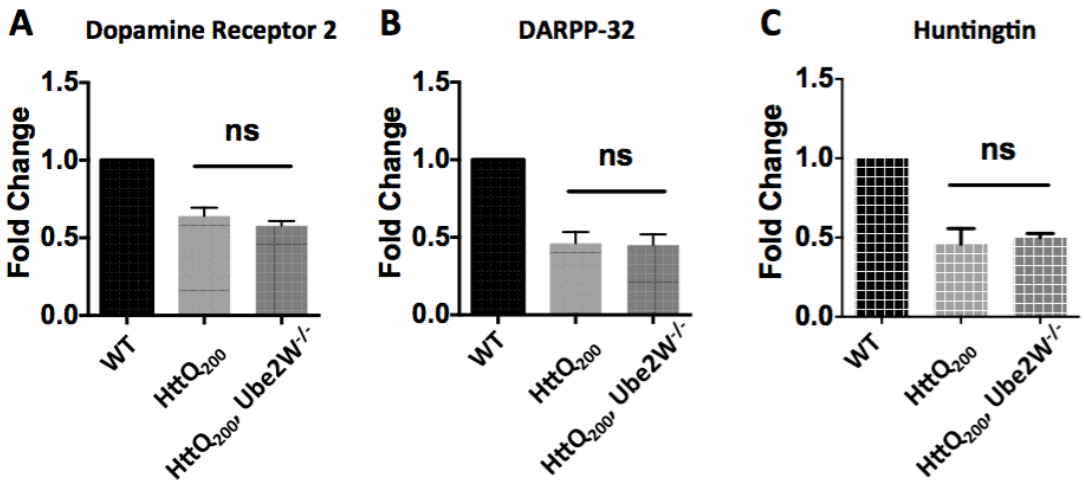

FIGURE 21. Ube2W deficiency does not cause significant changes in levels of major chaperone proteins.

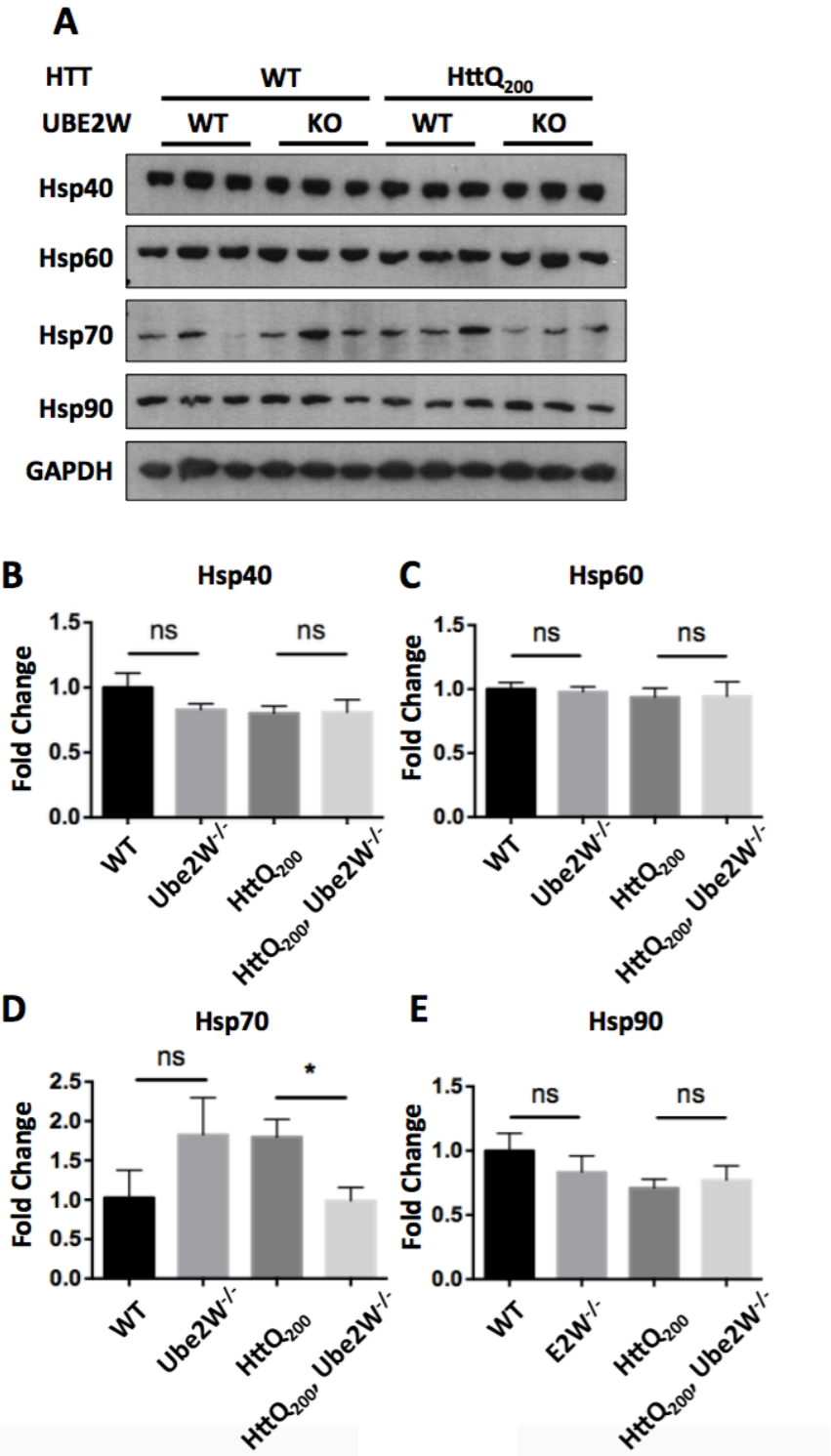

3.6 FIGURE LEGENDS

FIGURE 15. Ube2W alters $Htt^{ex1}Q_{103}$-GFP inclusion formation in HEK293 cells

$Htt^{ex1}Q_{103}$ inclusion is visualized by GFP fluorescence with co-overexpression of vector (A), Ube2W (B), W144E (C) and C91A (D). Scale bar=30 μm.

$Htt^{ex1}Q_{103}$ inclusion number (E) and size (F) from all four groups were plotted. Graphs show means +/- SEM; ***, p<0.001; ****, p<0.0001. n=8 (E), n>34 (F).

FIGURE 16. Ube2W alters solubility of $Htt^{ex1}Q_{103}$

A. Western Blot of lysates from cells transfected with $Htt^{ex1}Q_{103}$ and Ube2W or its mutants, W144E and C91A. Upper panel is the Triton-X100 soluble fraction and lower panel is the Triton-X100 insoluble fraction. Blotted with anti-GFP ($Htt^{ex1}Q_{103}$), anti-tubulin-α and anti-Ube2W. (15 μg total protein loaded per lane.) Arrowheads indicate $Htt^{ex1}Q_{103}$, Ube2W or tubulin, and bracket indicates high molecular weight $Htt^{ex1}Q_{103}$ in stacking gel.

B. Autoradiograph of a representative ^{35}S-methionine pulse-chase experiment followed by GFP-IP and gel electrophoresis. Arrowhead indicates $Htt^{ex1}Q_{103}$ signal.

C-E. Quantification of Western Blot in panel A. Graphs show means +/- SEM; ns, not significant; *, p<0.05; ***, p<0.001; ****, p<0.0001. n=3.

F. Quantification of autoradiograph in panel B. Graphs show means +/- SEM; ns, not significant. n=3.

FIGURE 17. Ube2W deficiency results in decreased $Htt^{ex1}Q_{72}$ inclusion formation and increased neuronal survival

A. Representative images from automated fluorescence microscopy. Primary cortical neurons from WT and *Ube2W* KO mice were transfected with mApple and $Htt^{ex1}Q_{72}$-EGFP, and survival was determined by repeated imaging at regular intervals. The last time at which the cell was noted to be alive (red arrows) was used as the time of death. Cells that survive the entire length of the experiment (blue arrow) were censored (analyzed as living cell at the end of experiment). Scale bar=25 μm.

B. Cumulative risk of death over time for WT and *Ube2W* KO neurons transfected with EGFP, $Htt^{ex1}Q_{17}$-EGFP and $Htt^{ex1}Q_{72}$-EGFP. Results were pooled from 16 wells per condition, with experiments performed in duplicate.

C-F. Quantification of EGFP signals or inclusion formation from experiments in panel A. Graphs show means +/- SEM; ns, not significant; *, $p<0.05$. $n>232$.

FIGURE 18. Ube2W deficiency increases soluble Htt levels in *HdhQ200* KI mice

A. Western Blot of mouse frontal brain lysates from WT, *Ube2W* KO, $HdhQ_{200}$ heterozygous (het) KI, $HdhQ_{200}$ het KI with *Ube2W* KO mice. Blotted with anti-Htt, anti-polyQ, anti-Ube2W and anti-GAPDH antibodies. (40 μg total protein loaded per lane.) Arrowheads represent mutant $HttQ_{200}$; arrow represents WT Htt.

B and C. Quantification of Western Blot in panel A. Graphs show means +/- SEM; ns, not significant; *, $p<0.05$; **, $p<0.01$. $n=3$.

FIGURE 19. Absence of Ube2W does not alter $HttQ_{200}$ inclusion levels in striatum of *HdhQ*$_{200}$ KI mice

A and B. Htt immunostaining of striatum showing $HttQ_{200}$ intranuclear inclusions in 46 weeks old *HdhQ*$_{200}$ het KI, *HdhQ*$_{200}$ het KI with *Ube2W* KO mice. Inserts show magnified region represented on the left panel. Scale bar on the left panel=200 μm; Scale bar of insert=50 μm.

$HTT^{ex1}Q_{103}$ inclusion number (C) and size (D) from both 32 weeks and 46 weeks old mice of both groups were plotted. Graphs show means +/- SEM; ns, not significant. n=10 (C), n>10 (D).

FIGURE 20. Ube2W deficiency does not alter transcript levels of striatal neuronal markers in *HdhQ*$_{200}$ KI mice.

Dopamine receptor 2 (Drd2) (A), DARPP-32 (Ppp1r1b) (B) and Huntingtin (Hdh) (C) transcript levels are measured by qRT-PCR amplification. RNAs were extracted from WT, *HdhQ*$_{200}$ het KI, *HdhQ*$_{200}$ het KI with *Ube2W* KO mice frontal brains. Results are normalized to β-actin (Actb) levels. Results were quantified and plotted as graphs. Graphs show means +/- SEM; ns, not significant. n=4.

FIGURE 21. Ube2W deficiency does not cause significant changes in levels of major chaperone proteins.

A. Western Blot of mouse frontal brain lysates from WT, *Ube2W* KO, *HdhQ*$_{200}$ het KI, *HdhQ*$_{200}$ het KI with *Ube2W* KO mice. Blotted with anti-Hsp40, anti-Hsp60, anti-Hsp70and anti-Hsp90 antibodies. (40 μg total protein loaded per lane.)

B-E. Quantification of Western Blot in panel A. Graphs show means +/- SEM; ns, not significant; *, $p<0.05$; n=3.

Chapter Four: Conclusions and future directions

In the previous three chapters, I investigated the biological functions of Ube2W and N-terminal ubiquitination. In chapter 1, I reviewed different ubiquitin pathways and their involvement in the pathogenesis of Huntington's disease. In chapter 2, I explored the potential in vivo functions of Ube2W, a N-terminal ubiquitinating E2, utilizing a novel *Ube2W* KO mouse model. I found that Ube2W plays an important function in mouse early post-natal survival, epidermal differentiation, and in the immune and male reproductive systems. In chapter 3, I investigated Ube2W's function in a prototypical protein-misfolding neurodegenerative disease, Huntington's disease; I showed that Ube2W regulates soluble level of Htt. In this final chapter, I discuss potential future studies building on the results of chapters 2 and 3, which should provide further insight into the biological functions of Ube2W-mediated N-terminal ubiquitination.

4.1 Ube2W involvement in skin differentiation

The sequential differentiation of epidermis is essential for post-natal survival. The loss of keratohyalin granules and altered Loricrin immunostaining in *Ube2W* KO P0 mice suggest a defect in barrier function, which can result in early postnatal lethality due to excessive water loss (reviewed in 37, 38). A similar phenotype was reported in other mouse models: for example, transient

knockdown of filaggrin, component of keratohyalin granules, results in reduced number of keratohyaline granules and reduced stratum corneum thickness(213); Filaggrin-null mice show a loss of skin barrier integrity analyzed by immunostaining and transepidermal water loss assay(214, 215). Detailed studies of skin barrier function and keratohyalin granule components in *Ube2W* KO mice will be helpful to further characterize the skin defect.

In *Ube2W* KO mice, the 60% postnatal lethality we observe is a similar percentage to that of the altered skin phenotype, suggesting a potential link between the epidermal differentiation defect and early postnatal lethality. In order to establish a direct cause-effect relationship between the skin defect and early postnatal lethality, I have already begun experiments to delete Ube2W selectively in epidermis using tissue-specific Cre-Lox recombination. Keratin-5 promoter-driven Cre expression results in confined Ube2W deletion in basal cell layer, and thus after epidermal differentiation, all epidermal layers will be deficient of Ube2W(216). By the time of my thesis defense, given the limited number of mice recovered I cannot yet reach a conclusion. If the same percentage of lethality and skin defect is observed in K5-driven *Ube2W* KO mice, it will suggest that Ube2W causes mouse early postnatal lethality due to a defect in skin differentiation.

4.2 Identification of N-terminal ubiquitin-modified proteome

To further investigate the function of N-terminal ubiquitination, more substrates should be identified and studied. The current identification of N-

terminal ubiquitination substrates has relied on two key methods: 1) mass spectrometry to identify fusion peptides directly linking the C-terminal glycine of Ub to the N-terminal methionine of the substrate; and 2) in vitro ubiquitination assays in which candidate substrates are mixed with E1, E2, E3, Ub and ATPs. If lysine-less substrate can still be ubiquitinated and blockade of α-amino group can abolish ubiquitination, the tested substrate is considered a N-terminal ubiquitination target. However, both methods identify targets individually instead of globally. Global identification of N-terminal ubiquitination targets performed in an unbiased manner would greatly facilitate future studies of the function of N-terminal modification.

The canonical ubiquitin-modified proteome has been widely studied in the past decade(217–220). Trypsin digestion of an ubiquitin-conjugated protein produces a signature peptide at the ubiquitination site containing a two-residue remnant (glycine-glycine) that is derived from the C terminus of ubiquitin and is still covalently attached to the target lysine residue via an isopeptide bond. This signature peptide (GGK) has a mass shift at the lysine residue of 114.1 Da, as well as a missed proteolytic cleavage because trypsin proteolysis cannot occur at these modified lysines. Due to this feature, ubiquitinated substrates can be identified by mass spectrometry(220). Under the same basis, monoclonal antibody derived from the signature peptide GGK can capture the ubiquitinated proteins by immunoprecipitation(217–219). The antibody is specific to Ub-modified lysines instead of linear peptide bond-linked lysines.

However, the systematic detection of N-terminal ubiquitination is more complicated. In the cellular microenvironment, a process called N-terminal methionine excision happens to approximately 60-70% of proteins(221). During this process, methionine aminopeptidase cleaves the N-terminal methionine, thus the new protein starts with the second amino acid(222, 223). Among the 30-40% of proteins whose starting methionine remains intact, a majority will be acetylated, physically blocking the N-terminus from ubiquitination. Accordingly, only 14-22% of proteins are predicted to be potential candidates for acquiring the signature peptide (GGM) seen upon N-terminal ubiquitination. In addition, unlike canonical lysine ubiquitination, the linkage between the ubiquitin C-terminus and N-terminal methionine is linear. Hence the linkage sequence GGM does not differ from GGM derived from internal protein sequences. The three-peptide sequence is too short to identify any protein specifically.

Since currently there is no specific method to identify fusion peptides of N-terminal ubiquitination, indirect methods have to be used. One possible alternative strategy is to utilize *Ube2W* KO cells or mice. Since Ube2W is the only E2 known to carry out N-terminal ubiquitination, deletion of Ube2W should abolish such ubiquitination. For N-terminally ubiquitinated substrates, the N-terminal protein sequence will differ in the presence or absence of Ube2W: the protein's N-terminus would start with ubiquitin in the WT proteome but with its own N-terminus in the *Ube2W* KO proteome. Protein N-terminus profiling enables these changes to be identified by mass spectrometry. There are both positive and negative selection methods to identify protein N-termini.

Strategies for positive selection in N-terminus profiling involve chemical or enzymatic tagging of protein N-termini before trypsination. For example, biotin can be tagged to the N-termini of proteins by a modified subtiligase; after trypsination, an avidin column captures biotin-ligated N-terminal peptides. The attached biotin can be cleaved by the tobacco etch virus (TEV) protease(224). However, positive selection has its limitations: 1) it is highly dependent on complete ligation efficiency and subtiligase specificity, especially when comparing protein abundance among different samples(225, 226); and 2) it can only identify free protein N-termini instead of naturally modified N-termini such as with acetylation.

Negative selection removes internal peptides, thus enriching both free and modified N-terminal peptides. The protein's α-amino group is first protected either by acetylation or dimethylation, followed by trypsin digestion to generate internal peptides with unprotected N-terminal amines. Using different methods, these newly generated internal peptides can be removed. Protected N-terminal peptides are preserved and can be sequenced thereafter. These negative selection approaches include: Combined Fractional Diagonal Chromatography (COFRADIC), Dimethyl Isotope-Coded Affinity Selection (DICAS), Terminal Amine Isotope Labeling of Substrates (TAILS), and phosphor tagging(225, 227–229).

Taken together, a combination of protein N-terminal profiling and stable isopeptide labeling (such as the TMT-labeling used in Chapter 2) can quantitatively assess the abundance of N-terminal peptides. Comparison

between the WT and *Ube2W* KO N-terminome will globally identify N-terminal ubiquitinated proteins and facilitate the functional study of such modification.

4.3 Protamine-2 as a potential target for Ube2W N-terminal ubiquitination

Consistent with the recent view that Ube2W may preferentially target substrates with disordered N-termini, our bioinformatic analysis revealed an accumulation of proteins with increased disorder in *Ube2W* KO testis. Protamine-2, an intrinsically disordered testicular protein, was confirmed by Western blot analysis to be increased in the absence of Ube2W. The N-terminus of protamine-2 is highly disordered: it starts with a continuous length disorder (CLD) region and 80% of its amino acids are disordered according to both IUPRED and DisEMBL prediction algorithms. Protamines are DNA binding proteins that are critical for testicular function. The association between DNA and protamines leads to substantial molecular remodeling and ultimately to 10-fold compaction of the male genome into toroidal nucleoprotamine structures. Protamines facilitate the hydrodynamic shape of the sperm head and protect the paternal genome from physical and chemical damage(230). In mature spermatozoa, about 85% of histones are replaced by the protamine-1 and protamine-2 in humans. Compared to the 51-amino-acid long protamine-1, the 107-amino-acid protamine-2 is twice the size, yet has fewer post-translational modifications. Protamine-1 is acetylated on the N-terminus amine, which potentially blocks other modifications, whereas protamine-2 retains a free α-amino group(231). Collectively this information

suggests that protamine-2 is a strong candidate target for Ube2W. Further experiments should be performed to validate this idea: 1) in vitro ubiquitination assay to prove that lysine-less mutant protamine can be ubiquitinated, and that blocking its N-terminus can abolish ubiquitination; 2) protamine-2 enrichment followed by mass spectrometry should identify the signature peptide of Ub modification on the protamine-2 N-terminus; and 3) cell-based experiments to study whether protamine-2 ubiquitination and degradation are altered by Ube2W overexpression or knock-down.

4.4 Ube2W's effect on insoluble Htt and HD disease progression

In chapter 3, I showed that Ube2W deficiency results in an increase of soluble Htt monomers in Htt KI mice, without significantly altering inclusion formation and HD severity at 32 weeks of age. As discussed in chapter 1, mutant Htt protein tends to misfold and accumulate in cells. Such accumulation can present as inclusion bodies or oligomers. When I analyze Htt expression by Western blotting, protein lysates are first denatured by detergents. This process generates two fractions of Htt: detergent-soluble and detergent-insoluble. A complete analysis of both fractions will help us understand the precise function of Ube2W with respect to Htt solubility and clearance

Currently there are two common methods to analyze the Htt insoluble fraction: 1) filter retardation assay (dot blot) where protein lysates are run through micropores on a cellulose acetate membrane trapping the insoluble material on the membrane (flow-through containing soluble Htt is discarded). 2) the use of

stronger detergents to further denature insoluble Htt (usually 4% SDS and 30mins boiling) and allow visualization of insoluble fraction by Western blotting. I hypothesize that Ube2W-driven N-terminal ubiquitination of Htt is a stabilizing signal that promotes Htt oligomer formation. When Ube2W is knocked-out in HD KI mice, the loss of this stabilizing signal triggers Htt to solubilize, leading to an increase in soluble Htt and a decrease in oligomeric, insoluble Htt. However, if the absence of Ube2W results in an increase in both soluble and insoluble Htt fractions, it would suggest that Ube2W mediates Htt clearance. This possibility is supported by the study in chapter 2 that showed a preferential accumulation of disordered protein in *Ube2W* KO testis, implying that Ube2W-mediated N-terminal ubiquitination can be a degradation signal.

Whether mutant Htt is indeed N-terminally ubiquitinated in vivo is still unknown. Given the published in vitro data(68), Htt is a compelling target for Ube2W. Mass spectrometry confirmation of Ube2W-driven N-terminal ubiquitination of Htt will be important to establish it as an actual target. The existence of signature peptide for N-terminal modification in WT brain, while missing in *Ube2W* KO brain, would prove that Ube2W indeed ubiquitinates Htt's α-amino group. However achieving this requires a clean immunoprecipitation (IP) of Htt, which is challenging since most mutant Htt exists as insoluble species that are not easily accessible to antibodies in an IP experiment. To address this issue, one could examine a different organ other than brain. As discussed earlier, the Htt mutation is present in every cell in the body although inclusion formation and signs of cytopathology are limited to nervous system. In other organs, Htt is more

soluble and accessible to IP antibodies. So, a Htt-IP from non-neuronal tissues followed by mass spectrometry might provide direct evidence for Htt N-terminal ubiquitination.

As introduced in chapter 1, mutant Htt accumulation is enhanced by Htt SUMOylation on K6 and K9 by PIAS1(144, 145). If Ube2W adds a bulky 8.5kDa ubiquitin to Htt's crowded N-terminus, such N-terminal ubiquitination conceivably could block or alter other modifications on Htt near the N-terminus (Fig 5). Moreover, SUMO-2 itself can be N-terminally ubiquitinated by Ube2W(67). Thus, alteration of mutant Htt levels in *Ube2W* KO mice might be explained by a secondary effect on SUMO-2 ubiquitination. In order to test this hypothesis, Htt SUMOylation levels can be measured by SUMO enrichment followed by Htt blotting. Additionally, I could use cultured cells to study this hypothesis: a SUMO-2 di-glycine mutation abolishes substrate binding, and thus if co-overexpression of this SUMO-2 mutant did not influence Ube2W's effects on Htt levels, it would indicate Ube2W does not act on Htt primarily through a SUMO-2 dependent mechanism.

4.5 Concluding remarks

Ubiquitin pathways are involved in many cellular processes and are implicated in a wide range of human diseases. N-terminal ubiquitination is easily missed by current methods, yet may play a key role in multiple organ systems. The recent identification of Ube2W as the only E2 that carries out N-terminal ubiquitination has helped to shed light on the potential roles of this noncanonical

ubiquitin pathway. My dissertation work explored the importance of this intriguing E2 in vivo, addressing its possible roles in different organ systems. It also provided in vivo support for the view that Ube2W preferably targets disordered substrates. Protein disorderness is implicated in protein-misfolding diseases such as Huntington's disease. While more work remains, my studies on Ube2W and HD have begun to provide insight into how the ubiquitin system can regulate misfolded proteins contributing to diseases. Alterations of ubiquitin pathways have the potential to influence the processing and clearance of disease proteins. Thus, they represent potential therapeutic targets in a large class of protein-misfolding diseases, many of which are currently untreatable and fatal disorders.

References:

1. Kravtsova-Ivantsiv, Y., and Ciechanover, A. (2012) Non-canonical ubiquitin-based signals for proteasomal degradation. *J. Cell Sci.* **125**, 539–548

2. Hoege, C., Pfander, B., Moldovan, G.-L., Pyrowolakis, G., and Jentsch, S. (2002) RAD6-dependent DNA repair is linked to modification of PCNA by ubiquitin and SUMO. *Nature*. **419**, 135–41

3. Hibbert, R. G., Huang, A., Boelens, R., and Sixma, T. K. (2011) E3 ligase Rad18 promotes monoubiquitination rather than ubiquitin chain formation by E2 enzyme Rad6. *Proc. Natl. Acad. Sci. U. S. A.* **108**, 5590–5

4. Bergink, S., and Jentsch, S. (2009) Principles of ubiquitin and SUMO modifications in DNA repair. *Nature*. **458**, 461–7

5. Christensen, D. E., Brzovic, P. S., and Klevit, R. E. (2007) E2-BRCA1 RING interactions dictate synthesis of mono- or specific polyubiquitin chain linkages. *Nat. Struct. Mol. Biol.* **14**, 941–948

6. Brzovic, P. S., Lissounov, A., Christensen, D. E., Hoyt, D. W., and Klevit, R. E. (2006) A UbcH5/ubiquitin noncovalent complex is required for processive BRCA1-directed ubiquitination. *Mol. Cell*. **21**, 873–80

7. Wu, K., Kovacev, J., and Pan, Z.-Q. (2010) Priming and extending: a UbcH5/Cdc34 E2 handoff mechanism for polyubiquitination on a SCF substrate. *Mol. Cell*. **37**, 784–96

8. Garcia-Higuera, I., Taniguchi, T., Ganesan, S., Meyn, M. S., Timmers, C., Hejna, J., Grompe, M., and D'Andrea, A. D. (2001) Interaction of the Fanconi anemia proteins and BRCA1 in a common pathway. *Mol. Cell*. **7**, 249–62

9. Rodrigo-Brenni, M. C., and Morgan, D. O. (2007) Sequential E2s drive polyubiquitin chain assembly on APC targets. *Cell*. **130**, 127–39

10. Jin, L., Williamson, A., Banerjee, S., Philipp, I., and Rape, M. (2008) Mechanism of ubiquitin-chain formation by the human anaphase-promoting complex. *Cell*. **133**, 653–65

11. Sadowski, M., and Sarcevic, B. (2010) Mechanisms of mono- and poly-ubiquitination: Ubiquitination specificity depends on compatibility between the E2 catalytic core and amino acid residues proximal to the lysine. *Cell Div.* **5**, 19

12. Dou, H., Buetow, L., Hock, A., Sibbet, G. J., Vousden, K. H., and Huang, D. T. (2012) Structural basis for autoinhibition and phosphorylation-dependent activation of c-Cbl. *Nat. Struct. Mol. Biol.* **19**, 184–92

13. Kobashigawa, Y., Tomitaka, A., Kumeta, H., Noda, N. N., Yamaguchi, M., and Inagaki, F. (2011) Autoinhibition and phosphorylation-induced activation mechanisms of human cancer and autoimmune disease-related E3 protein Cbl-b. *Proc. Natl. Acad. Sci. U. S. A.* **108**, 20579–84

14. Katzmann, D. J., Odorizzi, G., and Emr, S. D. (2002) Receptor downregulation and multivesicular-body sorting. *Nat. Rev. Mol. Cell Biol.* **3**, 893–905

15. Woelk, T., Oldrini, B., Maspero, E., Confalonieri, S., Cavallaro, E., Di Fiore, P. P., and Polo, S. (2006) Molecular mechanisms of coupled monoubiquitination. *Nat. Cell Biol.* **8**, 1246–54

16. Raiborg, C., Bache, K. G., Gillooly, D. J., Madshus, I. H., Stang, E., and Stenmark, H. (2002) Hrs sorts ubiquitinated proteins into clathrin-coated microdomains of early endosomes. *Nat. Cell Biol.* **4**, 394–8

17. Jura, N., Scotto-Lavino, E., Sobczyk, A., and Bar-Sagi, D. (2006) Differential modification of Ras proteins by ubiquitination. *Mol. Cell*. **21**, 679–87

18. Sasaki, A. T., Carracedo, A., Locasale, J. W., Anastasiou, D., Takeuchi, K., Kahoud, E. R., Haviv, S., Asara, J. M., Pandolfi, P. P., and Cantley, L. C. (2011) Ubiquitination of K-Ras enhances activation and facilitates binding to select downstream effectors. *Sci. Signal.* **4**, ra13

19. Baker, R., Lewis, S. M., Sasaki, A. T., Wilkerson, E. M., Locasale, J. W., Cantley, L. C., Kuhlman, B., Dohlman, H. G., and Campbell, S. L. (2013) Site-specific monoubiquitination activates Ras by impeding GTPase-activating protein function. *Nat. Struct. Mol. Biol.* **20**, 46–52

20. Baker, R., Wilkerson, E. M., Sumita, K., Isom, D. G., Sasaki, A. T., Dohlman, H. G., and Campbell, S. L. (2013) Differences in the regulation of K-Ras and H-Ras isoforms by monoubiquitination. *J. Biol. Chem.* **288**, 36856–62

21. Pan, M.-R., Peng, G., Hung, W.-C., and Lin, S.-Y. (2011) Monoubiquitination of H2AX protein regulates DNA damage response signaling. *J. Biol. Chem.* **286**, 28599–607

22. Rajendra, E., Oestergaard, V. H., Langevin, F., Wang, M., Dornan, G. L., Patel, K. J., and Passmore, L. A. (2014) The genetic and biochemical basis of FANCD2 monoubiquitination. *Mol. Cell*. **54**, 858–69

23. Zhang, Y., Zhou, X., Zhao, L., Li, C., Zhu, H., Xu, L., Shan, L., Liao, X., Guo, Z., and Huang, P. (2011) UBE2W interacts with FANCL and regulates the monoubiquitination of fanconi anemia protein FANCD2. *Mol. Cells*. **31**, 113–122

24. Alpi, A. F., Pace, P. E., Babu, M. M., and Patel, K. J. (2008) Mechanistic insight into site-restricted monoubiquitination of FANCD2 by Ube2t, FANCL, and FANCI. *Mol. Cell*. **32**, 767–77

25. Scaglione, K. M., Zavodszky, E., Todi, S. V., Patury, S., Xu, P., Rodríguez-Lebrón, E., Fischer, S., Konen, J., Djarmati, A., Peng, J., Gestwicki, J. E., and Paulson, H. L. (2011) Ube2w and Ataxin-3 Coordinately Regulate the Ubiquitin Ligase CHIP. *Mol. Cell*. **43**, 599–612

26. Thrower, J. S., Hoffman, L., Rechsteiner, M., and Pickart, C. M. (2000) Recognition of the polyubiquitin proteolytic signal. *EMBO J.* **19**, 94–102

27. Merkley, N., and Shaw, G. S. (2004) Solution structure of the flexible class II ubiquitin-conjugating enzyme Ubc1 provides insights for polyubiquitin chain assembly. *J. Biol. Chem.* **279**, 47139–47

28. Dai, R. M., and Li, C. C. (2001) Valosin-containing protein is a multi-ubiquitin chain-targeting factor required in ubiquitin-proteasome degradation. *Nat. Cell Biol.* **3**, 740–4

29. Williams, K. L., Warraich, S. T., Yang, S., Solski, J. A., Fernando, R., Rouleau, G. A., Nicholson, G. A., and Blair, I. P. (2012) UBQLN2/ubiquilin 2 mutation and pathology in familial amyotrophic lateral sclerosis. *Neurobiol. Aging*. **33**, 2527.e3–10

30. Deng, H.-X., Chen, W., Hong, S.-T., Boycott, K. M., Gorrie, G. H., Siddique, N., Yang, Y., Fecto, F., Shi, Y., Zhai, H., Jiang, H., Hirano, M., Rampersaud, E., Jansen, G. H., Donkervoort, S., Bigio, E. H., Brooks, B. R., Ajroud, K., Sufit, R. L., Haines, J. L., Mugnaini, E., Pericak-Vance, M. A., and Siddique, T. (2011) Mutations in UBQLN2 cause dominant X-linked juvenile and adult-onset ALS and ALS/dementia. *Nature*. **477**, 211–5

31. Bedford, L., Paine, S., Sheppard, P. W., Mayer, R. J., and Roelofs, J. (2010) Assembly, structure, and function of the 26S proteasome. *Trends Cell Biol.* **20**, 391–401

32. Wickliffe, K. E., Williamson, A., Meyer, H.-J., Kelly, A., and Rape, M. (2011) K11-linked ubiquitin chains as novel regulators of cell division. *Trends Cell Biol.* **21**, 656–63

33. Spence, J., Sadis, S., Haas, A., and Finley, D. (1995) A ubiquitin mutant with specific defects in DNA repair and multiubiquitination. *Mol. Cell. Biol.* **15**, 1265–1273

34. Arnason, T., and Ellison, M. J. (1994) Stress resistance in Saccharomyces cerevisiae is strongly correlated with assembly of a novel type of multiubiquitin chain. *Mol. Cell. Biol.* **14**, 7876–7883

35. Silva, G. M., Finley, D., and Vogel, C. (2015) K63 polyubiquitination is a new modulator of the oxidative stress response. *Nat. Struct. Mol. Biol.* **22**, 116–123

36. Mukhopadhyay, D., and Riezman, H. (2007) Proteasome-independent functions of ubiquitin in endocytosis and signaling. *Science*. **315**, 201–5

37. Sun, L., and Chen, Z. J. (2004) The novel functions of ubiquitination in signaling. *Curr. Opin. Cell Biol.* **16**, 119–26

38. Vucic, D., Dixit, V. M., and Wertz, I. E. (2011) Ubiquitylation in apoptosis: a post-translational modification at the edge of life and death. *Nat. Rev. Mol. Cell Biol.* **12**, 439–52

39. Seymour, R. E., Hasham, M. G., Cox, G. A., Shultz, L. D., Hogenesch, H., Roopenian, D. C., and Sundberg, J. P. (2007) Spontaneous mutations in the mouse Sharpin gene result in multiorgan inflammation, immune system dysregulation and dermatitis. *Genes Immun.* **8**, 416–21

40. Boisson, B., Laplantine, E., Prando, C., Giliani, S., Israelsson, E., Xu, Z., Abhyankar, A., Israël, L., Trevejo-Nunez, G., Bogunovic, D., Cepika, A.-M., MacDuff, D., Chrabieh, M., Hubeau, M., Bajolle, F., Debré, M., Mazzolari, E., Vairo, D., Agou, F., Virgin, H. W., Bossuyt, X., Rambaud, C., Facchetti, F., Bonnet, D., Quartier, P., Fournet, J.-C., Pascual, V., Chaussabel, D., Notarangelo, L. D., Puel, A., Israël, A., Casanova, J.-L., and Picard, C. (2012) Immunodeficiency, autoinflammation and amylopectinosis in humans with inherited HOIL-1 and LUBAC deficiency. *Nat. Immunol.* **13**, 1178–86

41. Williams, C., van den Berg, M., Sprenger, R. R., and Distel, B. (2007) A conserved cysteine is essential for Pex4p-dependent ubiquitination of the peroxisomal import receptor Pex5p. *J. Biol. Chem.* **282**, 22534–43

42. Kragt, A., Voorn-Brouwer, T., van den Berg, M., and Distel, B. (2005) The Saccharomyces cerevisiae peroxisomal import receptor Pex5p is monoubiquitinated in wild type cells. *J. Biol. Chem.* **280**, 7867–74

43. Carvalho, A. F., Pinto, M. P., Grou, C. P., Alencastre, I. S., Fransen, M., Sá-Miranda, C., and Azevedo, J. E. (2007) Ubiquitination of mammalian Pex5p, the peroxisomal import receptor. *J. Biol. Chem.* **282**, 31267–72

44. Léon, S., and Subramani, S. (2007) A conserved cysteine residue of Pichia pastoris Pex20p is essential for its recycling from the peroxisome to the cytosol. *J. Biol. Chem.* **282**, 7424–30

45. Grou, C. P., Carvalho, A. F., Pinto, M. P., Wiese, S., Piechura, H., Meyer, H. E., Warscheid, B., Sá-Miranda, C., and Azevedo, J. E. (2008) Members of the E2D (UbcH5) family mediate the ubiquitination of the conserved cysteine of Pex5p, the peroxisomal import receptor. *J. Biol. Chem.* **283**, 14190–7

46. Vosper, J. M. D., McDowell, G. S., Hindley, C. J., Fiore-Heriche, C. S., Kucerova, R., Horan, I., and Philpott, A. (2009) Ubiquitylation on canonical and non-canonical sites targets the transcription factor neurogenin for ubiquitin-mediated proteolysis. *J. Biol. Chem.* **284**, 15458–68

47. McDowell, G. S., Kucerova, R., and Philpott, A. (2010) Non-canonical ubiquitylation of the proneural protein Ngn2 occurs in both Xenopus embryos and mammalian cells. *Biochem. Biophys. Res. Commun.* **400**, 655–60

48. Wang, X., Herr, R. A., Chua, W.-J., Lybarger, L., Wiertz, E. J. H. J., and Hansen, T. H. (2007) Ubiquitination of serine, threonine, or lysine residues on the cytoplasmic tail can induce ERAD of MHC-I by viral E3 ligase mK3. *J. Cell Biol.* **177**, 613–24

49. Roark, R., Itzhaki, L., and Philpott, A. (2012) Complex regulation controls Neurogenin3 proteolysis. *Biol. Open*. **1**, 1264–72

50. Anania, V. G., Bustos, D. J., Lill, J. R., Kirkpatrick, D. S., and Coscoy, L. (2013) A Novel Peptide-Based SILAC Method to Identify the Posttranslational Modifications Provides Evidence for Unconventional Ubiquitination in the ER-Associated Degradation Pathway. *Int. J. Proteomics*. **2013**, 857918

51. Ikeda, M., Ikeda, A., and Longnecker, R. (2002) Lysine-independent ubiquitination of Epstein-Barr virus LMP2A. *Virology*. **300**, 153–9

52. Breitschopf, K., Bengal, E., Ziv, T., Admon, A., and Ciechanover, A. (1998) A novel site for ubiquitination: the N-terminal residue, and not internal lysines of MyoD, is essential for conjugation and degradation of the protein. *EMBO J.* **17**, 5964–73

53. Aviel, S., Winberg, G., Massucci, M., and Ciechanover, A. (2000) Degradation of the epstein-barr virus latent membrane protein 1 (LMP1) by the ubiquitin-proteasome pathway. Targeting via ubiquitination of the N-terminal residue. *J. Biol. Chem.* **275**, 23491–9

54. Chen, X., Barton, L. F., Chi, Y., Clurman, B. E., and Roberts, J. M. (2007) Ubiquitin-independent degradation of cell-cycle inhibitors by the REGgamma proteasome. *Mol. Cell*. **26**, 843–52

55. Coulombe, P., Rodier, G., Bonneil, E., Thibault, P., and Meloche, S. (2004) N-Terminal ubiquitination of extracellular signal-regulated kinase 3 and p21 directs their degradation by the proteasome. *Mol. Cell. Biol.* **24**, 6140–50

56. Scaglione, K. M., Basrur, V., Ashraf, N. S., Konen, J. R., Elenitoba-Johnson, K. S. J., Todi, S. V., and Paulson, H. L. (2013) The ubiquitin-conjugating enzyme (E2) ube2w ubiquitinates the N terminus of substrates. *J. Biol. Chem.* **288**, 18784–18788

57. Li, H., Okamoto, K., Peart, M. J., and Prives, C. (2009) Lysine-independent turnover of cyclin G1 can be stabilized by B'alpha subunits of protein phosphatase 2A. *Mol. Cell. Biol.* **29**, 919–28

58. Trausch-Azar, J. S., Lingbeck, J., Ciechanover, A., and Schwartz, A. L. (2004) Ubiquitin-Proteasome-mediated degradation of Id1 is modulated by MyoD. *J. Biol. Chem.* **279**, 32614–9

59. Fajerman, I., Schwartz, A. L., and Ciechanover, A. (2004) Degradation of the Id2 developmental regulator: targeting via N-terminal ubiquitination. *Biochem. Biophys. Res. Commun.* **314**, 505–12

60. Kuo, M.-L., den Besten, W., Bertwistle, D., Roussel, M. F., and Sherr, C. J. (2004) N-terminal polyubiquitination and degradation of the Arf tumor suppressor. *Genes Dev.* **18**, 1862–74

61. Trausch-Azar, J., Leone, T. C., Kelly, D. P., and Schwartz, A. L. (2010) Ubiquitin proteasome-dependent degradation of the transcriptional coactivator PGC-1{alpha} via the N-terminal pathway. *J. Biol. Chem.* **285**, 40192–200

62. Ben-Saadon, R., Fajerman, I., Ziv, T., Hellman, U., Schwartz, A. L., and Ciechanover, A. (2004) The tumor suppressor protein p16(INK4a) and the

human papillomavirus oncoprotein-58 E7 are naturally occurring lysine-less proteins that are degraded by the ubiquitin system. Direct evidence for ubiquitination at the N-terminal residue. *J. Biol. Chem.* **279**, 41414–21

63. Kimura, S. H., and Nojima, H. (2002) Cyclin G1 associates with MDM2 and regulates accumulation and degradation of p53 protein. *Genes Cells*. **7**, 869–80

64. Kimura, S. H., Ikawa, M., Ito, A., Okabe, M., and Nojima, H. (2001) Cyclin G1 is involved in G2/M arrest in response to DNA damage and in growth control after damage recovery. *Oncogene*. **20**, 3290–300

65. Sherr, C. J. (2004) Principles of Tumor Suppression. *Cell*. **116**, 235–246

66. Sharpless, E., and Chin, L. (2003) The INK4a/ARF locus and melanoma. *Oncogene*. **22**, 3092–8

67. Tatham, M. H., Plechanovová, A., Jaffray, E. G., Salmen, H., and Hay, R. T. (2013) Ube2W conjugates ubiquitin to α-amino groups of protein N-termini. *Biochem. J.* **453**, 137–45

68. Vittal, V., Shi, L., Wenzel, D. M., Scaglione, K. M., Duncan, E. D., Basrur, V., Elenitoba-Johnson, K. S. J., Baker, D., Paulson, H. L., Brzovic, P. S., and Klevit, R. E. (2014) Intrinsic disorder drives N-terminal ubiquitination by Ube2w. *Nat. Chem. Biol.* 10.1038/nchembio.1700

69. Fletcher, A. J., Christensen, D. E., Nelson, C., Tan, C. P., Schaller, T., Lehner, P. J., Sundquist, W. I., and Towers, G. J. (2015) TRIM5α requires Ube2W to anchor Lys63-linked ubiquitin chains and restrict reverse transcription. *EMBO J.* 10.15252/embj.201490361

70. Fletcher, A. J., Mallery, D. L., Watkinson, R. E., Dickson, C. F., and James, L. C. (2015) Sequential ubiquitination and deubiquitination enzymes synchronize the dual sensor and effector functions of TRIM21. *Proc. Natl. Acad. Sci. U. S. A.* 10.1073/pnas.1507534112

71. Wu, P.-Y., Hanlon, M., Eddins, M., Tsui, C., Rogers, R. S., Jensen, J. P., Matunis, M. J., Weissman, A. M., Weisman, A. M., Wolberger, C., Wolberger, C. P., and Pickart, C. M. (2003) A conserved catalytic residue in the ubiquitin-conjugating enzyme family. *EMBO J.* **22**, 5241–50

72. Eddins, M. J., Carlile, C. M., Gomez, K. M., Pickart, C. M., and Wolberger, C. (2006) Mms2-Ubc13 covalently bound to ubiquitin reveals the structural basis of linkage-specific polyubiquitin chain formation. *Nat. Struct. Mol. Biol.* **13**, 915–20

73. Saha, A., Lewis, S., Kleiger, G., Kuhlman, B., and Deshaies, R. J. (2011) Essential role for ubiquitin-ubiquitin-conjugating enzyme interaction in ubiquitin discharge from Cdc34 to substrate. *Mol. Cell*. **42**, 75–83

74. Wickliffe, K. E., Lorenz, S., Wemmer, D. E., Kuriyan, J., and Rape, M. (2011) The mechanism of linkage-specific ubiquitin chain elongation by a single-subunit E2. *Cell*. **144**, 769–81

75. Arnesen, T., Van Damme, P., Polevoda, B., Helsens, K., Evjenth, R., Colaert, N., Varhaug, J. E., Vandekerckhove, J., Lillehaug, J. R., Sherman, F., and Gevaert, K. (2009) Proteomics analyses reveal the evolutionary conservation and divergence of N-terminal acetyltransferases from yeast and humans. *Proc. Natl. Acad. Sci. U. S. A.* **106**, 8157–62

76. Goetze, S., Qeli, E., Mosimann, C., Staes, A., Gerrits, B., Roschitzki, B., Mohanty, S., Niederer, E. M., Laczko, E., Timmerman, E., Lange, V., Hafen, E., Aebersold, R., Vandekerckhove, J., Basler, K., Ahrens, C. H., Gevaert, K., and Brunner, E. (2009) Identification and functional characterization of N-terminally acetylated proteins in Drosophila melanogaster. *PLoS Biol.* **7**, e1000236

77. McNab, F. W., Rajsbaum, R., Stoye, J. P., and O'Garra, A. (2011) Tripartite-motif proteins and innate immune regulation. *Curr. Opin. Immunol.* **23**, 46–56

78. Shi, M., Deng, W., Bi, E., Mao, K., Ji, Y., Lin, G., Wu, X., Tao, Z., Li, Z., Cai, X., Sun, S., Xiang, C., and Sun, B. (2008) TRIM30 alpha negatively regulates TLR-mediated NF-kappa B activation by targeting TAB2 and TAB3 for degradation. *Nat. Immunol.* **9**, 369–77

79. Pertel, T., Hausmann, S., Morger, D., Züger, S., Guerra, J., Lascano, J., Reinhard, C., Santoni, F. A., Uchil, P. D., Chatel, L., Bisiaux, A., Albert, M. L., Strambio-De-Castillia, C., Mothes, W., Pizzato, M., Grütter, M. G., and Luban, J. (2011) TRIM5 is an innate immune sensor for the retrovirus capsid lattice. *Nature*. **472**, 361–5

80. Shi, C.-H., Schisler, J. C., Rubel, C. E., Tan, S., Song, B., McDonough, H., Xu, L., Portbury, A. L., Mao, C.-Y., True, C., Wang, R.-H., Wang, Q.-Z., Sun, S.-L., Seminara, S. B., Patterson, C., and Xu, Y.-M. (2014) Ataxia and hypogonadism caused by the loss of ubiquitin ligase activity of the U box protein CHIP. *Hum. Mol. Genet.* **23**, 1013–24

81. Ronnebaum, S. M., Patterson, C., and Schisler, J. C. (2014) Emerging evidence of coding mutations in the ubiquitin–proteasome system associated with cerebellar ataxias. *Hum. Genome Var.* **1**, 14018

82. Malzac, P., Webber, H., Moncla, A., Graham, J. M., Kukolich, M., Williams, C., Pagon, R. A., Ramsdell, L. A., Kishino, T., and Wagstaff, J. (1998) Mutation analysis of UBE3A in Angelman syndrome patients. *Am. J. Hum. Genet.* **62**, 1353–60

83. Fang, P. (1999) The spectrum of mutations in UBE3A causing Angelman syndrome. *Hum. Mol. Genet.* **8**, 129–135

84. Hartl, F. U., Bracher, A., and Hayer-Hartl, M. (2011) Molecular chaperones in protein folding and proteostasis. *Nature*. **475**, 324–32

85. Fujimoto, M., Takaki, E., Hayashi, T., Kitaura, Y., Tanaka, Y., Inouye, S., and Nakai, A. (2005) Active HSF1 significantly suppresses polyglutamine aggregate formation in cellular and mouse models. *J. Biol. Chem.* **280**, 34908–16

86. Hayashida, N., Fujimoto, M., Tan, K., Prakasam, R., Shinkawa, T., Li, L., Ichikawa, H., Takii, R., and Nakai, A. (2010) Heat shock factor 1 ameliorates proteotoxicity in cooperation with the transcription factor NFAT. *EMBO J.* **29**, 3459–69

87. Kondo, N., Katsuno, M., Adachi, H., Minamiyama, M., Doi, H., Matsumoto, S., Miyazaki, Y., Iida, M., Tohnai, G., Nakatsuji, H., Ishigaki, S., Fujioka, Y., Watanabe, H., Tanaka, F., Nakai, A., and Sobue, G. (2013) Heat shock factor-1 influences pathological lesion distribution of polyglutamine-induced neurodegeneration. *Nat. Commun.* **4**, 1405

88. Bersuker, K., Hipp, M. S., Calamini, B., Morimoto, R. I., and Kopito, R. R. (2013) Heat shock response activation exacerbates inclusion body formation in a cellular model of Huntington disease. *J. Biol. Chem.* **288**, 23633–8

89. Fernandez-Funez, P., Nino-Rosales, M. L., de Gouyon, B., She, W. C., Luchak, J. M., Martinez, P., Turiegano, E., Benito, J., Capovilla, M., Skinner, P. J., McCall, A., Canal, I., Orr, H. T., Zoghbi, H. Y., and Botas, J. (2000) Identification of genes that modify ataxin-1-induced neurodegeneration. *Nature*. **408**, 101–6

90. Kazemi-Esfarjani, P., and Benzer, S. (2000) Genetic suppression of polyglutamine toxicity in Drosophila. *Science*. **287**, 1837–40

91. Bilen, J., and Bonini, N. M. (2007) Genome-wide screen for modifiers of ataxin-3 neurodegeneration in Drosophila. *PLoS Genet.* **3**, 1950–64

92. Chuang, J.-Z., Zhou, H., Zhu, M., Li, S.-H., Li, X.-J., and Sung, C.-H. (2002) Characterization of a brain-enriched chaperone, MRJ, that inhibits

Huntingtin aggregation and toxicity independently. *J. Biol. Chem.* **277**, 19831–8

93. Rujano, M. A., Kampinga, H. H., and Salomons, F. A. (2007) Modulation of polyglutamine inclusion formation by the Hsp70 chaperone machine. *Exp. Cell Res.* **313**, 3568–78

94. Hageman, J., Rujano, M. A., van Waarde, M. A. W. H., Kakkar, V., Dirks, R. P., Govorukhina, N., Oosterveld-Hut, H. M. J., Lubsen, N. H., and Kampinga, H. H. (2010) A DNAJB chaperone subfamily with HDAC-dependent activities suppresses toxic protein aggregation. *Mol. Cell*. **37**, 355–69

95. Wang, A. M., Miyata, Y., Klinedinst, S., Peng, H.-M., Chua, J. P., Komiyama, T., Li, X., Morishima, Y., Merry, D. E., Pratt, W. B., Osawa, Y., Collins, C. A., Gestwicki, J. E., and Lieberman, A. P. (2013) Activation of Hsp70 reduces neurotoxicity by promoting polyglutamine protein degradation. *Nat. Chem. Biol.* **9**, 112–8

96. Kuo, Y., Ren, S., Lao, U., Edgar, B. A., and Wang, T. (2013) Suppression of polyglutamine protein toxicity by co-expression of a heat-shock protein 40 and a heat-shock protein 110. *Cell Death Dis.* **4**, e833

97. Tokui, K., Adachi, H., Waza, M., Katsuno, M., Minamiyama, M., Doi, H., Tanaka, K., Hamazaki, J., Murata, S., Tanaka, F., and Sobue, G. (2009) 17-DMAG ameliorates polyglutamine-mediated motor neuron degeneration through well-preserved proteasome function in an SBMA model mouse. *Hum. Mol. Genet.* **18**, 898–910

98. Waza, M., Adachi, H., Katsuno, M., Minamiyama, M., Sang, C., Tanaka, F., Inukai, A., Doyu, M., and Sobue, G. (2005) 17-AAG, an Hsp90 inhibitor, ameliorates polyglutamine-mediated motor neuron degeneration. *Nat. Med.* **11**, 1088–95

99. Sittler, A., Lurz, R., Lueder, G., Priller, J., Lehrach, H., Hayer-Hartl, M. K., Hartl, F. U., and Wanker, E. E. (2001) Geldanamycin activates a heat shock response and inhibits huntingtin aggregation in a cell culture model of Huntington's disease. *Hum. Mol. Genet.* **10**, 1307–15

100. Holmberg, C. I., Staniszewski, K. E., Mensah, K. N., Matouschek, A., and Morimoto, R. I. (2004) Inefficient degradation of truncated polyglutamine proteins by the proteasome. *EMBO J.* **23**, 4307–18

101. Venkatraman, P., Wetzel, R., Tanaka, M., Nukina, N., and Goldberg, A. L. (2004) Eukaryotic proteasomes cannot digest polyglutamine sequences

and release them during degradation of polyglutamine-containing proteins. *Mol. Cell*. **14**, 95–104

102. Mandrusiak, L. M., Beitel, L. K., Wang, X., Scanlon, T. C., Chevalier-Larsen, E., Merry, D. E., and Trifiro, M. A. (2003) Transglutaminase potentiates ligand-dependent proteasome dysfunction induced by polyglutamine-expanded androgen receptor. *Hum. Mol. Genet.* **12**, 1497–506

103. Díaz-Hernández, M., Valera, A. G., Morán, M. A., Gómez-Ramos, P., Alvarez-Castelao, B., Castaño, J. G., Hernández, F., and Lucas, J. J. (2006) Inhibition of 26S proteasome activity by huntingtin filaments but not inclusion bodies isolated from mouse and human brain. *J. Neurochem.* **98**, 1585–96

104. Juenemann, K., Schipper-Krom, S., Wiemhoefer, A., Kloss, A., Sanz Sanz, A., and Reits, E. A. J. (2013) Expanded polyglutamine-containing N-terminal huntingtin fragments are entirely degraded by mammalian proteasomes. *J. Biol. Chem.* **288**, 27068–84

105. Michalik, A., and Van Broeckhoven, C. (2004) Proteasome degrades soluble expanded polyglutamine completely and efficiently. *Neurobiol. Dis.* **16**, 202–11

106. Neefjes, J., and Dantuma, N. P. (2004) Fluorescent probes for proteolysis: tools for drug discovery. *Nat. Rev. Drug Discov.* **3**, 58–69

107. Dantuma, N. P., Lindsten, K., Glas, R., Jellne, M., and Masucci, M. G. (2000) Short-lived green fluorescent proteins for quantifying ubiquitin/proteasome-dependent proteolysis in living cells. *Nat. Biotechnol.* **18**, 538–43

108. Stack, J. H., Whitney, M., Rodems, S. M., and Pollok, B. A. (2000) A ubiquitin-based tagging system for controlled modulation of protein stability. *Nat. Biotechnol.* **18**, 1298–302

109. Bennett, E. J., Bence, N. F., Jayakumar, R., and Kopito, R. R. (2005) Global impairment of the ubiquitin-proteasome system by nuclear or cytoplasmic protein aggregates precedes inclusion body formation. *Mol. Cell*. **17**, 351–65

110. Bence, N. F., Sampat, R. M., and Kopito, R. R. (2001) Impairment of the ubiquitin-proteasome system by protein aggregation. *Science*. **292**, 1552–5

111. Lindsten, K., Menéndez-Benito, V., Masucci, M. G., and Dantuma, N. P. (2003) A transgenic mouse model of the ubiquitin/proteasome system. *Nat. Biotechnol.* **21**, 897–902

112. Maynard, C. J., Böttcher, C., Ortega, Z., Smith, R., Florea, B. I., Díaz-Hernández, M., Brundin, P., Overkleeft, H. S., Li, J.-Y., Lucas, J. J., and Dantuma, N. P. (2009) Accumulation of ubiquitin conjugates in a polyglutamine disease model occurs without global ubiquitin/proteasome system impairment. *Proc. Natl. Acad. Sci. U. S. A.* **106**, 13986–91

113. Ortega, Z., Díaz-Hernández, M., Maynard, C. J., Hernández, F., Dantuma, N. P., and Lucas, J. J. (2010) Acute polyglutamine expression in inducible mouse model unravels ubiquitin/proteasome system impairment and permanent recovery attributable to aggregate formation. *J. Neurosci.* **30**, 3675–88

114. Lim, K.-L., and Lim, G. G. Y. (2011) K63-linked ubiquitination and neurodegeneration. *Neurobiol. Dis.* **43**, 9–16

115. Liu, C., Fei, E., Jia, N., Wang, H., Tao, R., Iwata, A., Nukina, N., Zhou, J., and Wang, G. (2007) Assembly of lysine 63-linked ubiquitin conjugates by phosphorylated alpha-synuclein implies Lewy body biogenesis. *J. Biol. Chem.* **282**, 14558–66

116. Tan, J. M. M., Wong, E. S. P., Kirkpatrick, D. S., Pletnikova, O., Ko, H. S., Tay, S.-P., Ho, M. W. L., Troncoso, J., Gygi, S. P., Lee, M. K., Dawson, V. L., Dawson, T. M., and Lim, K.-L. (2008) Lysine 63-linked ubiquitination promotes the formation and autophagic clearance of protein inclusions associated with neurodegenerative diseases. *Hum. Mol. Genet.* **17**, 431–9

117. Tan, J. M. M., Wong, E. S. P., Dawson, V. L., Dawson, T. M., and Lim, K.-L. (2008) Lysine 63-linked polyubiquitin potentially partners with p62 to promote the clearance of protein inclusions by autophagy. [online] http://scholarbank.nus.edu.sg/handle/10635/101043 (Accessed July 9, 2015)

118. Harjes, P., and Wanker, E. E. (2003) The hunt for huntingtin function: interaction partners tell many different stories. *Trends Biochem. Sci.* **28**, 425–33

119. Gerber, H. P., Seipel, K., Georgiev, O., Höfferer, M., Hug, M., Rusconi, S., and Schaffner, W. (1994) Transcriptional activation modulated by homopolymeric glutamine and proline stretches. *Science (80-.).* **263**, 808–811

120. Zoghbi, H. Y., and Orr, H. T. (2000) Glutamine repeats and neurodegeneration. *Annu. Rev. Neurosci.* **23**, 217–47

121. Duyao, M., Ambrose, C., Myers, R., Novelletto, A., Persichetti, F., Frontali, M., Folstein, S., Ross, C., Franz, M., Abbott, M., Gray, J., Conneally, P., Young, A., Penney, J., Hollingsworth, Z., Shoulson, I., Lazzarini, A., Falek, A., Koroshetz, W., Sax, D., Bird, E., Vonsattel, J., Bonilla, E., Alvir, J., Bickham Conde, J., Cha, J.-H., Dure, L., Gomez, F., Ramos, M., Sanchez-Ramos, J., Snodgrass, S., de Young, M., Wexler, N., Moscowitz, C., Penchaszadeh, G., MacFarlane, H., Anderson, M., Jenkins, B., Srinidhi, J., Barnes, G., Gusella, J., and MacDonald, M. (1993) Trinucleotide repeat length instability and age of onset in Huntington's disease. *Nat. Genet.* **4**, 387–392

122. Snell, R. G., MacMillan, J. C., Cheadle, J. P., Fenton, I., Lazarou, L. P., Davies, P., MacDonald, M. E., Gusella, J. F., Harper, P. S., and Shaw, D. J. (1993) Relationship between trinucleotide repeat expansion and phenotypic variation in Huntington's disease. *Nat. Genet.* **4**, 393–7

123. Nance, M. A., and Myers, R. H. (2001) Juvenile onset Huntington's disease--clinical and research perspectives. *Ment. Retard. Dev. Disabil. Res. Rev.* **7**, 153–7

124. Augood, S. J., Faull, R. L., Love, D. R., and Emson, P. C. (1996) Reduction in enkephalin and substance P messenger RNA in the striatum of early grade Huntington's disease: a detailed cellular in situ hybridization study. *Neuroscience*. **72**, 1023–36

125. Ginovart, N., Lundin, A., Farde, L., Halldin, C., Bäckman, L., Swahn, C. G., Pauli, S., and Sedvall, G. (1997) PET study of the pre- and post-synaptic dopaminergic markers for the neurodegenerative process in Huntington's disease. *Brain*. **120 (Pt 3**, 503–14

126. Sapp, E., Ge, P., Aizawa, H., Bird, E., Penney, J., Young, A. B., Vonsattel, J. P., and DiFiglia, M. (1995) Evidence for a preferential loss of enkephalin immunoreactivity in the external globus pallidus in low grade Huntington's disease using high resolution image analysis. *Neuroscience*. **64**, 397–404

127. Crook, Z. R., and Housman, D. E. (2012) Dysregulation of dopamine receptor D2 as a sensitive measure for Huntington disease pathology in model mice. *Proc. Natl. Acad. Sci. U. S. A.* **109**, 7487–92

128. Rosas, H. D., Hevelone, N. D., Zaleta, A. K., Greve, D. N., Salat, D. H., and Fischl, B. (2005) Regional cortical thinning in preclinical Huntington disease and its relationship to cognition. *Neurology*. **65**, 745–7

129. Sax, D. S., Powsner, R., Kim, A., Tilak, S., Bhatia, R., Cupples, L. A., and Myers, R. H. (1996) Evidence of cortical metabolic dysfunction in early Huntington's disease by single-photon-emission computed tomography. *Mov. Disord.* **11**, 671–7

130. Vonsattel, J. P., Myers, R. H., Stevens, T. J., Ferrante, R. J., Bird, E. D., and Richardson, E. P. (1985) Neuropathological classification of Huntington's disease. *J. Neuropathol. Exp. Neurol.* **44**, 559–77

131. DiFiglia, M. (1997) Aggregation of Huntingtin in Neuronal Intranuclear Inclusions and Dystrophic Neurites in Brain. *Science (80-.).* **277**, 1990–1993

132. Davies, S. W., Turmaine, M., Cozens, B. A., DiFiglia, M., Sharp, A. H., Ross, C. A., Scherzinger, E., Wanker, E. E., Mangiarini, L., and Bates, G. P. (1997) Formation of neuronal intranuclear inclusions underlies the neurological dysfunction in mice transgenic for the HD mutation. *Cell*. **90**, 537–48

133. Gutekunst, C. A., Li, S. H., Yi, H., Mulroy, J. S., Kuemmerle, S., Jones, R., Rye, D., Ferrante, R. J., Hersch, S. M., and Li, X. J. (1999) Nuclear and neuropil aggregates in Huntington's disease: relationship to neuropathology. *J. Neurosci.* **19**, 2522–34

134. Rockabrand, E., Slepko, N., Pantalone, A., Nukala, V. N., Kazantsev, A., Marsh, J. L., Sullivan, P. G., Steffan, J. S., Sensi, S. L., and Thompson, L. M. (2007) The first 17 amino acids of Huntingtin modulate its sub-cellular localization, aggregation and effects on calcium homeostasis. *Hum. Mol. Genet.* **16**, 61–77

135. Atwal, R. S., Xia, J., Pinchev, D., Taylor, J., Epand, R. M., and Truant, R. (2007) Huntingtin has a membrane association signal that can modulate huntingtin aggregation, nuclear entry and toxicity. *Hum. Mol. Genet.* **16**, 2600–15

136. Maiuri, T., Woloshansky, T., Xia, J., and Truant, R. (2013) The huntingtin N17 domain is a multifunctional CRM1 and Ran-dependent nuclear and cilial export signal. *Hum. Mol. Genet.* **22**, 1383–94

137. Zheng, Z., Li, A., Holmes, B. B., Marasa, J. C., and Diamond, M. I. (2013) An N-terminal nuclear export signal regulates trafficking and aggregation of Huntingtin (Htt) protein exon 1. *J. Biol. Chem.* **288**, 6063–71

138. Thakur, A. K., Jayaraman, M., Mishra, R., Thakur, M., Chellgren, V. M., Byeon, I.-J. L., Anjum, D. H., Kodali, R., Creamer, T. P., Conway, J. F., Gronenborn, A. M., and Wetzel, R. (2009) Polyglutamine disruption of the

huntingtin exon 1 N terminus triggers a complex aggregation mechanism. *Nat. Struct. Mol. Biol.* **16**, 380–9

139. Tam, S., Spiess, C., Auyeung, W., Joachimiak, L., Chen, B., Poirier, M. A., and Frydman, J. (2009) The chaperonin TRiC blocks a huntingtin sequence element that promotes the conformational switch to aggregation. *Nat. Struct. Mol. Biol.* **16**, 1279–85

140. Gu, X., Cantle, J. P., Greiner, E. R., Lee, C. Y. D., Barth, A. M., Gao, F., Park, C. S., Zhang, Z., Sandoval-Miller, S., Zhang, R. L., Diamond, M., Mody, I., Coppola, G., and Yang, X. W. (2015) N17 Modifies Mutant Huntingtin Nuclear Pathogenesis and Severity of Disease in HD BAC Transgenic Mice. *Neuron*. **85**, 726–41

141. Lee, C. Y. D., Cantle, J. P., and Yang, X. W. (2013) Genetic manipulations of mutant huntingtin in mice: new insights into Huntington's disease pathogenesis. *FEBS J.* **280**, 4382–94

142. Thompson, L. M., Aiken, C. T., Kaltenbach, L. S., Agrawal, N., Illes, K., Khoshnan, A., Martinez-Vincente, M., Arrasate, M., O'Rourke, J. G., Khashwji, H., Lukacsovich, T., Zhu, Y.-Z., Lau, A. L., Massey, A., Hayden, M. R., Zeitlin, S. O., Finkbeiner, S., Green, K. N., LaFerla, F. M., Bates, G., Huang, L., Patterson, P. H., Lo, D. C., Cuervo, A. M., Marsh, J. L., and Steffan, J. S. (2009) IKK phosphorylates Huntingtin and targets it for degradation by the proteasome and lysosome. *J. Cell Biol.* **187**, 1083–99

143. Bhat, K. P., Yan, S., Wang, C.-E., Li, S., and Li, X.-J. (2014) Differential ubiquitination and degradation of huntingtin fragments modulated by ubiquitin-protein ligase E3A. *Proc. Natl. Acad. Sci. U. S. A.* **111**, 5706–11

144. Steffan, J. S., Agrawal, N., Pallos, J., Rockabrand, E., Trotman, L. C., Slepko, N., Illes, K., Lukacsovich, T., Zhu, Y.-Z., Cattaneo, E., Pandolfi, P. P., Thompson, L. M., and Marsh, J. L. (2004) SUMO modification of Huntingtin and Huntington's disease pathology. *Science*. **304**, 100–4

145. O'Rourke, J. G., Gareau, J. R., Ochaba, J., Song, W., Raskó, T., Reverter, D., Lee, J., Monteys, A. M., Pallos, J., Mee, L., Vashishtha, M., Apostol, B. L., Nicholson, T. P., Illes, K., Zhu, Y.-Z., Dasso, M., Bates, G. P., Difiglia, M., Davidson, B., Wanker, E. E., Marsh, J. L., Lima, C. D., Steffan, J. S., and Thompson, L. M. (2013) SUMO-2 and PIAS1 modulate insoluble mutant huntingtin protein accumulation. *Cell Rep.* **4**, 362–75

146. Jana, N. R., Zemskov, E. A., Wang Gh, and Nukina, N. (2001) Altered proteasomal function due to the expression of polyglutamine-expanded truncated N-terminal huntingtin induces apoptosis by caspase activation

through mitochondrial cytochrome c release. *Hum. Mol. Genet.* **10**, 1049–59

147. Hipp, M. S., Patel, C. N., Bersuker, K., Riley, B. E., Kaiser, S. E., Shaler, T. A., Brandeis, M., and Kopito, R. R. (2012) Indirect inhibition of 26S proteasome activity in a cellular model of Huntington's disease. *J. Cell Biol.* **196**, 573–87

148. Duennwald, M. L., and Lindquist, S. (2008) Impaired ERAD and ER stress are early and specific events in polyglutamine toxicity. *Genes Dev.* **22**, 3308–19

149. Bett, J. S., Cook, C., Petrucelli, L., and Bates, G. P. (2009) The ubiquitin-proteasome reporter GFPu does not accumulate in neurons of the R6/2 transgenic mouse model of Huntington's disease. *PLoS One*. **4**, e5128

150. Paine, S., Bedford, L., Thorpe, J. R., Mayer, R. J., Cavey, J. R., Bajaj, N., Sheppard, P. W., Lowe, J., and Layfield, R. (2009) Immunoreactivity to Lys63-linked polyubiquitin is a feature of neurodegeneration. *Neurosci. Lett.* **460**, 205–8

151. Babu, J. R., Geetha, T., and Wooten, M. W. (2005) Sequestosome 1/p62 shuttles polyubiquitinated tau for proteasomal degradation. *J. Neurochem.* **94**, 192–203

152. Saeki, Y., Kudo, T., Sone, T., Kikuchi, Y., Yokosawa, H., Toh-e, A., and Tanaka, K. (2009) Lysine 63-linked polyubiquitin chain may serve as a targeting signal for the 26S proteasome. *EMBO J.* **28**, 359–71

153. Gareau, J. R., and Lima, C. D. (2010) The SUMO pathway: emerging mechanisms that shape specificity, conjugation and recognition. *Nat. Rev. Mol. Cell Biol.* **11**, 861–71

154. Cubeñas-Potts, C., and Matunis, M. J. (2013) SUMO: a multifaceted modifier of chromatin structure and function. *Dev. Cell*. **24**, 1–12

155. Bohren, K. M., Nadkarni, V., Song, J. H., Gabbay, K. H., and Owerbach, D. (2004) A M55V polymorphism in a novel SUMO gene (SUMO-4) differentially activates heat shock transcription factors and is associated with susceptibility to type I diabetes mellitus. *J. Biol. Chem.* **279**, 27233–8

156. Johnson, E. S. (2004) Protein modification by SUMO. *Annu. Rev. Biochem.* **73**, 355–82

157. Berndsen, C. E., and Wolberger, C. (2014) New insights into ubiquitin E3 ligase mechanism. *Nat. Struct. Mol. Biol.* **21**, 301–7

158. Reinstein, E., Scheffner, M., Oren, M., Ciechanover, A., and Schwartz, A. (2000) Degradation of the E7 human papillomavirus oncoprotein by the ubiquitin-proteasome system: targeting via ubiquitination of the N-terminal residue. *Oncogene*. **19**, 5944–50

159. Knipscheer, P., Räschle, M., Smogorzewska, A., Enoiu, M., Ho, T. V., Schärer, O. D., Elledge, S. J., and Walter, J. C. (2009) The Fanconi anemia pathway promotes replication-dependent DNA interstrand cross-link repair. *Science*. **326**, 1698–701

160. Verma, R., Oania, R., Graumann, J., and Deshaies, R. J. (2004) Multiubiquitin chain receptors define a layer of substrate selectivity in the ubiquitin-proteasome system. *Cell*. **118**, 99–110

161. Iwai, K. (2012) Diverse ubiquitin signaling in NF-κB activation. *Trends Cell Biol.* **22**, 355–64

162. Fricker, M., O'Prey, J., Tolkovsky, A. M., and Ryan, K. M. (2010) Phosphorylation of Puma modulates its apoptotic function by regulating protein stability. *Cell Death Dis.* **1**, e59

163. Starita, L. M., Pruneda, J. N., Lo, R. S., Fowler, D. M., Kim, H. J., Hiatt, J. B., Shendure, J., Brzovic, P. S., Fields, S., and Klevit, R. E. (2013) Activity-enhancing mutations in an E3 ubiquitin ligase identified by high-throughput mutagenesis. *Proc. Natl. Acad. Sci. U. S. A.* **110**, E1263–72

164. Vittal, V., Wenzel, D. M., Brzovic, P. S., and Klevit, R. E. (2013) Biochemical and Structural Characterization of the Ubiquitin-Conjugating Enzyme UBE2W Reveals the Formation of a Noncovalent Homodimer. *Cell Biochem. Biophys.* **67**, 103–110

165. Salmon, A. B., Murakami, S., Bartke, A., Kopchick, J., Yasumura, K., and Miller, R. A. (2005) Fibroblast cell lines from young adult mice of long-lived mutant strains are resistant to multiple forms of stress. *Am. J. Physiol. Endocrinol. Metab.* **289**, E23–9

166. Dosztányi, Z., Csizmok, V., Tompa, P., and Simon, I. (2005) IUPred: web server for the prediction of intrinsically unstructured regions of proteins based on estimated energy content. *Bioinformatics*. **21**, 3433–4

167. Linding, R., Jensen, L. J., Diella, F., Bork, P., Gibson, T. J., and Russell, R. B. (2003) Protein disorder prediction: implications for structural proteomics. *Structure*. **11**, 1453–9

168. Ward, J. J., Sodhi, J. S., McGuffin, L. J., Buxton, B. F., and Jones, D. T. (2004) Prediction and Functional Analysis of Native Disorder in Proteins from the Three Kingdoms of Life. *J. Mol. Biol.* **337**, 635–645

169. Haynes, C., Oldfield, C. J., Ji, F., Klitgord, N., Cusick, M. E., Radivojac, P., Uversky, V. N., Vidal, M., and Iakoucheva, L. M. (2006) Intrinsic disorder is a common feature of hub proteins from four eukaryotic interactomes. *PLoS Comput. Biol.* **2**, 0890–0901

170. Marseglia, L., D'Angelo, G., Manti, S., Arrigo, T., Barberi, I., Reiter, R. J., and Gitto, E. (2014) Oxidative stress-mediated aging during the fetal and perinatal periods. *Oxid. Med. Cell. Longev.* **2014**, 358375

171. Gitto, E., Reiter, R. J., Karbownik, M., Tan, D., Gitto, P., Barberi, S., and Barberi, I. (2002) Causes of oxidative stress in the pre- and perinatal period. *Biol. Neonate*. **81**, 146–57

172. Bueter, W., Dammann, O., and Leviton, A. (2009) Endoplasmic reticulum stress, inflammation, and perinatal brain damage. *Pediatr. Res.* **66**, 487–94

173. Ye, Y., and Rape, M. (2009) Building ubiquitin chains: E2 enzymes at work. *Nat. Rev. Mol. Cell Biol.* **10**, 755–64

174. Nacerddine, K., Lehembre, F., Bhaumik, M., Artus, J., Cohen-Tannoudji, M., Babinet, C., Pandolfi, P. P., and Dejean, A. (2005) The SUMO pathway is essential for nuclear integrity and chromosome segregation in mice. *Dev. Cell*. **9**, 769–79

175. Harbers, K., Müller, U., Grams, A., Li, E., Jaenisch, R., and Franz, T. (1996) Provirus integration into a gene encoding a ubiquitin-conjugating enzyme results in a placental defect and embryonic lethality. *Proc. Natl. Acad. Sci. U. S. A.* **93**, 12412–7

176. Yamamoto, M., Okamoto, T., Takeda, K., Sato, S., Sanjo, H., Uematsu, S., Saitoh, T., Yamamoto, N., Sakurai, H., Ishii, K. J., Yamaoka, S., Kawai, T., Matsuura, Y., Takeuchi, O., and Akira, S. (2006) Key function for the Ubc13 E2 ubiquitin-conjugating enzyme in immune receptor signaling. *Nat. Immunol.* **7**, 962–70

177. Zhao, G. Y., Sonoda, E., Barber, L. J., Oka, H., Murakawa, Y., Yamada, K., Ikura, T., Wang, X., Kobayashi, M., Yamamoto, K., Boulton, S. J., and Takeda, S. (2007) A critical role for the ubiquitin-conjugating enzyme Ubc13 in initiating homologous recombination. *Mol. Cell*. **25**, 663–75

178. Ren, J., Shi, M., Liu, R., Yang, Q.-H., Johnson, T., Skarnes, W. C., and Du, C. (2005) The Birc6 (Bruce) gene regulates p53 and the mitochondrial

pathway of apoptosis and is essential for mouse embryonic development. *Proc. Natl. Acad. Sci. U. S. A.* **102**, 565–70

179. Roest, H. P., Baarends, W. M., de Wit, J., van Klaveren, J. W., Wassenaar, E., Hoogerbrugge, J. W., van Cappellen, W. A., Hoeijmakers, J. H. J., and Grootegoed, J. A. (2004) The ubiquitin-conjugating DNA repair enzyme HR6A is a maternal factor essential for early embryonic development in mice. *Mol. Cell. Biol.* **24**, 5485–95

180. Bedard, N., Hingamp, P., Pang, Z., Karaplis, A., Morales, C., Trasler, J., Cyr, D., Gagnon, C., and Wing, S. S. (2005) Mice lacking the UBC4-testis gene have a delay in postnatal testis development but normal spermatogenesis and fertility. *Mol. Cell. Biol.* **25**, 6346–54

181. Byrne, C., Hardman, M., and Nield, K. (2003) Covering the limb--formation of the integument. *J. Anat.* **202**, 113–23

182. Madison, K. C. (2003) Barrier function of the skin: “la raison d’être” of the epidermis. *J. Invest. Dermatol.* **121**, 231–41

183. Santos, M. A., Huen, M. S. Y., Jankovic, M., Chen, H.-T., López-Contreras, A. J., Klein, I. A., Wong, N., Barbancho, J. L. R., Fernandez-Capetillo, O., Nussenzweig, M. C., Chen, J., and Nussenzweig, A. (2010) Class switching and meiotic defects in mice lacking the E3 ubiquitin ligase RNF8. *J. Exp. Med.* **207**, 973–81

184. Lu, L.-Y., Wu, J., Ye, L., Gavrilina, G. B., Saunders, T. L., and Yu, X. (2010) RNF8-dependent histone modifications regulate nucleosome removal during spermatogenesis. *Dev. Cell*. **18**, 371–84

185. Li, L., Halaby, M.-J., Hakem, A., Cardoso, R., El Ghamrasni, S., Harding, S., Chan, N., Bristow, R., Sanchez, O., Durocher, D., and Hakem, R. (2010) Rnf8 deficiency impairs class switch recombination, spermatogenesis, and genomic integrity and predisposes for cancer. *J. Exp. Med.* **207**, 983–97

186. Zeng, L., Tallaksen-Greene, S. J., Wang, B., Albin, R. L., and Paulson, H. L. (2013) The de-ubiquitinating enzyme ataxin-3 does not modulate disease progression in a knock-in mouse model of Huntington disease. *J. Huntingtons. Dis.* **2**, 201–15

187. Zeng, L., Wang, B., Merillat, S. A., N Minakawa, E., Perkins, M. D., Ramani, B., Tallaksen-Greene, S. J., Costa, M. do C., Albin, R. L., and Paulson, H. L. (2015) Differential recruitment of UBQLN2 to nuclear inclusions in the polyglutamine diseases HD and SCA3. *Neurobiol. Dis.* **82**, 281–288

188. Barmada, S. J., Ju, S., Arjun, A., Batarse, A., Archbold, H. C., Peisach, D., Li, X., Zhang, Y., Tank, E. M. H., Qiu, H., Huang, E. J., Ringe, D., Petsko, G. A., and Finkbeiner, S. (2015) Amelioration of toxicity in neuronal models of amyotrophic lateral sclerosis by hUPF1. *Proc. Natl. Acad. Sci. U. S. A.* **112**, 7821–6

189. Barmada, S. J., Serio, A., Arjun, A., Bilican, B., Daub, A., Ando, D. M., Tsvetkov, A., Pleiss, M., Li, X., Peisach, D., Shaw, C., Chandran, S., and Finkbeiner, S. (2014) Autophagy induction enhances TDP43 turnover and survival in neuronal ALS models. *Nat. Chem. Biol.* **10**, 677–85

190. Miller, J., Arrasate, M., Shaby, B. A., Mitra, S., Masliah, E., and Finkbeiner, S. (2010) Quantitative relationships between huntingtin levels, polyglutamine length, inclusion body formation, and neuronal death provide novel insight into huntington's disease molecular pathogenesis. *J. Neurosci.* **30**, 10541–50

191. Saudou, F., Finkbeiner, S., Devys, D., and Greenberg, M. E. (1998) Huntingtin acts in the nucleus to induce apoptosis but death does not correlate with the formation of intranuclear inclusions. *Cell*. **95**, 55–66

192. Barmada, S. J., Skibinski, G., Korb, E., Rao, E. J., Wu, J. Y., and Finkbeiner, S. (2010) Cytoplasmic mislocalization of TDP-43 is toxic to neurons and enhanced by a mutation associated with familial amyotrophic lateral sclerosis. *J. Neurosci.* **30**, 639–49

193. Livak, K. J., and Schmittgen, T. D. (2001) Analysis of relative gene expression data using real-time quantitative PCR and the 2(-Delta Delta C(T)) Method. *Methods*. **25**, 402–8

194. Takahashi, T., Kikuchi, S., Katada, S., Nagai, Y., Nishizawa, M., and Onodera, O. (2008) Soluble polyglutamine oligomers formed prior to inclusion body formation are cytotoxic. *Hum. Mol. Genet.* **17**, 345–56

195. Arrasate, M., Mitra, S., Schweitzer, E. S., Segal, M. R., and Finkbeiner, S. (2004) Inclusion body formation reduces levels of mutant huntingtin and the risk of neuronal death. *Nature*. **431**, 805–10

196. Heng, M. Y., Duong, D. K., Albin, R. L., Tallaksen-Greene, S. J., Hunter, J. M., Lesort, M. J., Osmand, A., Paulson, H. L., and Detloff, P. J. (2010) Early autophagic response in a novel knock-in model of Huntington disease. *Hum. Mol. Genet.* **19**, 3702–20

197. Heng, M. Y., Tallaksen-Greene, S. J., Detloff, P. J., and Albin, R. L. (2007) Longitudinal evaluation of the Hdh(CAG)150 knock-in murine model of Huntington's disease. *J. Neurosci.* **27**, 8989–98

198. Bibb, J. A., Yan, Z., Svenningsson, P., Snyder, G. L., Pieribone, V. A., Horiuchi, A., Nairn, A. C., Messer, A., and Greengard, P. (2000) Severe deficiencies in dopamine signaling in presymptomatic Huntington's disease mice. *Proc. Natl. Acad. Sci.* **97**, 6809–6814

199. Van Dellen, A., Welch, J., Dixon, R. M., Cordery, P., York, D., Styles, P., Blakemore, C., and Hannan, A. J. (2000) N-Acetylaspartate and DARPP-32 levels decrease in the corpus striatum of Huntington's disease mice. *Neuroreport*. **11**, 3751–7

200. Tallaksen-Greene, S. J., Sadagurski, M., Zeng, L., Mauch, R., Perkins, M., Banduseela, V. C., Lieberman, A. P., Miller, R. A., Paulson, H. L., and Albin, R. L. (2014) Differential effects of delayed aging on phenotype and striatal pathology in a murine model of Huntington disease. *J. Neurosci.* **34**, 15658–68

201. Hay, D. G., Sathasivam, K., Tobaben, S., Stahl, B., Marber, M., Mestril, R., Mahal, A., Smith, D. L., Woodman, B., and Bates, G. P. (2004) Progressive decrease in chaperone protein levels in a mouse model of Huntington's disease and induction of stress proteins as a therapeutic approach. *Hum. Mol. Genet.* **13**, 1389–405

202. Wang, J., Wang, C.-E., Orr, A., Tydlacka, S., Li, S.-H., and Li, X.-J. (2008) Impaired ubiquitin-proteasome system activity in the synapses of Huntington's disease mice. *J. Cell Biol.* **180**, 1177–89

203. Miller, V. M., Nelson, R. F., Gouvion, C. M., Williams, A., Rodriguez-Lebron, E., Harper, S. Q., Davidson, B. L., Rebagliati, M. R., and Paulson, H. L. (2005) CHIP suppresses polyglutamine aggregation and toxicity in vitro and in vivo. *J. Neurosci.* **25**, 9152–61

204. Weiss, A., Klein, C., Woodman, B., Sathasivam, K., Bibel, M., Régulier, E., Bates, G. P., and Paganetti, P. (2008) Sensitive biochemical aggregate detection reveals aggregation onset before symptom development in cellular and murine models of Huntington's disease. *J. Neurochem.* **104**, 846–58

205. Leitman, J., Ulrich Hartl, F., and Lederkremer, G. Z. (2013) Soluble forms of polyQ-expanded huntingtin rather than large aggregates cause endoplasmic reticulum stress. *Nat. Commun.* **4**, 2753

206. Ehrnhoefer, D. E., Duennwald, M., Markovic, P., Wacker, J. L., Engemann, S., Roark, M., Legleiter, J., Marsh, J. L., Thompson, L. M., Lindquist, S., Muchowski, P. J., and Wanker, E. E. (2006) Green tea (-)-epigallocatechin-gallate modulates early events in huntingtin misfolding and reduces toxicity in Huntington's disease models. *Hum. Mol. Genet.* **15**, 2743–51

207. Nucifora, L. G., Burke, K. A., Feng, X., Arbez, N., Zhu, S., Miller, J., Yang, G., Ratovitski, T., Delannoy, M., Muchowski, P. J., Finkbeiner, S., Legleiter, J., Ross, C. A., and Poirier, M. A. (2012) Identification of novel potentially toxic oligomers formed in vitro from mammalian-derived expanded huntingtin exon-1 protein. *J. Biol. Chem.* **287**, 16017–28

208. Slow, E. J., Graham, R. K., Osmand, A. P., Devon, R. S., Lu, G., Deng, Y., Pearson, J., Vaid, K., Bissada, N., Wetzel, R., Leavitt, B. R., and Hayden, M. R. (2005) Absence of behavioral abnormalities and neurodegeneration in vivo despite widespread neuronal huntingtin inclusions. *Proc. Natl. Acad. Sci. U. S. A.* **102**, 11402–7

209. Kim, M., Lee, H. S., LaForet, G., McIntyre, C., Martin, E. J., Chang, P., Kim, T. W., Williams, M., Reddy, P. H., Tagle, D., Boyce, F. M., Won, L., Heller, A., Aronin, N., and DiFiglia, M. (1999) Mutant huntingtin expression in clonal striatal cells: dissociation of inclusion formation and neuronal survival by caspase inhibition. *J. Neurosci.* **19**, 964–73

210. Taylor, J. P., Tanaka, F., Robitschek, J., Sandoval, C. M., Taye, A., Markovic-Plese, S., and Fischbeck, K. H. (2003) Aggresomes protect cells by enhancing the degradation of toxic polyglutamine-containing protein. *Hum. Mol. Genet.* **12**, 749–57

211. Lajoie, P., and Snapp, E. L. (2013) Detecting soluble polyQ oligomers and investigating their impact on living cells using split-GFP. *Methods Mol. Biol.* **1017**, 229–39

212. Cheroni, C., Marino, M., Tortarolo, M., Veglianese, P., De Biasi, S., Fontana, E., Zuccarello, L. V., Maynard, C. J., Dantuma, N. P., and Bendotti, C. (2009) Functional alterations of the ubiquitin-proteasome system in motor neurons of a mouse model of familial amyotrophic lateral sclerosis. *Hum. Mol. Genet.* **18**, 82–96

213. Pendaries, V., Malaisse, J., Pellerin, L., Le Lamer, M., Nachat, R., Kezic, S., Schmitt, A.-M., Paul, C., Poumay, Y., Serre, G., and Simon, M. (2014) Knockdown of filaggrin in a three-dimensional reconstructed human epidermis impairs keratinocyte differentiation. *J. Invest. Dermatol.* **134**, 2938–46

214. Brown, S. J., and McLean, W. H. I. (2012) One remarkable molecule: filaggrin. *J. Invest. Dermatol.* **132**, 751–62

215. Kawasaki, H., Nagao, K., Kubo, A., Hata, T., Shimizu, A., Mizuno, H., Yamada, T., and Amagai, M. (2012) Altered stratum corneum barrier and enhanced percutaneous immune responses in filaggrin-null mice. *J. Allergy Clin. Immunol.* **129**, 1538–46.e6

216. Indra, A. K., Warot, X., Brocard, J., Bornert, J. M., Xiao, J. H., Chambon, P., and Metzger, D. (1999) Temporally-controlled site-specific mutagenesis in the basal layer of the epidermis: comparison of the recombinase activity of the tamoxifen-inducible Cre-ER(T) and Cre-ER(T2) recombinases. *Nucleic Acids Res.* **27**, 4324–7

217. Xu, G., Paige, J. S., and Jaffrey, S. R. (2010) Global analysis of lysine ubiquitination by ubiquitin remnant immunoaffinity profiling. *Nat. Biotechnol.* **28**, 868–73

218. Danielsen, J. M. R., Sylvestersen, K. B., Bekker-Jensen, S., Szklarczyk, D., Poulsen, J. W., Horn, H., Jensen, L. J., Mailand, N., and Nielsen, M. L. (2011) Mass spectrometric analysis of lysine ubiquitylation reveals promiscuity at site level. *Mol. Cell. Proteomics*. **10**, M110.003590

219. Kim, W., Bennett, E. J., Huttlin, E. L., Guo, A., Li, J., Possemato, A., Sowa, M. E., Rad, R., Rush, J., Comb, M. J., Harper, J. W., and Gygi, S. P. (2011) Systematic and quantitative assessment of the ubiquitin-modified proteome. *Mol. Cell*. **44**, 325–40

220. Peng, J., Schwartz, D., Elias, J. E., Thoreen, C. C., Cheng, D., Marsischky, G., Roelofs, J., Finley, D., and Gygi, S. P. (2003) A proteomics approach to understanding protein ubiquitination. *Nat. Biotechnol.* **21**, 921–6

221. Martinez, A., Traverso, J. A., Valot, B., Ferro, M., Espagne, C., Ephritikhine, G., Zivy, M., Giglione, C., and Meinnel, T. (2008) Extent of N-terminal modifications in cytosolic proteins from eukaryotes. *Proteomics*. **8**, 2809–31

222. Polevoda, B., and Sherman, F. (2000) Nalpha -terminal acetylation of eukaryotic proteins. *J. Biol. Chem.* **275**, 36479–82

223. Bradshaw, R. A., Brickey, W. W., and Walker, K. W. (1998) N-terminal processing: the methionine aminopeptidase and N alpha-acetyl transferase families. *Trends Biochem. Sci.* **23**, 263–7

224. Mahrus, S., Trinidad, J. C., Barkan, D. T., Sali, A., Burlingame, A. L., and Wells, J. A. (2008) Global sequencing of proteolytic cleavage sites in apoptosis by specific labeling of protein N termini. *Cell*. **134**, 866–76

225. Huesgen, P. F., and Overall, C. M. (2012) N- and C-terminal degradomics: new approaches to reveal biological roles for plant proteases from substrate identification. *Physiol. Plant.* **145**, 5–17

226. Agard, N. J., and Wells, J. A. (2009) Methods for the proteomic identification of protease substrates. *Curr. Opin. Chem. Biol.* **13**, 503–9

227. Kleifeld, O., Doucet, A., auf dem Keller, U., Prudova, A., Schilling, O., Kainthan, R. K., Starr, A. E., Foster, L. J., Kizhakkedathu, J. N., and Overall, C. M. (2010) Isotopic labeling of terminal amines in complex samples identifies protein N-termini and protease cleavage products. *Nat. Biotechnol.* **28**, 281–8

228. Mommen, G. P. M., van de Waterbeemd, B., Meiring, H. D., Kersten, G., Heck, A. J. R., and de Jong, A. P. J. M. (2012) Unbiased selective isolation of protein N-terminal peptides from complex proteome samples using phospho tagging (PTAG) and TiO(2)-based depletion. *Mol. Cell. Proteomics*. **11**, 832–42

229. Shen, P.-T., Hsu, J.-L., and Chen, S.-H. (2007) Dimethyl isotope-coded affinity selection for the analysis of free and blocked N-termini of proteins using LC-MS/MS. *Anal. Chem.* **79**, 9520–30

230. Rathke, C., Baarends, W. M., Awe, S., and Renkawitz-Pohl, R. (2014) Chromatin dynamics during spermiogenesis. *Biochim. Biophys. Acta*. **1839**, 155–68

231. Brunner, A. M., Nanni, P., and Mansuy, I. M. (2014) Epigenetic marking of sperm by post-translational modification of histones and protamines. *Epigenetics Chromatin*. **7**, 2